A UNITED STATES DEPARTMENT OF COMMERCE PUBLICATION

EASTROPAC ATLAS

U.S. DEPARTMENT OF COMMERCE
National Oceanic and Atmospheric Administration
National Marine Fisheries Service

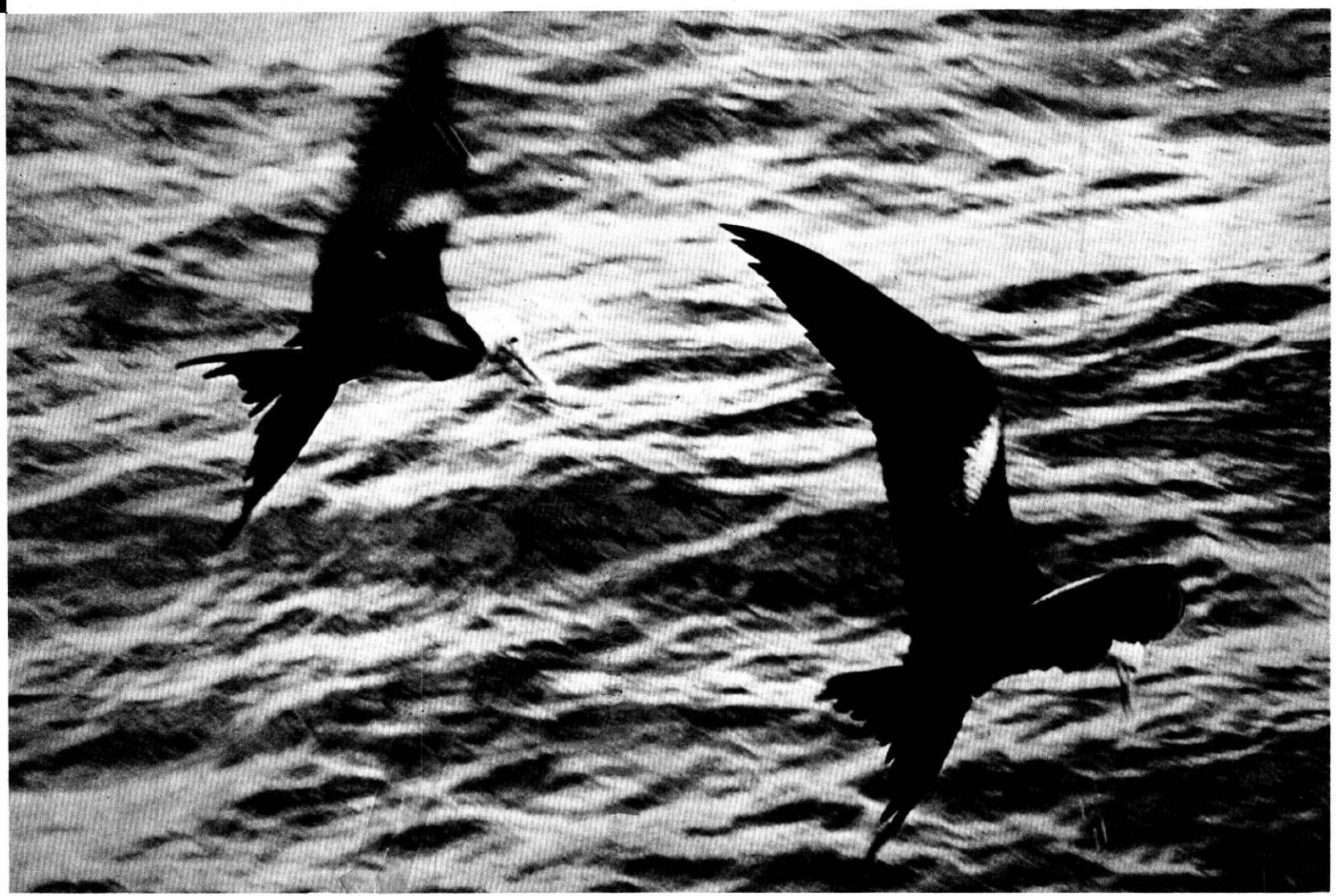

CIRCULAR
330
VOLUME 5
SEPTEMBER
1972

EASTROPAC *Atlas*

Volume 1	Physical oceanographic and meteorological data from principal participating ships, first survey cruise, February-March 1967.	Published June 1972
Volume 2	Biological and nutrient chemistry data from principal participating ships, first survey cruise, February-March 1967.	Published April 1971
Volume 3	Physical oceanographic and meteorological data from principal participating ships, first and second monitor cruises, April-July 1967.	Published September 1971
Volume 4	Biological and nutrient chemistry data from principal participating ships, first and second monitor cruises, April-July 1967.	Published November 1970
Volume 5	Physical oceanographic and meteorological data from principal participating ships, second survey cruise, August-September 1967.	Published September 1972
Volume 6	Biological and nutrient chemistry data from principal participating ships, second survey cruise, August-September 1967.	In preparation
Volume 7	Physical oceanographic and meteorological data from principal participating ships and *Oceanographer*, third and fourth monitor cruises, October 1967-January 1968.	In preparation
Volume 8	Biological and nutrient chemistry data from principal participating ships and *Oceanographer*, third and fourth monitor cruises, October 1967-January 1968.	In preparation
Volume 9	Physical oceanographic and meteorological data from principal participating ships, third survey cruise, February-March 1968.	In preparation
Volume 10	Biological and nutrient chemistry data from principal participating ships, third survey cruise, February-March 1968.	In preparation
Volume 11	Data from Latin American cooperating ships and ships of opportunity, all cruises, February 1967-March 1968.	In preparation

Cover. Immature magnificent frigatebirds near Cocos Island.
Photo by John H. Taylor, Scripps Institution of Oceanography.

ABSTRACT

This atlas contains charts depicting the distribution of physical, chemical, and biological oceanographic properties and associated meteorological properties observed during EASTROPAC. EASTROPAC was an international cooperative investigation of the eastern tropical Pacific Ocean (20° N. to 20° S., and from the west coasts of the American continents to 119° W.) which was intended to provide data necessary for a more effective use of the marine resources of the area, especially tropical tunas, and also to increase knowledge of the ocean circulation, air-sea interaction, and ecology. The Bureau of Commercial Fisheries (now National Marine Fisheries Service) was the coordinating agency. The field work, from February 1967 through March 1968, was divided into seven 2-month cruise periods. During each cruise period one or more ships were operating in the study area.

On completion of the field work the data seemed too numerous for a classical data report. Instead, it was decided to produce an 11-volume atlas of the results, with 5 volumes containing physical oceanographic and meteorological data from the principal participating ships, 5 volumes containing biological and nutrient chemistry data from the same ships, and 1 volume containing all data from Latin American cooperating ships and ships of opportunity. Extensive use was made of a computer and automatic plotter in preparation of the atlas charts. Methods used to collect and process the data upon which the atlas is based are described in detail by the contributors of the following categories of charts: temperature, salinity, and derived quantities; thickness of the upper mixed layer; dissolved oxygen; meteorology; nutrient chemistry; phytoplankton standing stocks and production; zooplankton and fish larvae; micronekton; birds, fish schools, and marine mammals.

EASTROPAC *Atlas*

VOLUME 2

ERRATA

May 1972

FIGURE 14-NO_3-v8. The labeling on the latitude scale is incorrect. The tick mark at the right hand end of the chart should be labeled 5 N instead of 1 S.

EASTROPAC Atlas

VOLUME 5

ERRATA Number 1

November 1972

FIGURE 46-S-v3. The two intersecting lines at lower left, below the 34.6 contour, are extraneous and should be disregarded.

UNITED STATES DEPARTMENT OF COMMERCE
Peter G. Peterson, *Secretary*

NATIONAL OCEANIC AND ATMOSPHERIC ADMINISTRATION
Robert M. White, *Administrator*

NATIONAL MARINE FISHERIES SERVICE
Philip M. Roedel, *Director*

EASTROPAC ATLAS

VOLUME 5

PHYSICAL OCEANOGRAPHIC AND METEOROLOGICAL DATA FROM
PRINCIPAL PARTICIPATING SHIPS
SECOND SURVEY CRUISE, AUGUST-SEPTEMBER 1967

CUTHBERT M. LOVE, *Editor*

CIRCULAR 330
WASHINGTON, D.C.
SEPTEMBER 1972

For sale by the Superintendent of Documents, U.S. Government Printing Office, Washington, D.C. 20402—Price $4.75 per volume

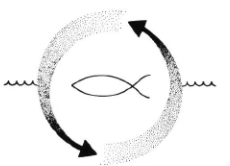

COORDINATOR, EASTROPAC PROJECT

WARREN S. WOOSTER, Scripps Institution of Oceanography, June 27, 1966-May 15, 1967
ALAN R. LONGHURST, National Marine Fisheries Service, May 15, 1967-June 30, 1970

ATLAS CONTRIBUTORS

ELBERT H. AHLSTROM—National Marine Fisheries Service, Fish Larvae
MAURICE BLACKBURN—Scripps Institution of Oceanography, Micronekton
WITOLD L. KLAWE—Inter-American Tropical Tuna Commission, Scombroid Larvae
R. MICHAEL LAURS—National Marine Fisheries Service, Zooplankton, Micronekton, Bird and Mammal Observations
FORREST R. MILLER—Inter-American Tropical Tuna Commission, Meteorology
ROBERT W. OWEN, Jr.—National Marine Fisheries Service, Phytoplankton, Oxygen, Mixed Layer Depth
BRUCE A. TAFT—Scripps Institution of Oceanography, Physical Oceanography
WILLIAM H. THOMAS—Scripps Institution of Oceanography, Nutrient Chemistry
MIZUKI TSUCHIYA—Scripps Institution of Oceanography, Physical Oceanography
BERNT ZEITZSCHEL—Scripps Institution of Oceanography, Phytoplankton

EDITORIAL COMMITTEE

CUTHBERT M. LOVE, National Marine Fisheries Service
BRUCE A. TAFT, Scripps Institution of Oceanography
R. MICHAEL LAURS, National Marine Fisheries Service

National Marine Fisheries Service
Southwest Fisheries Center
La Jolla, California 92037

Scripps Institution of Oceanography
University of California, San Diego
La Jolla, California 92037

Inter-American Tropical Tuna Commission
% Scripps Institution of Oceanography
La Jolla, California 92037

INTRODUCTION

EASTROPAC was an international cooperative investigation of the eastern tropical Pacific Ocean which was intended to provide data necessary for a more effective use of the marine resources of the area, especially tropical tunas, and also to increase knowledge of the ocean circulation, air-sea interaction, and ecology. The National Marine Fisheries Service (NMFS)—the Bureau of Commercial Fisheries (BCF) at the time of the investigations—was the coordinating agency. The field work, from February 1967 through March 1968, was divided into seven 2-month cruise periods.

At a meeting of the EASTROPAC Coordinating Committee held at La Jolla in April 1968, it was decided that the data derived from the cruises were so numerous as to render classical data reports impractical and that a comprehensive atlas of the physical and biological results of the project should be produced instead. The atlas has been divided into 11 volumes, with five volumes containing physical oceanographic and meteorological data from the principal participating ships, five volumes containing biological and nutrient chemistry data from the same ships, and one volume containing all data from Latin-American cooperating ships and ships of opportunity.

Volume 5 contains physical oceanographic and meteorological data collected mainly by the principal participating ships during the second survey cruise period (40-series cruises), August-September 1967. The companion volume presenting the corresponding biological and nutrient chemistry data is volume 6. The locations of stations occupied by principal participating ships and Latin-American cooperating ships are shown in figures 40-TC-a and 40-TC-b.

Information concerning the history and organization of the EASTROPAC Project, a description of the cruises undertaken, the program of observations, the methods used for preparation of the charts, and remarks on the organization of the atlas are contained in volumes 1 and 4 with descriptions by the contributing scientists of the methods used to collect and process the data upon which the atlas charts are based.

CUTHBERT M. LOVE
Editor

Abbreviations used in figure designation system

Cruise or cruise period	Property represented	Mnemonic to explain choice of letters	Indicator for vertical sections or type of horizontal surface
Numbers 11, 12, 13, etc., indicate principal cruises. See figure 1.	T Temperature		v1, v2, etc., indicate vertical sections.
	S Salinity		Vertical sections are assigned consecutive numbers within each cruise which follow the chronological order in which the ship ran the sections.
Letters or letter-number combinations indicate cruises of Latin American cooperating ships or ships of opportunity, as follows:	δ Thermosteric anomaly (δ_T)		
	G Geostrophic velocity		
	O_2 Oxygen concentration		
	O_2Sa Oxygen saturation		Number 10 or 100 following O_2Sa or horizontal P, Si, NO_3, NO_2, or NH_3 charts indicates distribution at that depth (m.).
	ML Thickness of the mixed layer		
	§300 300 cl./t. thermosteric anomaly surface		s Distribution at the sea surface
	AP Acceleration Potential		§300 Distribution on the surface where δ_T=300 cl./t.
	P Phosphate-phosphorus		ei Distribution integrated over the euphotic layer
	Si Silicate-silicon		150i Distribution integrated to 150 m. depth
	NO_3 Nitrate-nitrogen		z Depth of a surface
	NO_2 Nitrite-nitrogen		
	NH_3 Ammonia-nitrogen		Number 1 or 2 following SP or SW charts indicates one of two 6-month periods into which those observations were divided.
	Ch Chlorophyll-a		
	Ph Phaeophytin		
	PP Primary production		
	EL Thickness of the euphotic layer		
	FCp Fish and cephalopod standing stock		
	Cr Crustacean standing stock		
	Nk Total micronekton standing stock		
	ZhN Zooplankton standing stock from 50-cm. net hauls, night	Zooplankton, half-meter, Night	
	Z1N Zooplankton standing stock from 1-m. net hauls, night	Zooplankton, 1-meter, Night	
	ZhD Zooplankton standing stock from 50-cm. net hauls, day	Zooplankton, half-meter, Day	
	Z1D Zooplankton standing stock from 1-m. net hauls, day	Zooplankton, 1-meter, Day	
	FLN Total fish larvae, night hauls	Fish Larvae, Night	Numbers 1 to 4 or 1 to 6 following MT or MW charts indicate one of the approximate 2-week periods into which those observations were divided. For all cruise periods except 40, the MT and MW charts were drawn for four 2-week periods. For the 40 cruise period these charts were drawn for six periods ranging from 12 to 16 days in length, but with several days overlap between some periods. Number 1 or 2 following MC charts indicates one of the monthly periods for which those charts were drawn.
	FLD Total fish larvae, day hauls	Fish Larvae, Day	
	FE Total fish eggs		
	FS Total skipjack tuna larvae	Fish, Skipjack	
	FA Total *Auxis* larvae	Fish, *Auxis*	
	FC Total *Coryphaena* larvae	Fish, *Coryphaena*	
	FMN Total myctophid larvae, night hauls	Fish, Myctophid, Night	
	FMD Total myctophid larvae, day hauls	Fish, Myctophid, Day	
	FGN Total gonostomatid and sternoptychid larvae, night hauls	Fish, Gonostomatid, Night	
	FGD Total gonostomatid and sternoptychid larvae, day hauls	Fish, Gonostomatid, Day	
	BP Relative abundance of plankton-feeding birds	Birds, Plankton-feeding	
	BF Relative abundance of fish and cephalopod-feeding birds	Birds, Fish-feeding	
	SP Porpoise sightings	Sightings, Porpoise	
	SW Whale sightings	Sightings, Whales	
	ST Tuna school sightings, all cruises	Sightings, Tuna	
	UA Upper atmosphere meteorology		
	MW Surface meteorological analysis, winds and pressure	Meteorology, Winds	
	MC Surface meteorological analysis, clouds, dewpoint, temperature	Meteorology, Clouds	
	MT Surface meteorological analysis, sea temperature, sea-air temperature difference, sea temperature anomaly	Meteorology, Temperature	
	RM Reference map		
	TC Track chart		

Cruise or cruise period
MZ-4 *Yolanda*, MZ-4
MZ-5 *Yolanda*, MZ-5
MZ-6 *Yolanda*, MZ-6
MZ-7 *Defiance*, MZ-7
MZ-8 *Tuxpan*, MZ-8
H1 *Huayaipe-1*
H2 *Huayaipe-2*
H3 *Huayaipe-3*
U1 *Unanue* 6702
U2 *Unanue* 6708
U3 *Unanue* 6802
Y5 *Yelcho* MARCHILE V
Y6 *Yelcho* MARCHILE VI
Y7 *Yelcho* MARCHILE VII
E6 *Esmeralda* BE VI
OP *Oceanographer*
CD *Charles H. Davis*
T3 *Te Vega* 13
T4 *Te Vega* 14
T5 *Te Vega* 15
T6 *Te Vega* 16
T7 *Te Vega* 17
Numbers 10, 20, 30, 40, 50, 60, 70, indicate 2-month cruise periods.

LIST OF FIGURES

FIGURE 40-MT-1.—Analysis of sea surface temperatures based on averages for 2-degree (latitude-longitude) squares from all available ship observations for the period August 1-12, 1967. Solid lines are sea surface isotherms (°C.); the isotherms are dashed where data are sparse. Dark hatching outlines areas with positive temperature anomalies (computed from mean sea surface temperatures averaged over 22 years) greater than 1° C.; light hatching shows areas with negative anomalies greater than 1° C. Sea surface temperature (°C. x 10) averaged for 5-degree squares is plotted above the mean position of the square; sea temperature minus air temperature difference (°C. x 10) is plotted below the symbol.

FIGURE 40-MT-2.—Analysis of sea surface temperatures based on averages for 2-degree (latitude-longitude) squares from all available ship observations for the period August 13-26, 1967. Solid lines are sea surface isotherms (°C.); the isotherms are dashed where data are sparse. Dark hatching outlines areas with positive temperature anomalies (computed from mean sea surface temperatures averaged over 22 years) greater than 1° C.; light hatching shows areas with negative anomalies greater than 1° C. Sea surface temperature (°C. x 10) averaged for 5-degree squares is plotted above the mean position of the square; sea temperature minus air temperature difference (°C. x 10) is plotted below the symbol.

FIGURE 40-MT-3.—Analysis of sea surface temperatures based on averages for 2-degree (latitude-longitude) squares from all available ship observations for the period August 20-31, 1967. Solid lines are sea surface isotherms (°C.); the isotherms are dashed where data are sparse. Dark hatching outlines areas with positive temperature anomalies (computed from mean sea surface temperatures averaged over 22 years) greater than 1° C.; light hatching shows areas with negative anomalies greater than 1° C. Sea surface temperature (°C. x 10) averaged for 5-degree squares is plotted above the mean position of the square; sea temperature minus air temperature difference (°C. x 10) is plotted below the symbol.

FIGURE 40-MT-4.—Analysis of sea surface temperatures based on averages for 2-degree (latitude-longitude) squares from all available ship observations for the period September 1-16, 1967. Solid lines are sea surface isotherms (°C.); the isotherms are dashed where data are sparse. Dark hatching outlines areas with positive temperature anomalies (computed from mean sea surface temperatures averaged over 22 years) greater than 1° C.; light hatching shows areas with negative anomalies greater than 1° C. Sea surface temperature (°C. x 10) averaged for 5-degree squares is plotted above the mean position of the square; sea temperature minus air temperature difference (°C. x 10) is plotted below the symbol.

FIGURE 40-MT-5.—Analysis of sea surface temperatures based on averages for 2-degree (latitude-longitude) squares from all available ship observations for the period September 10-23, 1967. Solid lines are sea surface isotherms (°C.); the isotherms are dashed where data are sparse. Dark hatching outlines areas with positive temperature anomalies (computed from mean sea surface temperatures averaged over 22 years) greater than 1° C.; light hatching shows areas with negative anomalies greater than 1° C. Sea surface temperature (°C. x 10) averaged for 5-degree squares is plotted above the mean position of the square; sea temperature minus air temperature difference (°C. x 10) is plotted below the symbol.

FIGURE 40-MT-6.—Analysis of sea surface temperatures based on averages for 2-degree (latitude-longitude) squares from all available ship observations for the period September 17-30, 1967. Solid lines are sea surface isotherms (°C.); the isotherms are dashed where data are sparse. Dark hatching outlines areas with positive temperature anomalies (computed from mean sea surface temperatures averaged over 22 years) greater than 1° C.; light hatching shows areas with negative anomalies greater than 1° C. Sea surface temperature (°C. x 10) averaged for 5-degree squares is plotted above the mean position of the square; sea temperature minus air temperature difference (°C. x 10) is plotted below the symbol.

FIGURE 40-MC-1.—Analyses of the surface dew-point temperature of the air and total cloud cover based on 2-degree (latitude-longitude) averages from all available ship observations for the month of August 1967. Solid lines depict the monthly mean total cloud cover in oktas; the lines are dashed where data are sparse. Dash-dot lines are isotherms of the mean monthly dew-point temperature at 2-degree (C.) intervals. Areas where 15 percent or more of the ships reported rain of any type at or within sight of the ship are shaded. Dew-point temperature (°C. x 10) averaged for 5-degree squares is plotted above the mean position of the square, with total cloud cover (oktas) below the rainfall frequency (%) to the right of the symbol.

FIGURE 40-MC-2.—Analyses of the surface dew-point temperature of the air and total cloud cover based on 2-degree (latitude-longitude) averages from all available ship observations for the month of September 1967. Solid lines depict the monthly mean total cloud cover in oktas; the lines are dashed where data are sparse. Dash-dot lines are isotherms of the mean monthly dew-point temperature at 2-degree (C.) intervals. Areas where 15 percent or more of the ships reported rain of any type at or within sight of the ship are shaded. Dew-point temperature (°C. x 10) averaged for 5-degree squares is plotted above the mean position of the square, with total cloud cover (oktas) below the rainfall frequency (%) to the right of the symbol.

Temperature and salinity—White pages

FIGURE 45-T-v1.—Vertical distribution of temperature (°C.) along 119° W., August 3-21, 1967. The data from Stations 1-15 were not calibrated against Nansen cast data.

FIGURE 45-T-v2.—Vertical distribution of temperature (°C.) along 10° S., August 21-23, 1967.

FIGURE 45-T-v5.—Vertical distribution of temperature (°C.) along a section from 12° N., 112° W. to Manzanillo, September 7-10, 1967.

FIGURE 45-T-v6.—Vertical distribution of temperature (°C.) along 19°30′ N. from Manzanillo to 111°25′ W., September 13-15, 1967.

FIGURE 45-T-v3.—Vertical distribution of temperature (°C.) along 112° W., August 23-September 7, 1967. The interruption in the contours indicates a 4-day interval between Stations 206 and 282 in the upper (0-500 m.) portion of the section, or between Stations 202 and 282 in the lower portion.

FIGURE 45-T-v4.—Vertical distribution of temperature (°C.) along 112° W. from 2°27′ N. to 2°29′ S., August 30-September 1, 1967. These data are part of a special series of observations made during the time interval indicated by the interrupted contours on figure 45-T-v3.

FIGURE 45-S-v1.—Vertical distribution of salinity (‰) along 119° W., August 3-21, 1967. The data from Stations 1-15 were not calibrated against Nansen cast data.

FIGURE 45-S-v2.—Vertical distribution of salinity (‰) along 10° S., August 21-23, 1967.

FIGURE 45-S-v5.—Vertical distribution of salinity (‰) along a section from 12° N., 112° W. to Manzanillo, September 7-10, 1967.

FIGURE 45-S-v6.—Vertical distribution of salinity (‰) along 19°30′ N. from Manzanillo to 111°25′ W., September 13-15, 1967.

FIGURE 45-S-v3.—Vertical distribution of salinity (‰) along 112° W., August 23-September 7, 1967. The interruption in the contours indicates a 4-day interval between Stations 206 and 282 in the upper (0-500 m.) portion of the section, or between Stations 202 and 282 in the lower portion.

FIGURE 45-S-v4.—Vertical distribution of salinity (‰) along 112° W. from 2°27′ N. to 2°29′ S., August 30-September 1, 1967. These data are part of a special series of observations made during the time interval indicated by the interrupted contours on figure 45-S-v3.

Thermosteric anomaly and geostrophic velocity—Yellow pages

FIGURE 45-δ-v1.—Vertical distribution of thermosteric anomaly, δ_x, (cl./t.) along 119° W., August 3-21, 1967. The temperature and salinity data from Stations 1-15 were not calibrated against Nansen cast data.

FIGURE 45-δ-v2.—Vertical distribution of thermosteric anomaly, δ_x, (cl./t.) along 10° S., August 21-23, 1967.

FIGURE 45-δ-v5.—Vertical distribution of thermosteric anomaly, δ_x, (cl./t.) along a section from 12° N., 112° W. to Manzanillo, September 7-10, 1967.

FIGURE 45-δ-v6.—Vertical distribution of thermosteric anomaly, δ_x, (cl./t.) along 19°30′ N. from Manzanillo to 111°25′ W., September 13-15, 1967.

FIGURE 45-δ-v3.—Vertical distribution of thermosteric anomaly, δ_x, (cl./t.) along 112° W., August 23-September 7, 1967. The interruption in the contours indicates a 4-day interval between Stations 206 and 282 in the upper (0-500 m.) portion of the section, or between Stations 202 and 282 in the lower portion.

FIGURE 45-δ-v4.—Vertical distribution of thermosteric anomaly, δ_x, (cl./t.) along 112° W. from 2°27′ N. to 2°29′ S., August 30-September 1, 1967. These data are part of a special series of observations made during the time interval indicated by the interrupted contours on figure 45-δ-v3.

FIGURE 45-G-v1.—Vertical distribution of the zonal component of geostrophic velocity (cm./sec.), relative to 500 db., along 119° W., August 3-21, 1967. Dark shading indicates eastward flow with a velocity greater than 5 cm./sec.; light shading indicates westward flow with a velocity greater than 5 cm./sec.

FIGURE 45-G-v2.—Vertical distribution of the meridional component of geostrophic velocity (cm./sec.), relative to 500 db., along 10° S., August 21-23, 1967. Dark shading indicates northward flow with a velocity greater than 5 cm./sec.; light shading indicates southward flow with a velocity greater than 5 cm./sec.

FIGURE 47-S-v2.—Vertical distribution of salinity (‰) along a northwest-southeast section in the central portion of the Panama Bight from Peninsula de Azuero, Panama, to the coast of Colombia, August 3-5, 1967. These contours are based on STD data read from analog traces.

FIGURE 47-S-v3.—Vertical distribution of salinity (‰) along 1°20′ N. from the coast of Colombia to 82° W., August 5, 1967. These contours are based on STD data read from analog traces.

FIGURE 47-S-v9.—Vertical distribution of salinity (‰) along the coasts of Costa Rica and Nicaragua from 85°52′ W., to 88°02′ W., August 30-31, 1967. These contours are based on STD data read from analog traces.

FIGURE 47-S-v4.—Vertical distribution of salinity (‰) along 82° W., August 5-12, 1967. These contours are based on STD data read from analog traces.

FIGURE 47-S-v6.—Vertical distribution of salinity (‰) along the coast of Peru from 9°22′ S. to 12°12′ S., August 13-16, 1967. These contours are based on STD data read from analog traces.

FIGURE 47-S-v5.—Vertical distribution of salinity (‰) along a southwest-northeast section from 10°09′ S., 82°09′ W. to the coast of Peru, August 12-13, 1967. These contours are based on STD data read from analog traces.

FIGURE 47-S-v7.—Vertical distribution of salinity (‰) along a northeast-southwest section from the coast of Peru to 15° S., 85° W., August 16-19, 1967. These contours are based on STD data read from analog traces.

FIGURE 47-S-v11.—Vertical distribution of salinity (‰) along 15° S., September 10-12, 1967. These contours are based on STD data read from analog traces.

FIGURE 47-S-v8.—Vertical distribution of salinity (‰) along 85° W., August 19-28, 1967. These contours are based on STD data read from analog traces.

FIGURE 47-S-v10.—Vertical distribution of salinity (‰) along 88° W., August 31-September 10, 1967. These contours are based on STD data read from analog traces.

FIGURE 47-S-v12.—Vertical distribution of salinity (‰) along 95° W., September 12-23, 1967. These contours are based on STD data read from analog traces.

Thermosteric anomaly and geostrophic velocity—Yellow pages

FIGURE 47-δ-v1.—Vertical distribution of thermosteric anomaly, δ_T, (cl./t.) across the northern portion of the Panama Bight from the coast of Colombia to Cabo Mala, Panama, August 1-2, 1967. These contours are based on STD data read from analog traces.

FIGURE 47-δ-v2.—Vertical distribution of thermosteric anomaly, δ_T, (cl./t.) along a northwest-southeast section in the central portion of the Panama Bight from Peninsula de Azuero, Panama, to the coast of Colombia, August 3-5, 1967. These contours are based on STD data read from analog traces.

FIGURE 47-δ-v3.—Vertical distribution of thermosteric anomaly, δ_T, (cl./t.) along 1°20′ N. from the coast of Colombia to 82° W., August 5, 1967. These contours are based on STD data read from analog traces.

FIGURE 47-δ-v9.—Vertical distribution of thermosteric anomaly, δ_T, (cl./t.) along the coasts of Costa Rica and Nicaragua from 85°52′ W. to 88°02′ W., August 30-31, 1967. These contours are based on STD data read from analog traces.

FIGURE 47-δ-v4.—Vertical distribution of thermosteric anomaly, δ_T, (cl./t.) along 82° W., August 5-12, 1967. These contours are based on STD data read from analog traces.

FIGURE 47-δ-v6.—Vertical distribution of thermosteric anomaly, δ_T, (cl./t.) along the coast of Peru from 9°22′ S. to 12°12′ S., August 13-16, 1967. These contours are based on STD data read from analog traces.

FIGURE 47-δ-v5.—Vertical distribution of thermosteric anomaly, δ_T, (cl./t.) along a southwest-northeast section from 10°09′ S., 82°09′ W. to the coast of Peru, August 12-13, 1967. These contours are based on STD data read from analog traces.

FIGURE 47-δ-v7.—Vertical distribution of thermosteric anomaly, δ_T, (cl./t.) along a northeast-southwest section from the coast of Peru to 15° S., 85° W., August 16-19, 1967. These contours are based on STD data read from analog traces.

FIGURE 47-δ-v11.—Vertical distribution of thermosteric anomaly, δ_T, (cl./t.) along 15° S., September 10-12, 1967. These contours are based on STD data read from analog traces.

FIGURE 47-δ-v8.—Vertical distribution of thermosteric anomaly, δ_T, (cl./t.) along 85° W., August 19-28, 1967. These contours are based on STD data read from analog traces.

FIGURE 47-δ-v10.—Vertical distribution of thermosteric anomaly, δ_T, (cl./t.) along 88° W., August 31-September 10, 1967. These contours are based on STD data read from analog traces.

FIGURE 47-δ-v12.—Vertical distribution of thermosteric anomaly, δ_T, (cl./t.) along 95° W., September 12-23, 1967. These contours are based on STD data read from analog traces.

FIGURE 47-G-v1.—Vertical distribution of the component of geostrophic velocity (cm./sec.), relative to 500 db., normal to a section across the northern portion of the Panama Bight from the coast of Colombia to Cabo Mala, Panama, August 1-2, 1967. The dark shading indicates flow toward the northeast with a velocity greater than 5 cm./sec.

FIGURE 47-G-v2.—Vertical distribution of the component of geostrophic velocity (cm./sec.), relative to 500 db., normal to a northwest-southeast section in the central portion of the Panama Bight from Peninsula de Azuero, Panama, to the coast of Colombia, August 3-5, 1967. Dark shading indicates flow toward the northeast with a velocity greater than 5 cm./sec.; light shading indicates flow toward the southwest with a velocity greater than 5 cm./sec.

FIGURE 47-G-v7.—Vertical distribution of the component of geostrophic velocity (cm./sec.), relative to 500 db., normal to a northeast-southwest section from the coast of Peru to 15° S., 85° W., August 16-19, 1967. The light shading indicates flow toward the northwest with a velocity greater than 5 cm./sec.

FIGURE 47-G-v4.—Vertical distribution of the zonal component of geostrophic velocity (cm./sec.), relative to 500 db., along 82° W., August 6-12, 1967. Dark shading indicates eastward flow with a velocity greater than 5 cm./sec.; light shading indicates westward flow with a velocity greater than 5 cm./sec.

FIGURE 47-G-v5.—Vertical distribution of the component of geostrophic velocity (cm./sec.), relative to 500 db., normal to a southwest-northeast section from 10°09′ S., 82°09′ W. to the coast of Peru, August 12-13, 1967. The light shading indicates flow toward the northwest with a velocity greater than 5 cm./sec.

FIGURE 47-G-v8.—Vertical distribution of the zonal component of geostrophic velocity (cm./sec.), relative to 500 db., along 85° W., August 19-28, 1967. Dark shading indicates eastward flow with a velocity greater than 5 cm./sec.; light shading indicates westward flow with a velocity greater than 5 cm./sec.

FIGURE 47-G-v10.—Vertical distribution of the zonal component of geostrophic velocity (cm./sce.), relative to 500 db., along 88° W., August 31-September 10, 1967. Dark shading indicates eastward flow with a velocity greater than 5 cm./sec.; light shading indicates westward flow with a velocity greater than 5 cm./sec.

FIGURE 47-G-v12.—Vertical distribution of the zonal component of geostrophic velocity (cm./sec.), relative to 500 db., along 95° W., September 12-22, 1967. Dark shading indicates eastward flow with a velocity greater than 5 cm./sec.; light shading indicates westward flow with a velocity greater than 5 cm./sec.

Oxygen—Green pages

FIGURE 47-O_2-v1.—Vertical distribution of oxygen (ml./l.) across the northern portion of the Panama Bight from the coast of Colombia to Cabo Mala, Panama, August 1-2, 1967.

FIGURE 47-O_2-v2.—Vertical distribution of oxygen (ml./l.) along a northwest-southeast section in the central portion of the Panama Bight from Peninsula de Azuero, Panama, to the coast of Colombia, August 3-4, 1967.

FIGURE 47-O_2-v7.—Vertical distribution of oxygen (ml./l.) along a northeast-southwest section from the coast of Peru to 15° S., 85° W., August 17-19, 1967.

FIGURE 47-O_2-v4.—Vertical distribution of oxygen (ml./l.) along 82° W., August 6-12, 1967.

FIGURE 47-O_2-v5.—Vertical distribution of oxygen (ml./l.) along a southwest-northeast section from 10°09′ S., 82°09′ W. to the coast of Peru, August 12, 1967.

FIGURE 47-O_2-v8.—Vertical distribution of oxygen (ml./l.) along 85° W., August 19-28, 1967.

FIGURE 47-O_2-v10.—Vertical distribution of oxygen (ml./l.) along 88° W., August 31-September 10, 1967.

FIGURE 47-O_2-v12.—Vertical distribution of oxygen (ml./l.) along 95° W., September 12-23, 1967.

FIGURE 47-UA-v4.—Vertical section of the atmosphere along 82° W., August 2-12, 1967. Solid lines are isotherms of air temperature (°C.). Dashed lines are isopleths of mixing ratio of the air (g./kg.). Surface air temperature is plotted above surface mixing ratio and below a base line representing the surface pressure (mb.). The computed height (m.) of each standard pressure surface is plotted for the northernmost radiosonde station of the section. At other stations the difference of computed height minus the corresponding height at the northern station is shown at each standard level.

FIGURE 47-UA-v8.—Vertical section of the atmosphere along 85° W., August 19-31, 1967. Solid lines are isotherms of air temperature (°C.). Dashed lines are isopleths of mixing ratio of the air (g./kg.). Surface air temperature is plotted above surface mixing ratio and below a base line representing the surface pressure (mb.). The computed height (m.) of each standard pressure surface is plotted for the northernmost radiosonde station of the section. At other stations the difference of computed height minus the corresponding height at the northern station is shown at each standard level.

FIGURE 47-UA-v10.—Vertical section of the atmosphere along 88° W., August 31-September 11, 1967. Solid lines are isotherms of air temperature (°C.). Dashed lines are isopleths of mixing ratio of the air (g./kg.). Surface air temperature is plotted above surface mixing ratio and below a base line representing the surface pressure (mb.). The computed height (m.) of each standard pressure surface is plotted for the northernmost radiosonde station of the section. At other stations the difference of computed height minus the corresponding height at the northern station is shown at each standard level.

FIGURE 47-UA-v12.—Vertical section of the atmosphere along 95° W., September 12-22, 1967. Solid lines are isotherms of air temperature (°C.). Dashed lines are isopleths of mixing ratio of the air (g./kg.). Surface air temperature is plotted above surface mixing ratio and below a base line representing the surface pressure (mb.). The computed height (m.) of each standard pressure surface is plotted for the northernmost radiosonde station of the section. At other stations the difference of computed height minus the corresponding height at the northern station is shown at each standard level.

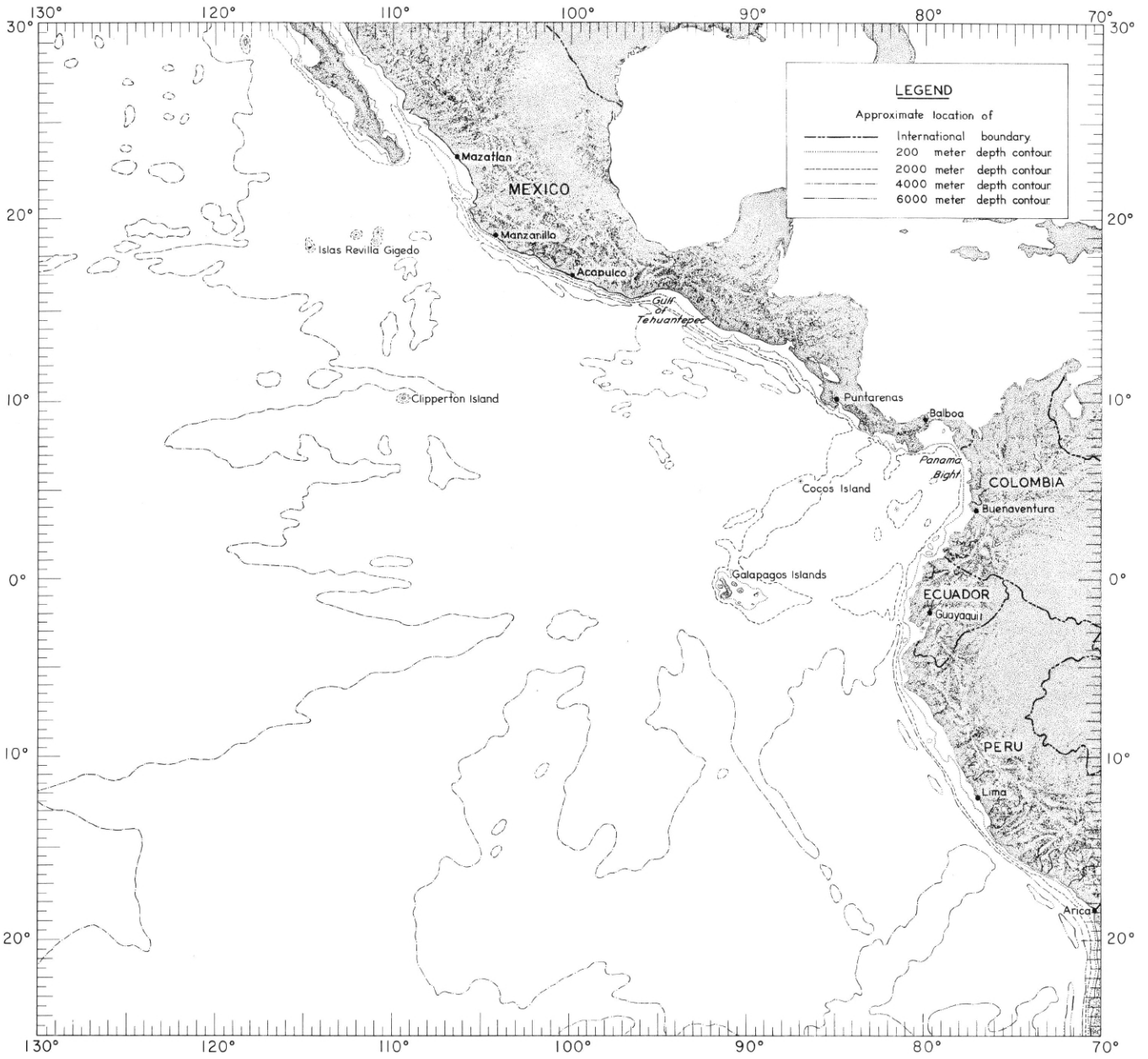

RM-a.

FIGURE RM-a. — Reference map of the main portion of the EASTROPAC area. The topographic shading and bathymetric contours are approximate only and should not be considered as portraying the latest available information.

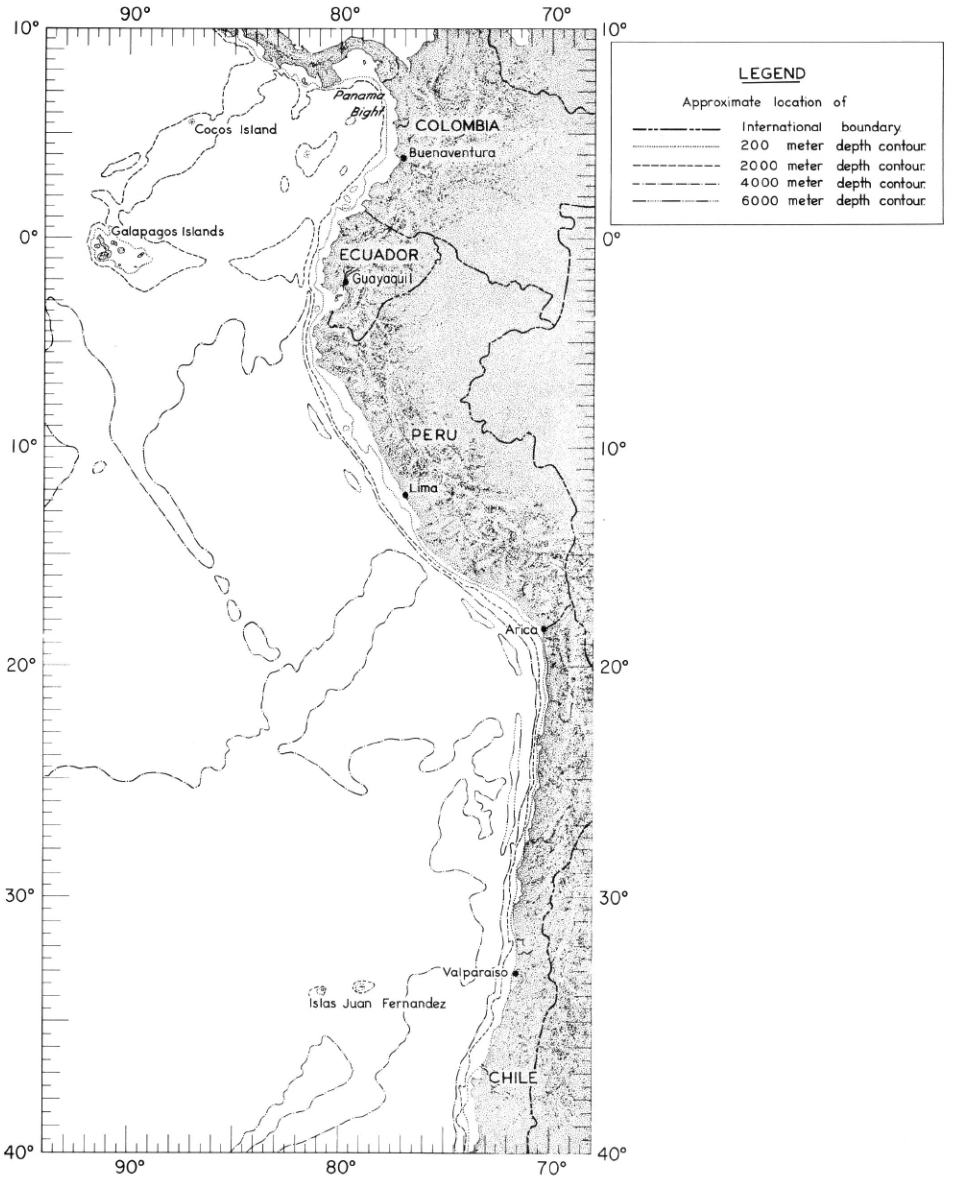

FIGURE RM-b — Reference map of the southern coastal portion of the EASTROPAC area. The topographic shading and bathymetric contours are approximate only and should not be considered as portraying the latest available information.

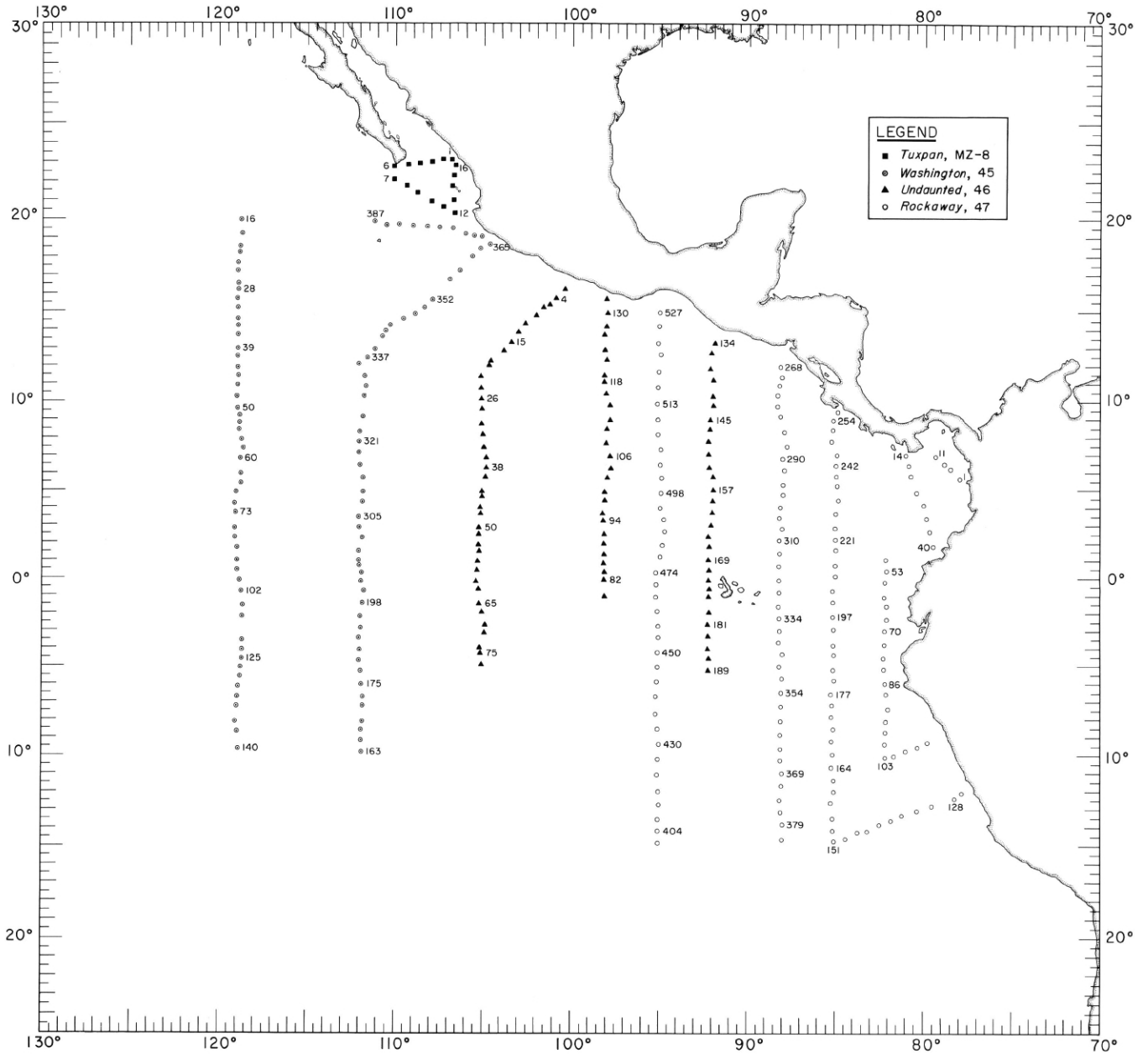

40-TC-a.

FIGURE 40-TC-a. — Locations of stations occupied by participating ships in the main portion of the EASTROPAC area during the second survey period, August-September 1967.

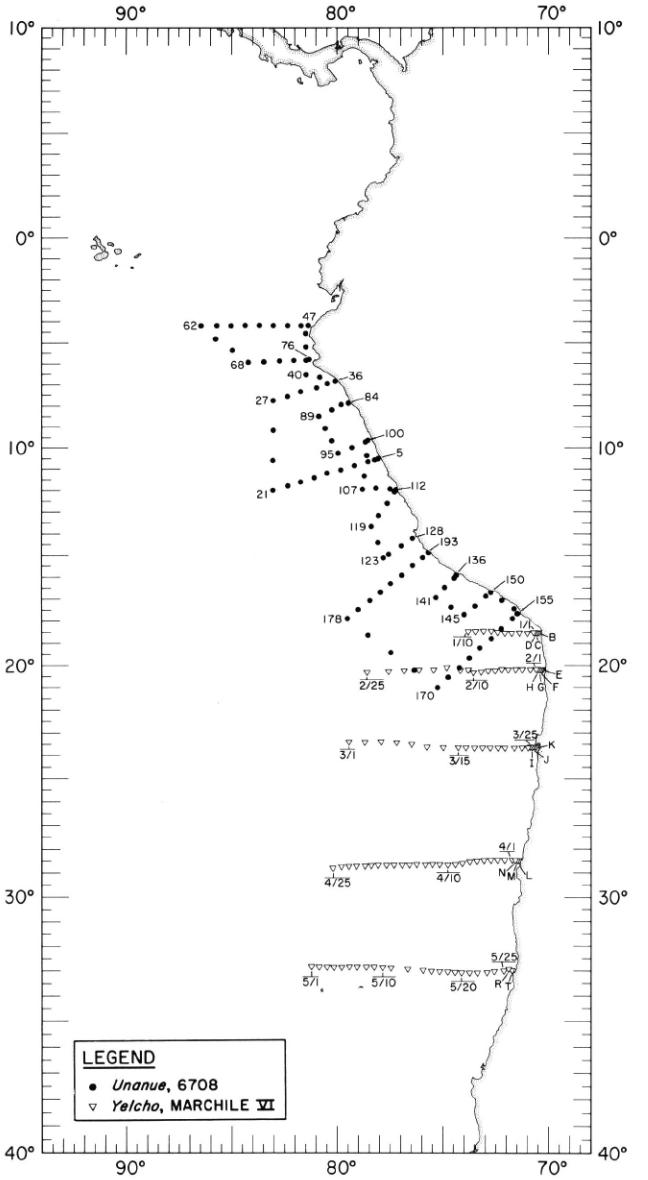

40-TC-b.

FIGURE 40-TC-b. — Locations of stations occupied by participating ships in the southern coastal portion of the EASTROPAC area during the second survey period, August-September 1967.

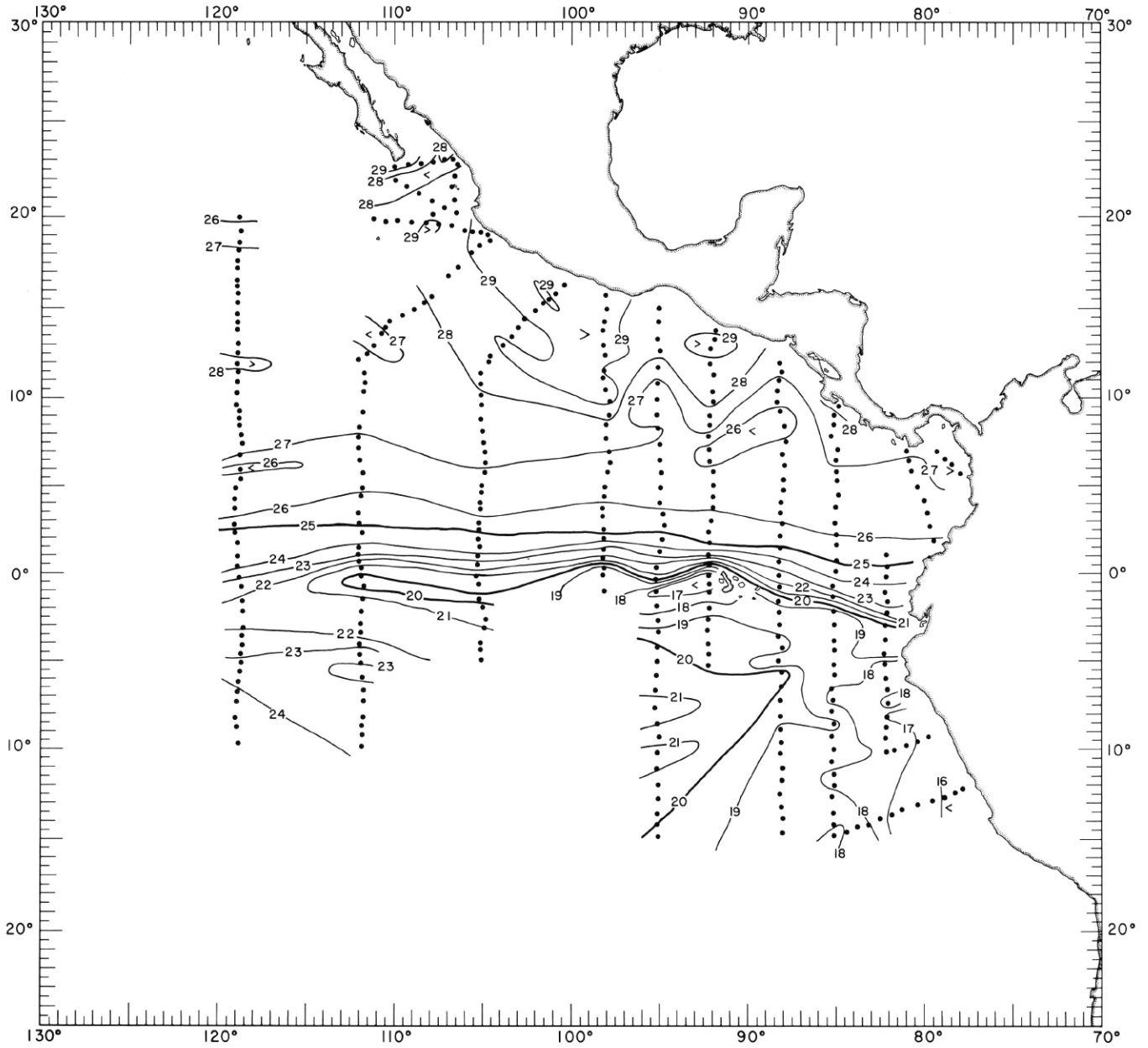

FIGURE 40-T-s(a).—Temperature (°C.) at the sea surface in the main portion of the EASTROPAC area, August-September 1967. These contours are based on Nansen cast data.

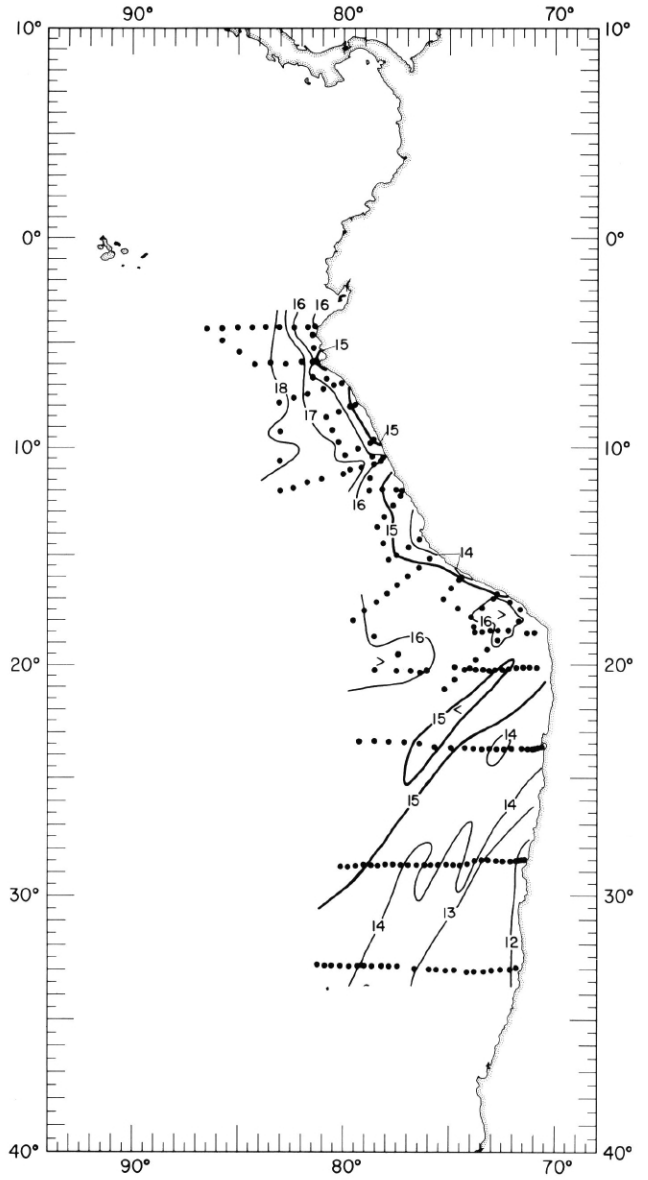

40-T-s(b).

FIGURE 40-T-s(b).—Temperature (°C.) at the sea surface in the southern coastal portion of the EASTROPAC area, August-September 1967. These contours are based on Nansen cast data.

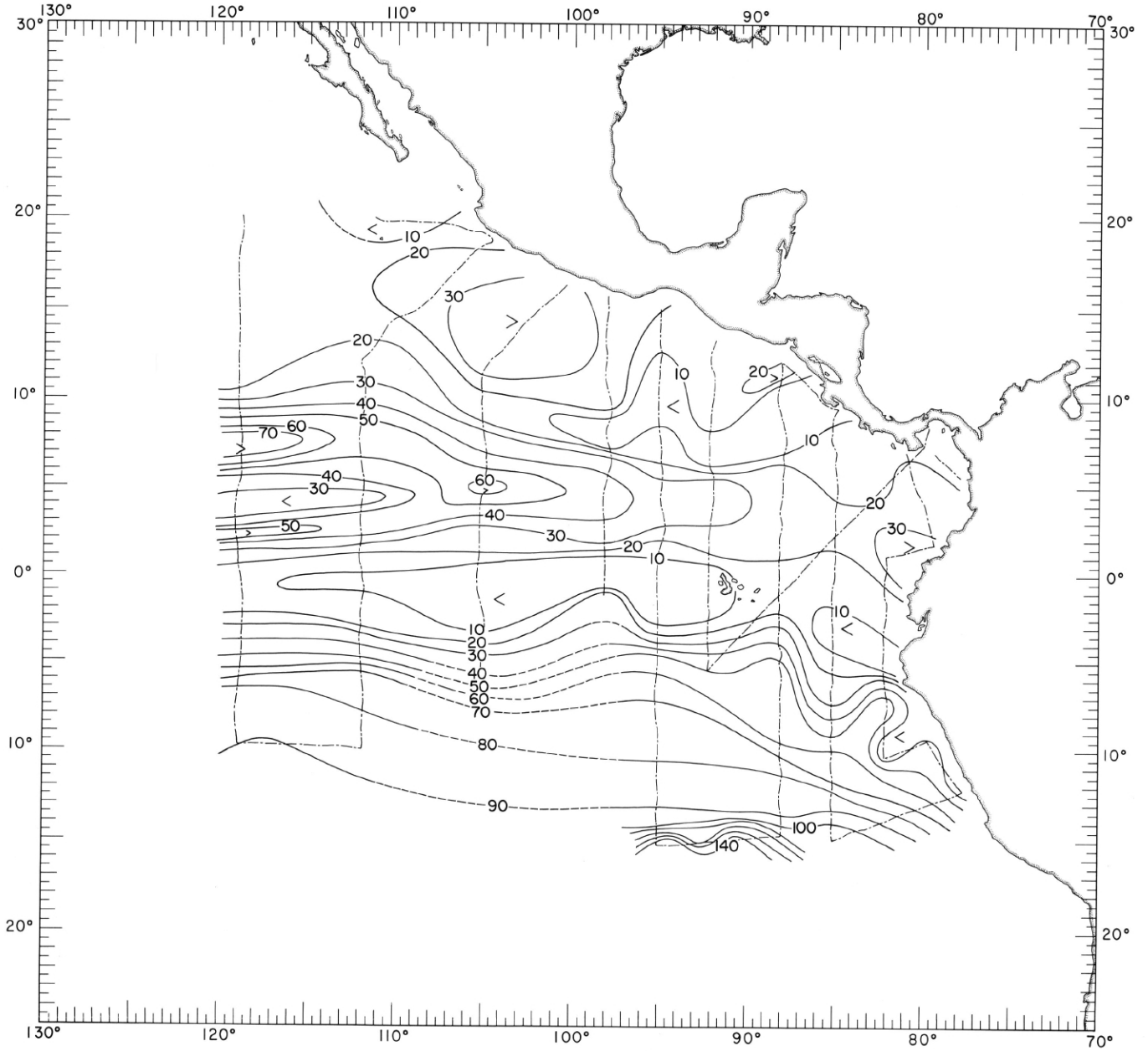

40-ML.

FIGURE 40-ML.—Thickness of the mixed layer in meters, August-September 1967. Dashed lines indicate portions of the cruise tracks where such data were collected.

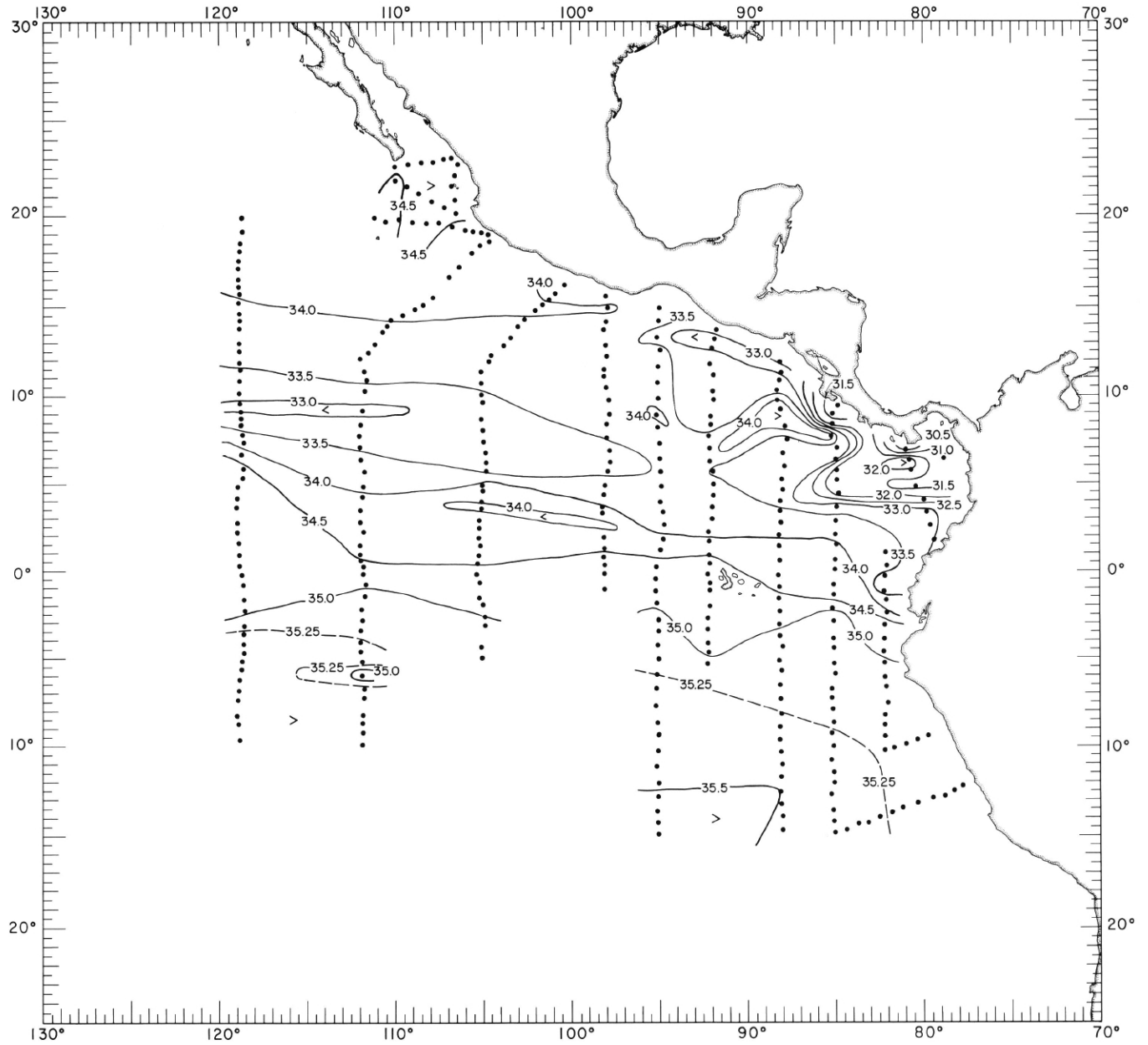

FIGURE 40-S-s(a).—Salinity (‰) at the sea surface in the main portion of the EASTROPAC area, August-September 1967. These contours are based on Nansen cast data.

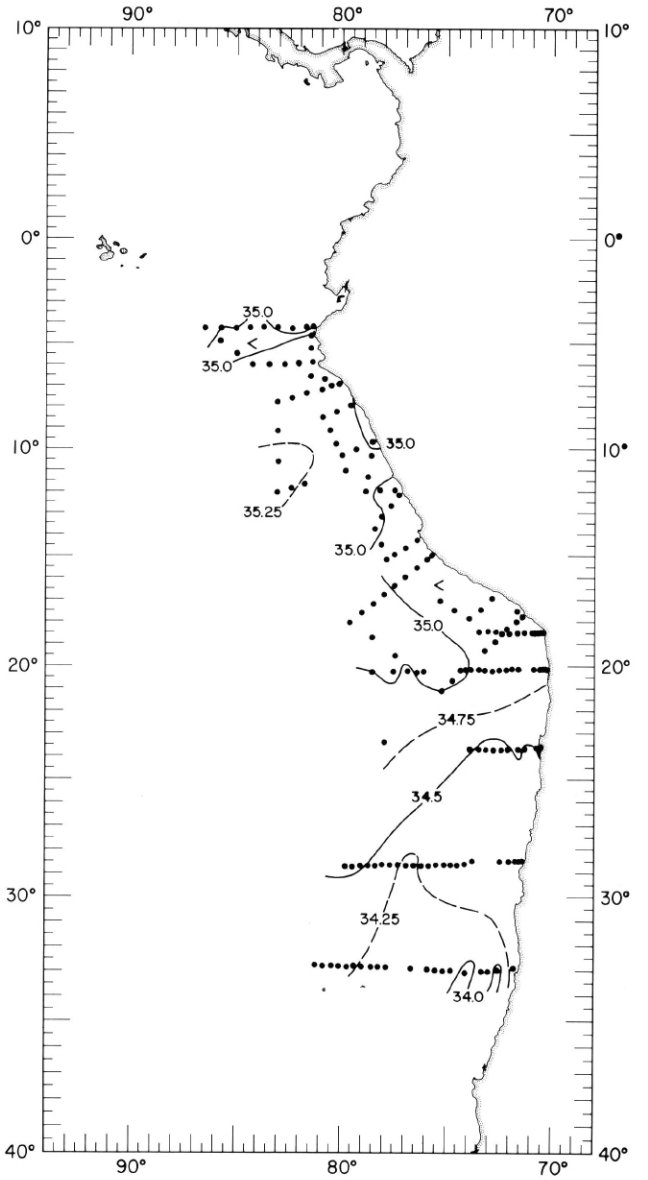

FIGURE 40-S-s(b).—Salinity (‰) at the sea surface in the southern coastal portion of the EASTROPAC area, August-September 1967. These contours are based on Nansen cast data.

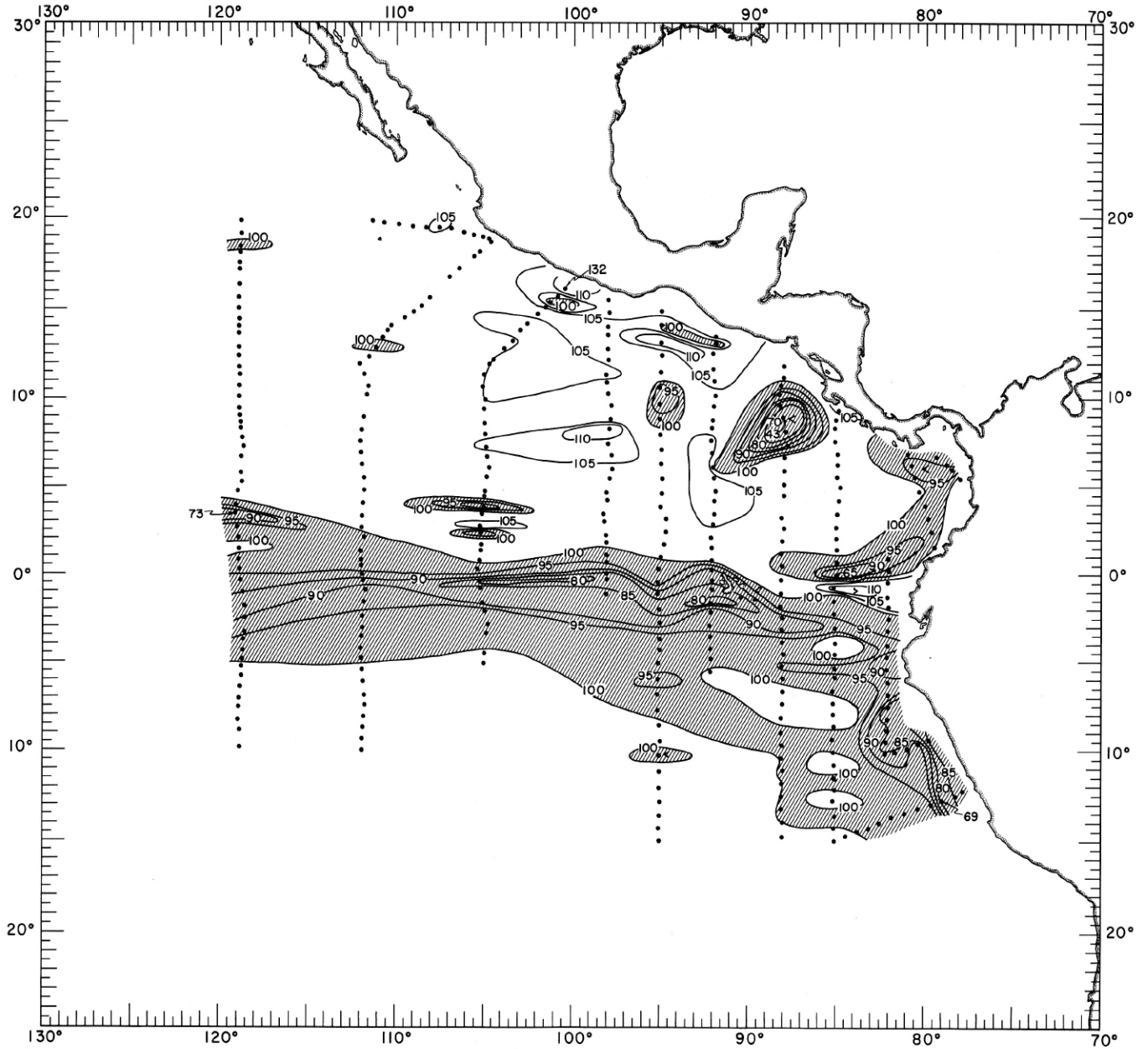

FIGURE 40-O2Sa-10.—Oxygen saturation (%) at 10 meters, August-September 1967. Areas with less than 100% saturation are shaded.

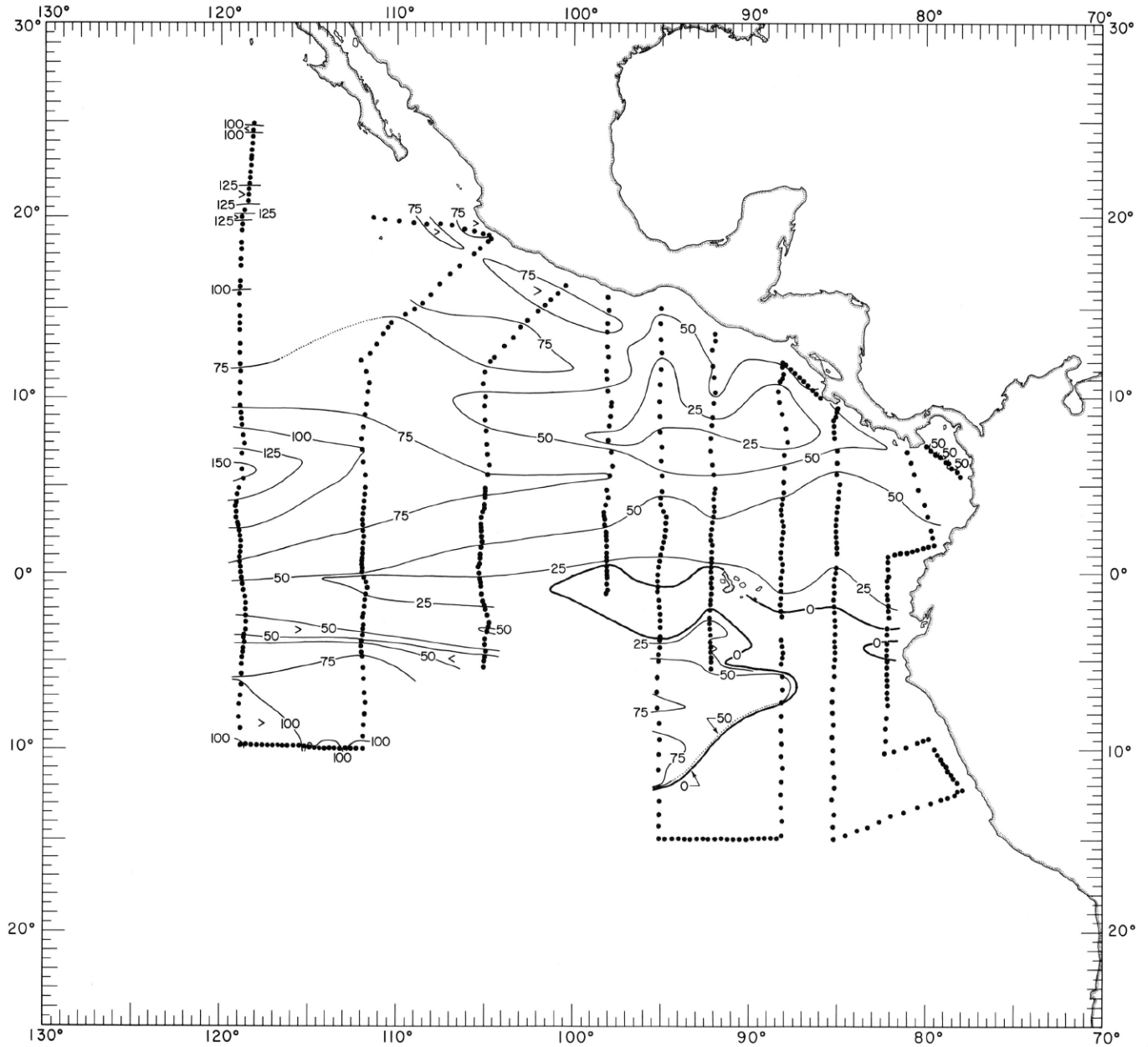

FIGURE 40-δ300-z.—Depth (m.) of the surface where $\delta_T = 300$ cl./t., August-September 1967. The zero contours indicate the intersections of this surface with the sea surface.

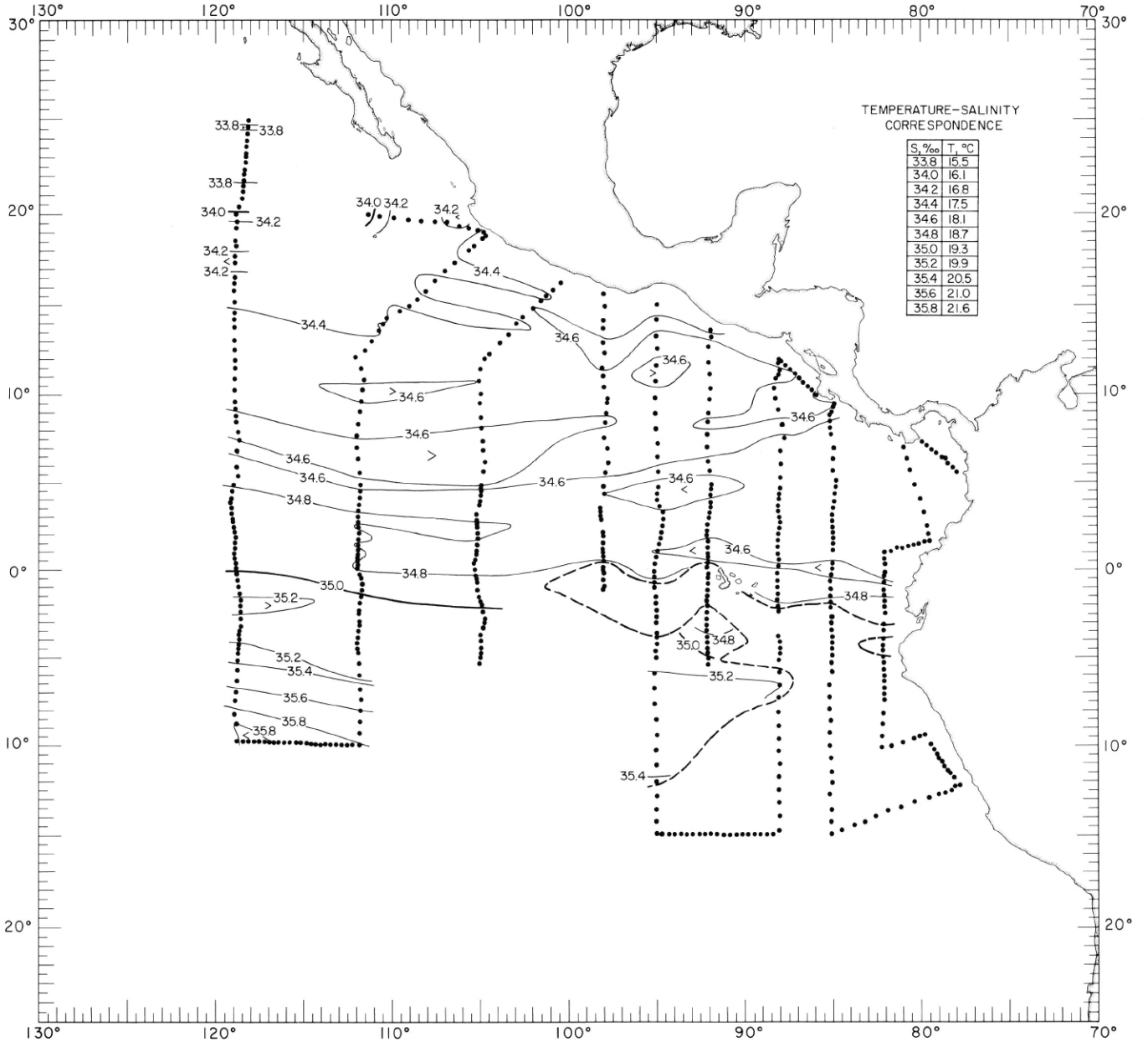

FIGURE 40-S-δ300.—Salinity (‰) on the surface where $\delta_T = 300$ cl./t., August-September 1967. The heavy dashed lines indicate the intersections of this surface with the sea surface. The table shows the temperature corresponding to each isohaline on the chart.

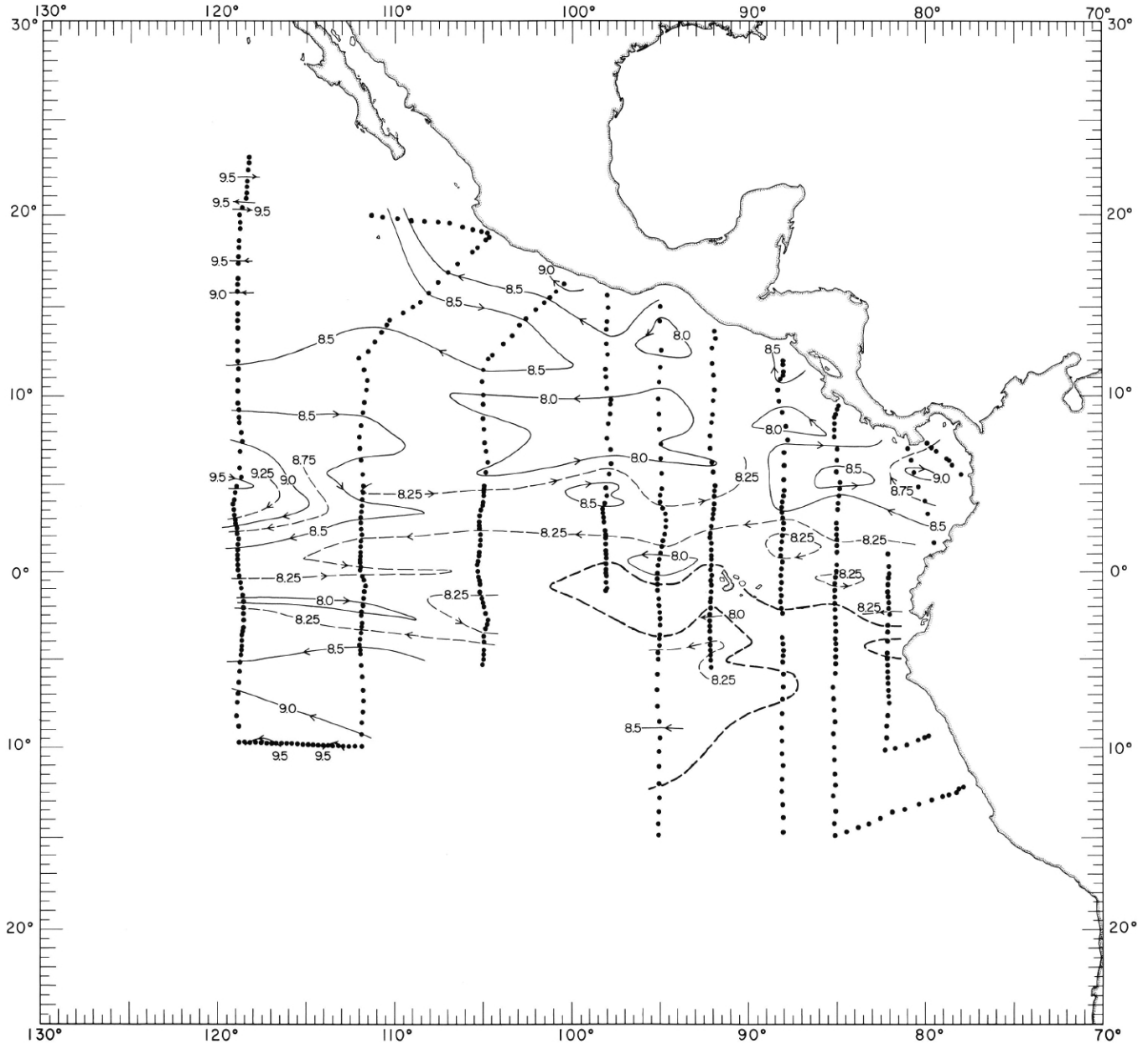

40-AP-δ300.

FIGURE 40-AP-δ300.—Acceleration potential (j./kg.), relative to 500 db., on the surface where $\delta_T = 300$ cl./t., August-September 1967. The heavy dashed lines indicate the intersections of this surface with the sea surface. For computing acceleration potential, thermosteric anomaly, δ_T, was used instead of specific volume anomaly, δ.

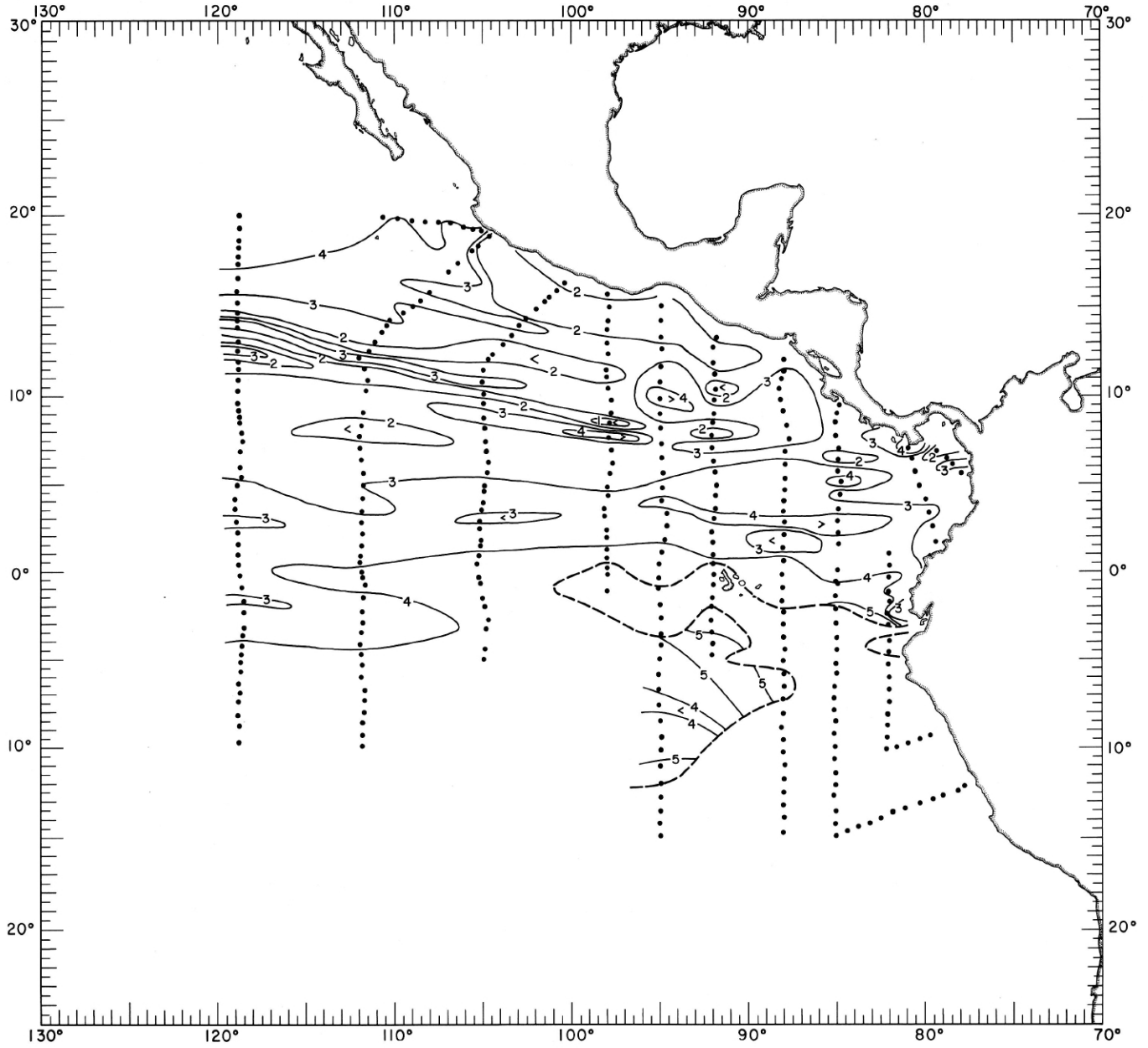

FIGURE 40-O_2-δ300.—Oxygen (ml./l.) on the surface where $\delta_T = 300$ cl./t., August-September 1967. The heavy dashed lines indicate the intersections of this surface with the sea surface.

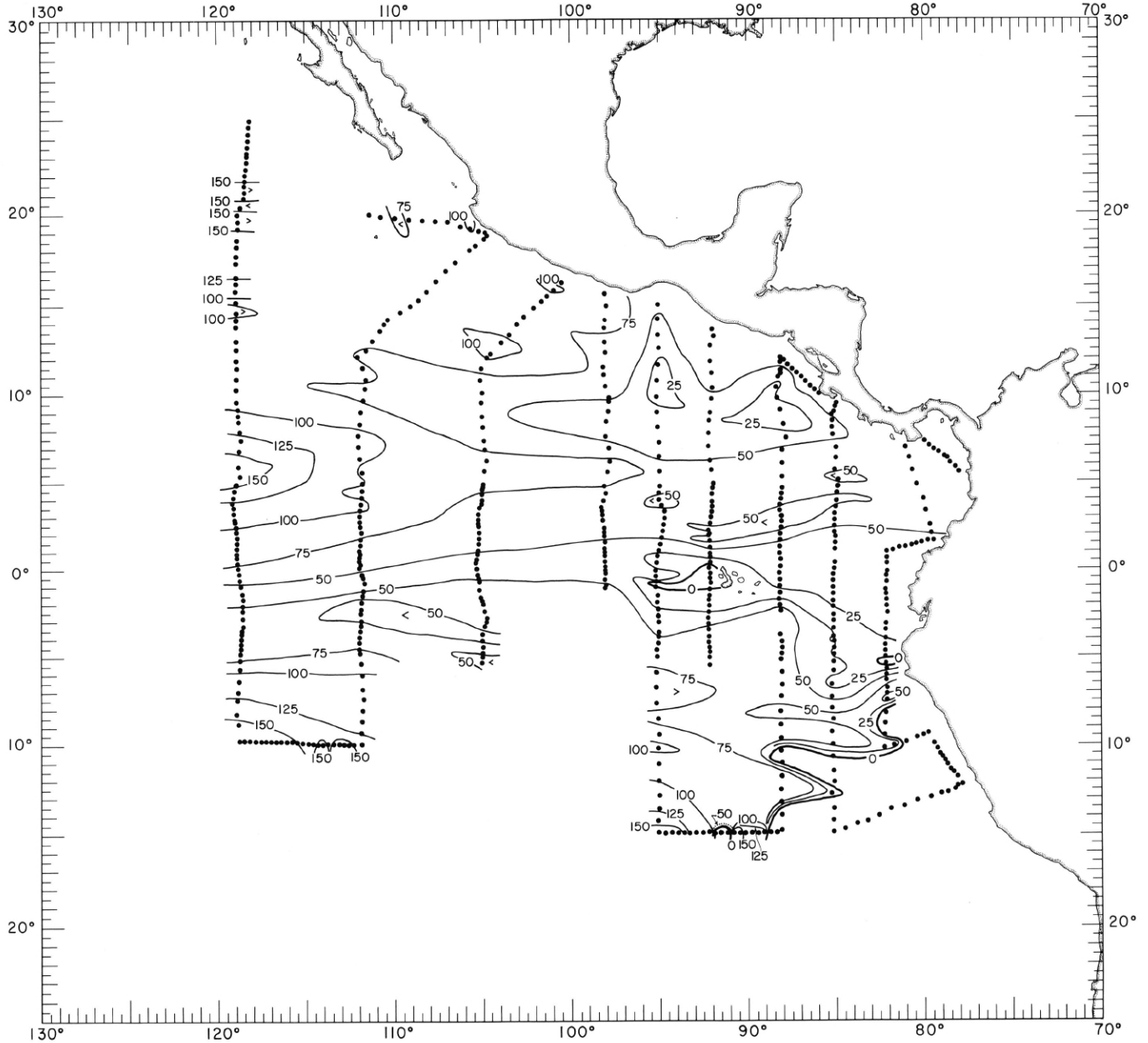

FIGURE 40-δ250-z.—Depth (m.) of the surface where $\delta_T = 250$ cl./t., August-September 1967. The zero contours indicate the intersections of this surface with the sea surface.

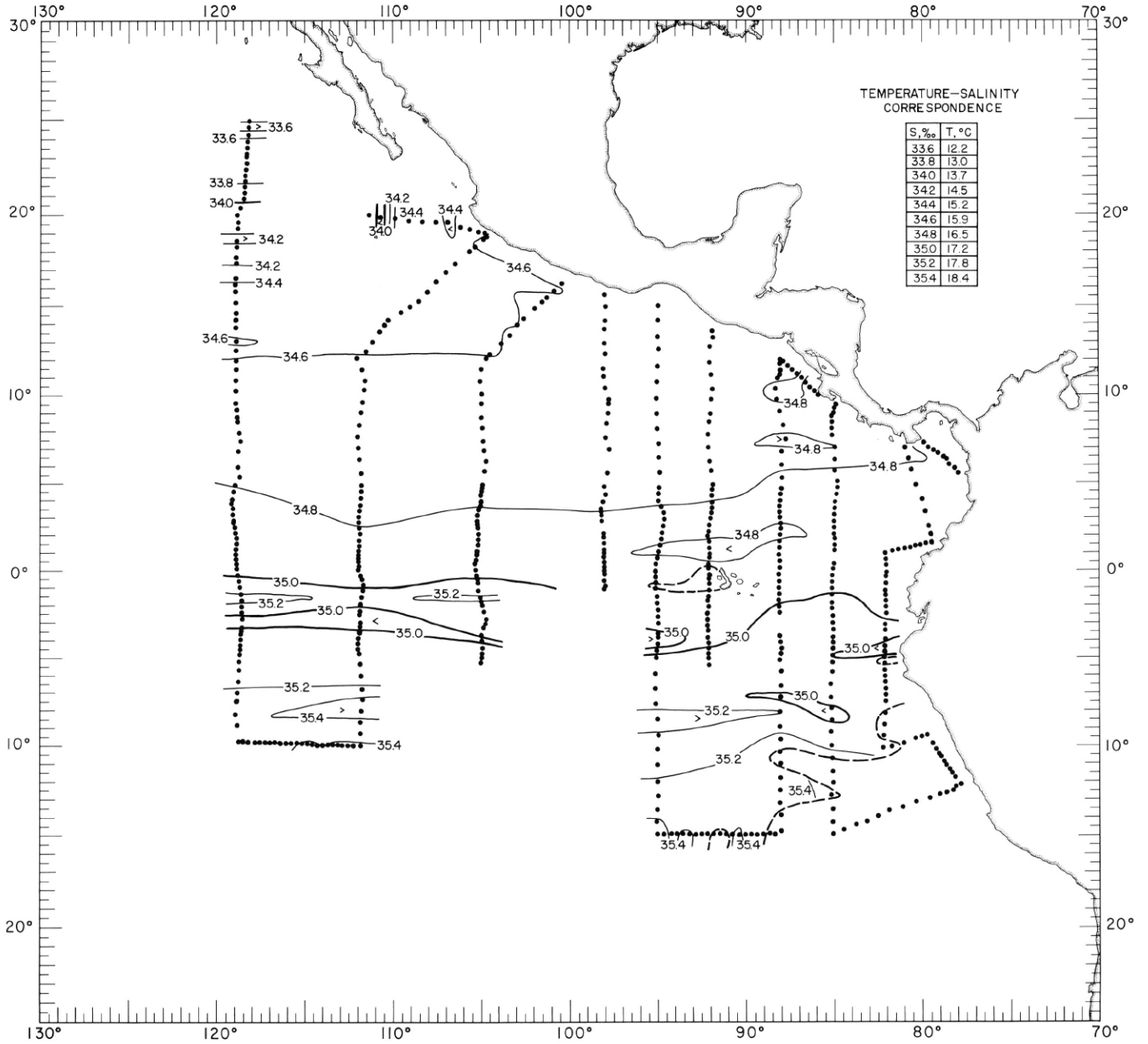

40-S-δ250.

FIGURE 40-S-δ250.—Salinity (‰) on the surface where $\delta_T = 250$ cl./t., August-September 1967. The heavy dashed lines indicate the intersections of this surface with the sea surface. The table shows the temperature corresponding to each isohaline on the chart.

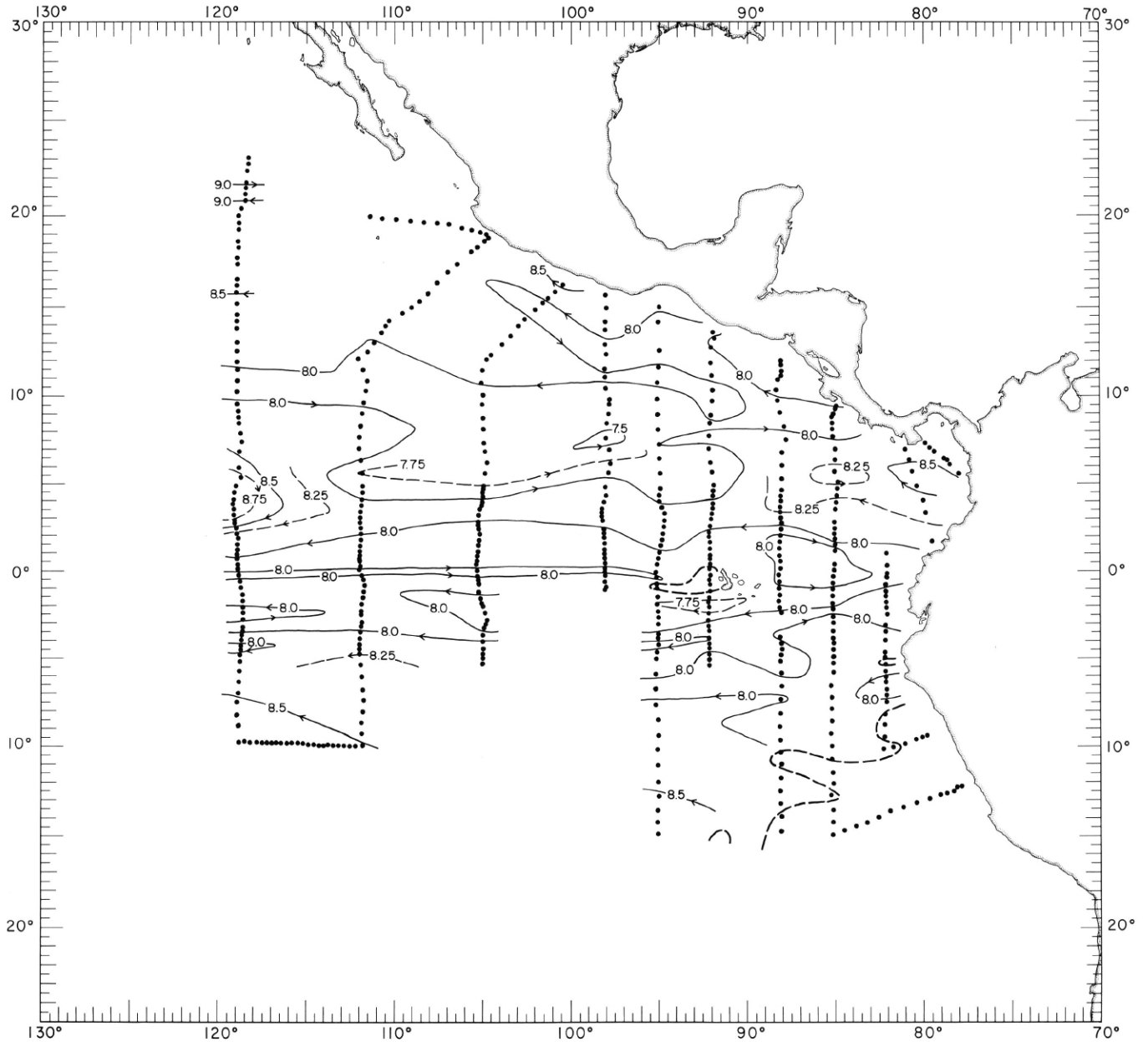

FIGURE 40-AP-δ250.—Acceleration potential (j./kg.), relative to 500 db., on the surface where $\delta_T = 250$ cl./t., August-September 1967. The heavy dashed lines indicate the intersections of this surface with the sea surface. For computing acceleration potential, thermosteric anomaly, δ_T, was used instead of specific volume anomaly, δ.

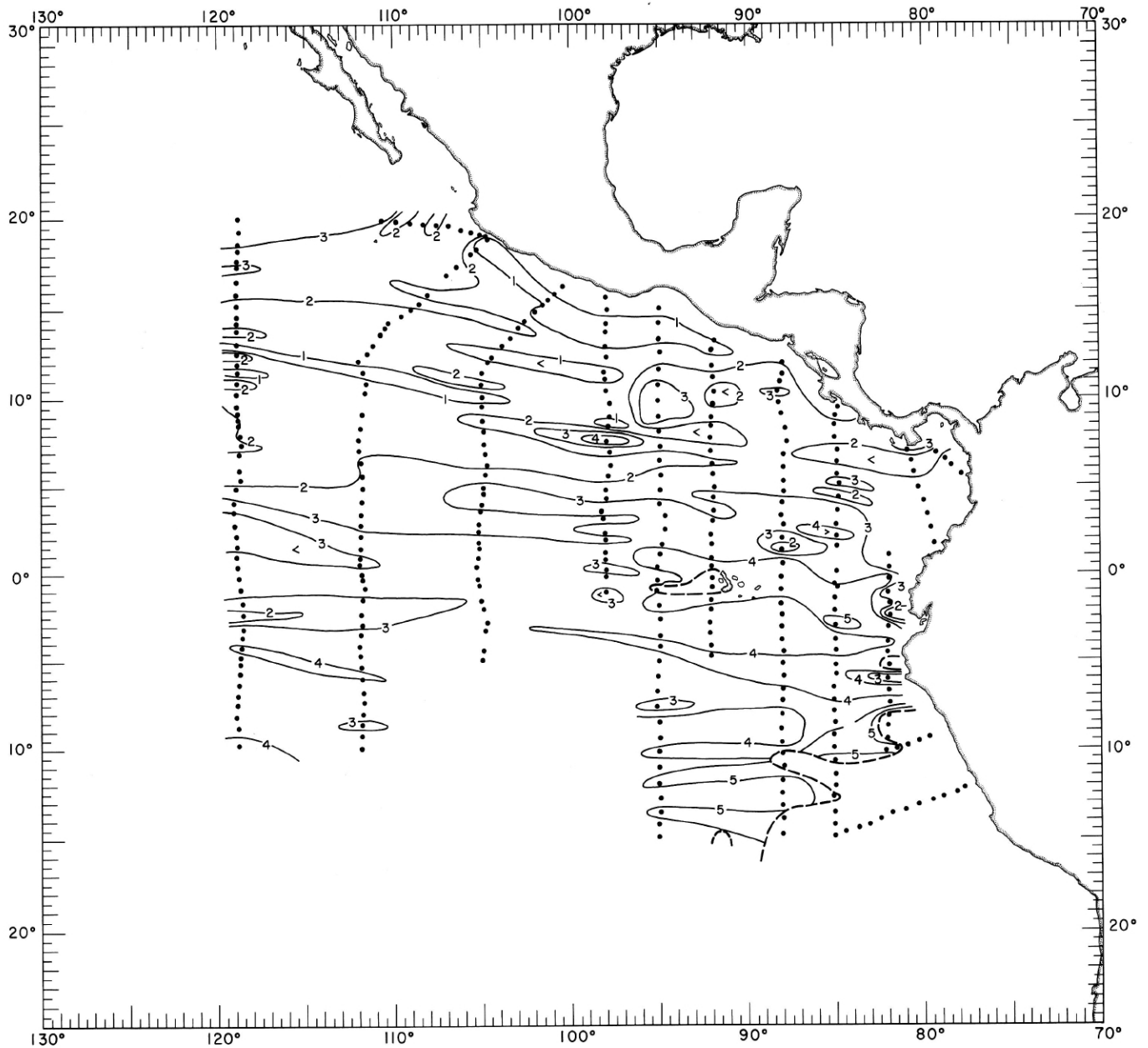

40-O_2-δ250.

FIGURE 40-O_2-δ250.—Oxygen (ml./l.) on the surface where $\delta_T = 250$ cl./t., August-September 1967. The heavy dashed lines indicate the intersections of this surface with the sea surface.

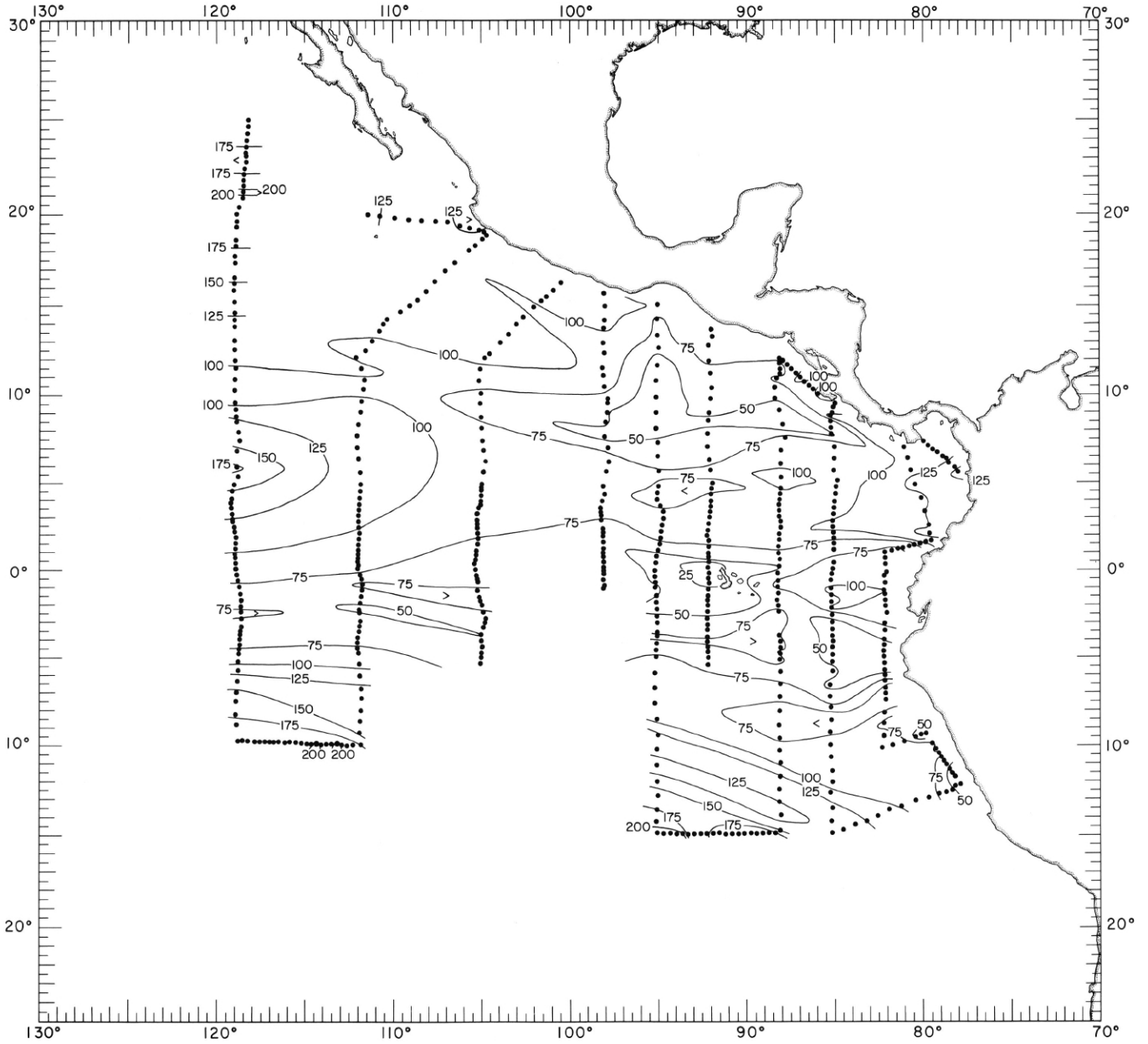

40-δ200-z.

FIGURE 40-δ200-z.—Depth (m.) of the surface where δ_T = 200 cl./t., August-September 1967.

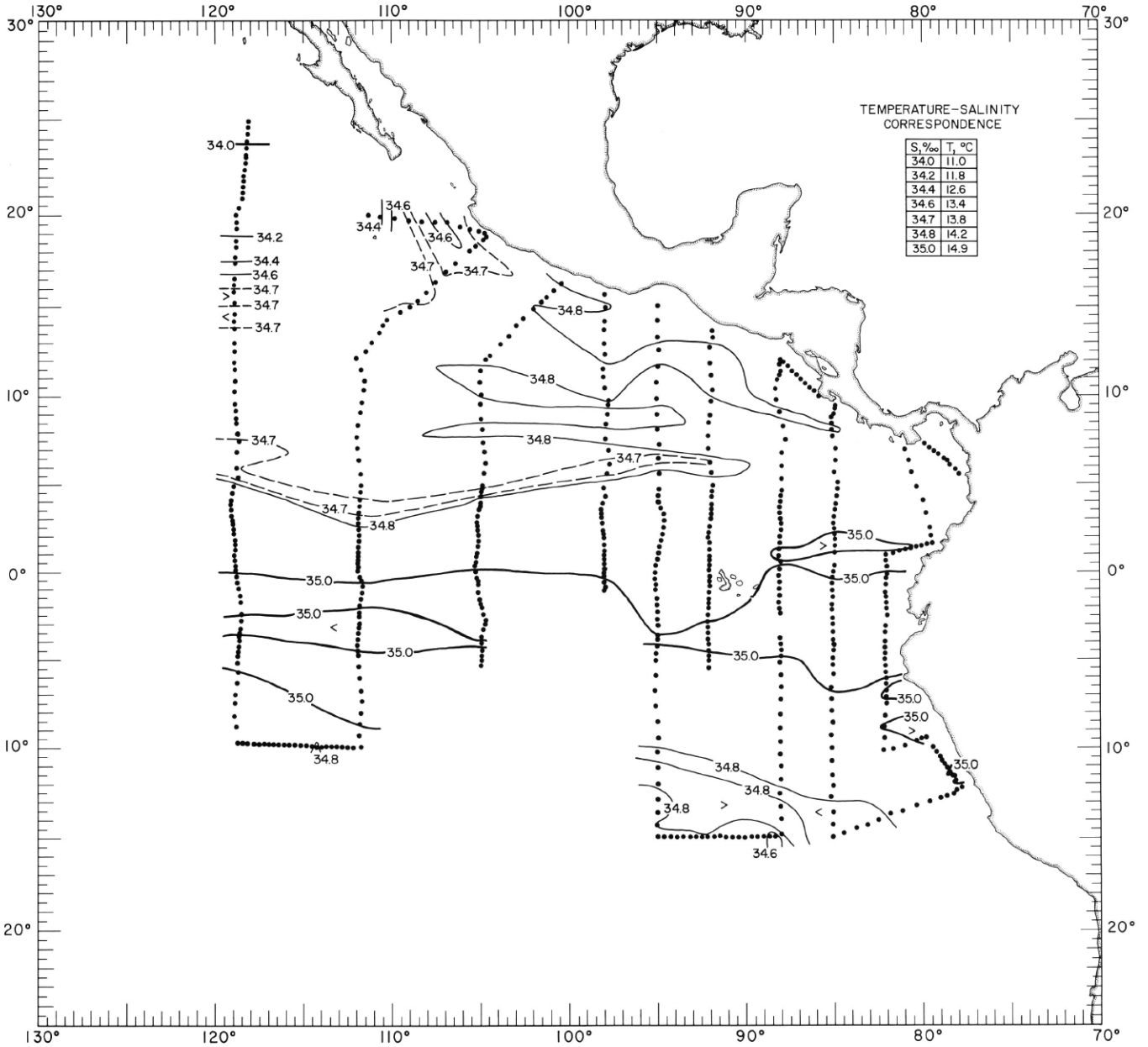

40-S-δ200.

FIGURE 40-S-δ200.—Salinity (‰) on the surface where $\delta_T = 200$ cl./t., August-September 1967. The table shows the temperature corresponding to each isohaline on the chart.

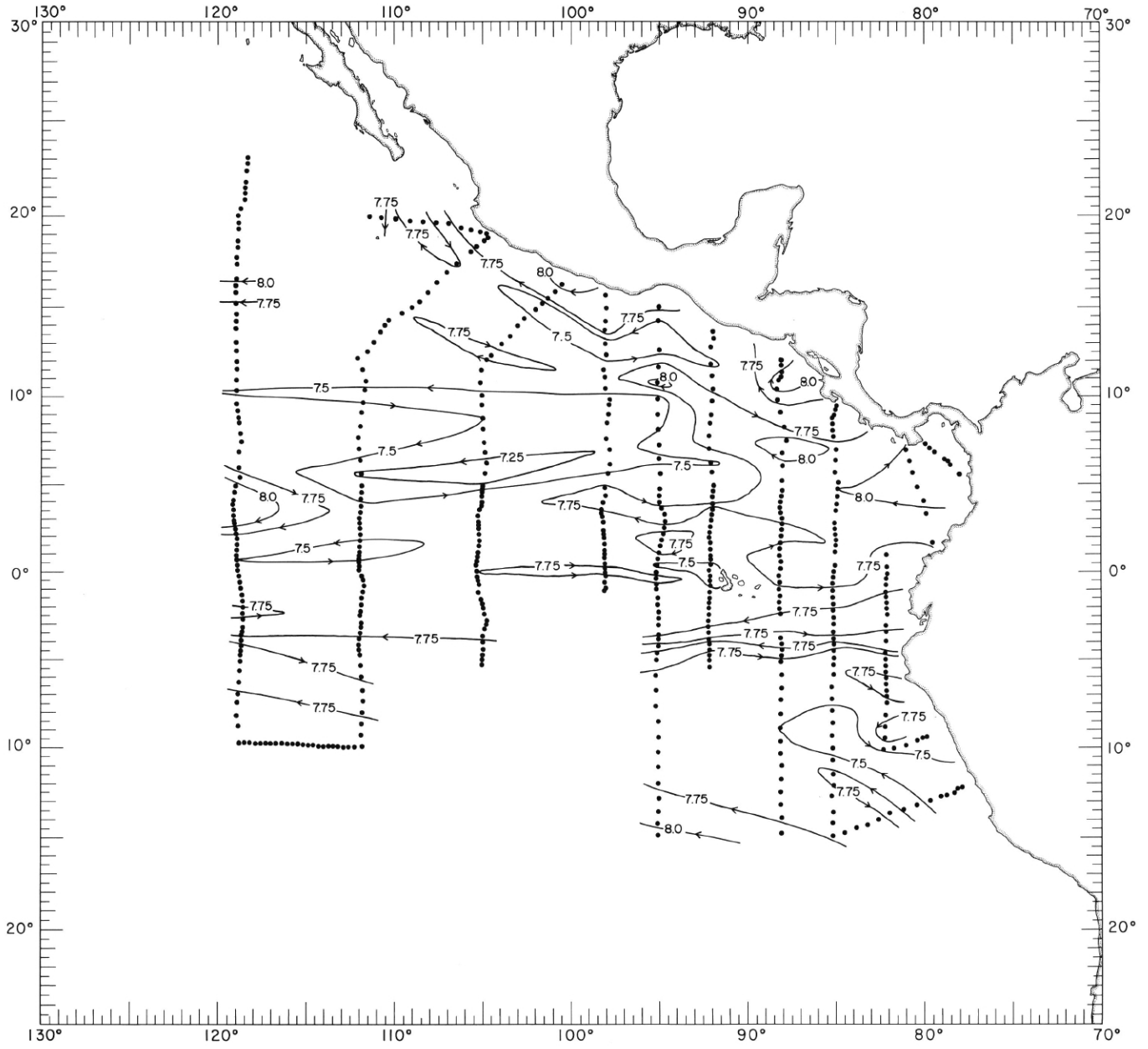

FIGURE 40-AP-δ200.—Acceleration potential (j./kg.), relative to 500 db., on the surface where $\delta_T = 200$ cl./t., August-September 1967. For computing acceleration potential, thermosteric anomaly, δ_T, was used instead of specific volume anomaly, δ.

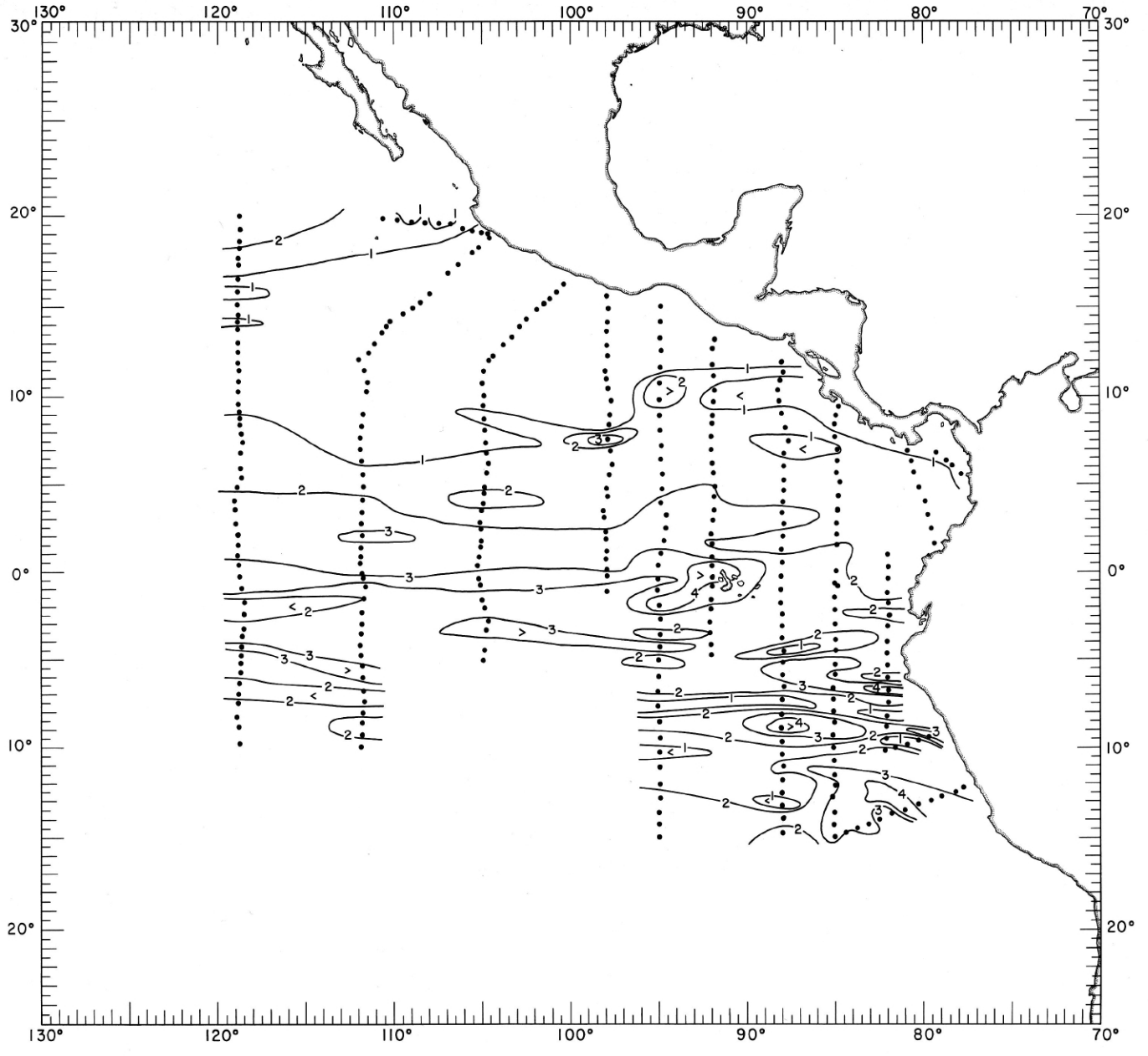

FIGURE 40-O2-δ200.—Oxygen (ml./l.) on the surface where $\delta_T = 200$ cl./t., August-September 1967.

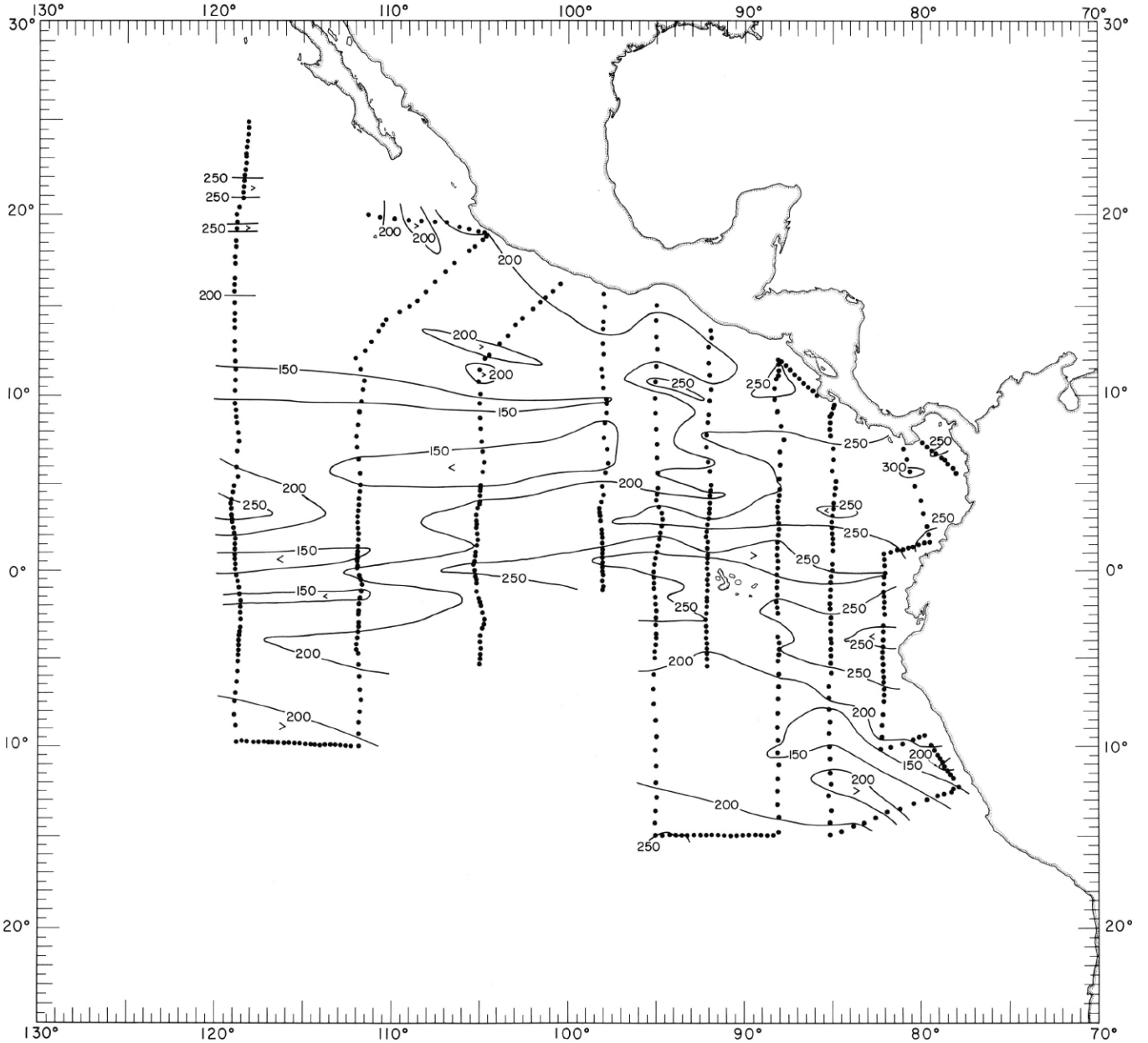

40-δ160-z.

FIGURE 40-δ160-z.—Depth (m.) of the surface where $\delta_T = 160$ cl./t., August-September 1967.

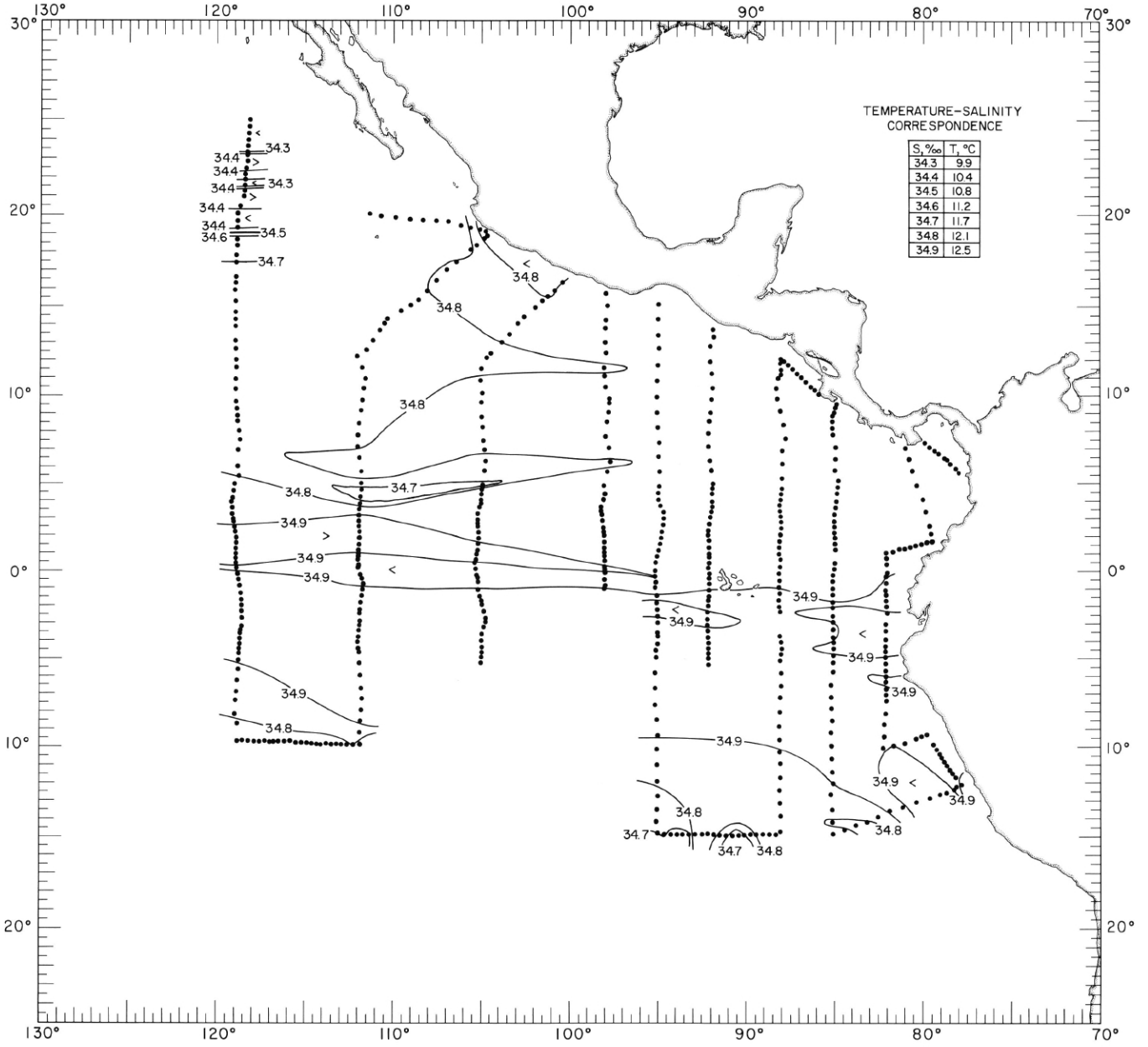

40-S-δ160.

FIGURE 40-S-δ160.—Salinity (‰) on the surface where $\delta_T = 160$ cl./t., August-September 1967. The table shows the temperature corresponding to each isohaline on the chart.

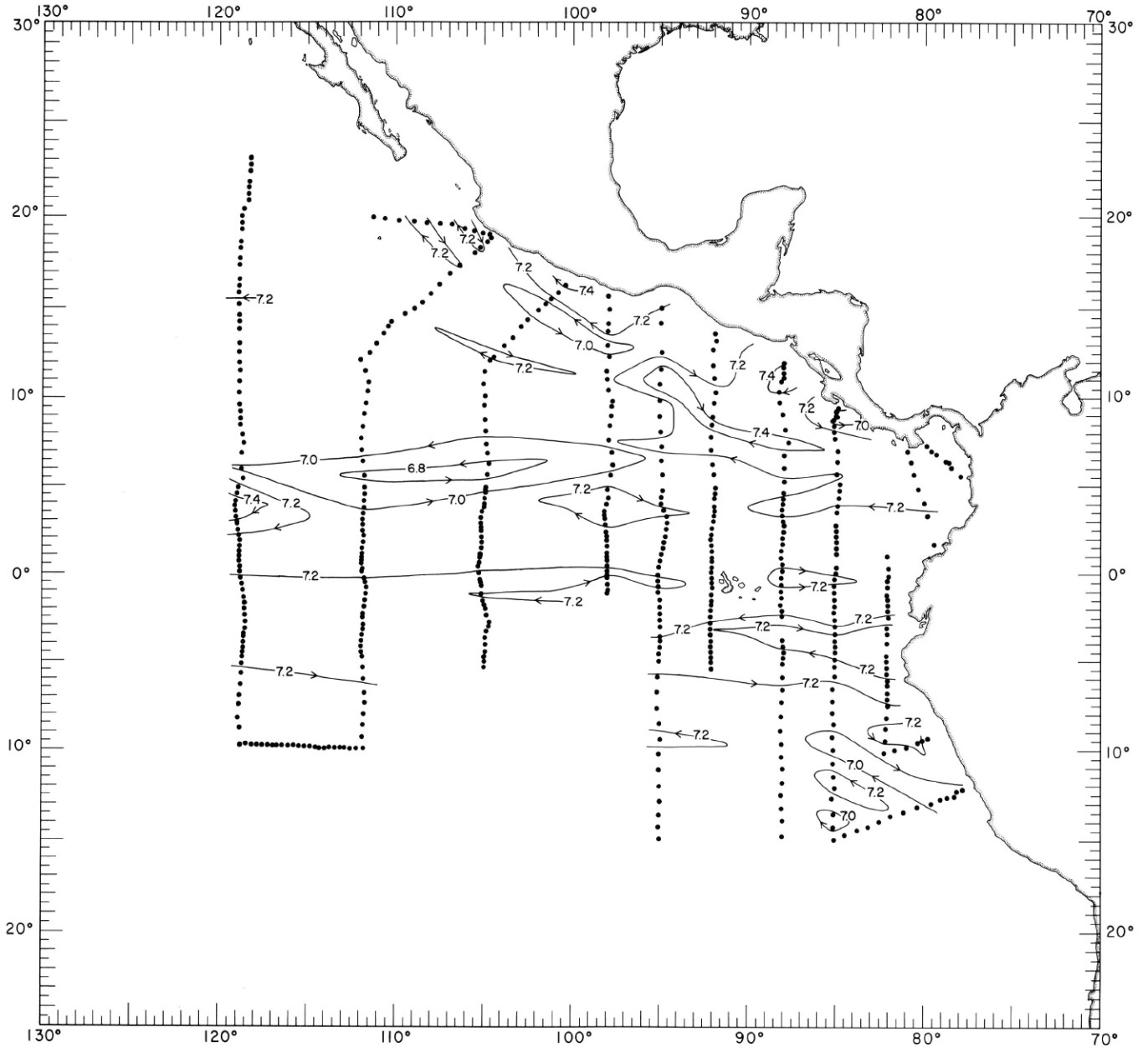

FIGURE 40-AP-δ160.—Acceleration potential (j./kg.), relative to 500 db., on the surface where $\delta_T = 160$ cl./t., August-September 1967. For computing acceleration potential, thermosteric anomaly, δ_T, was used instead of specific volume anomaly, δ.

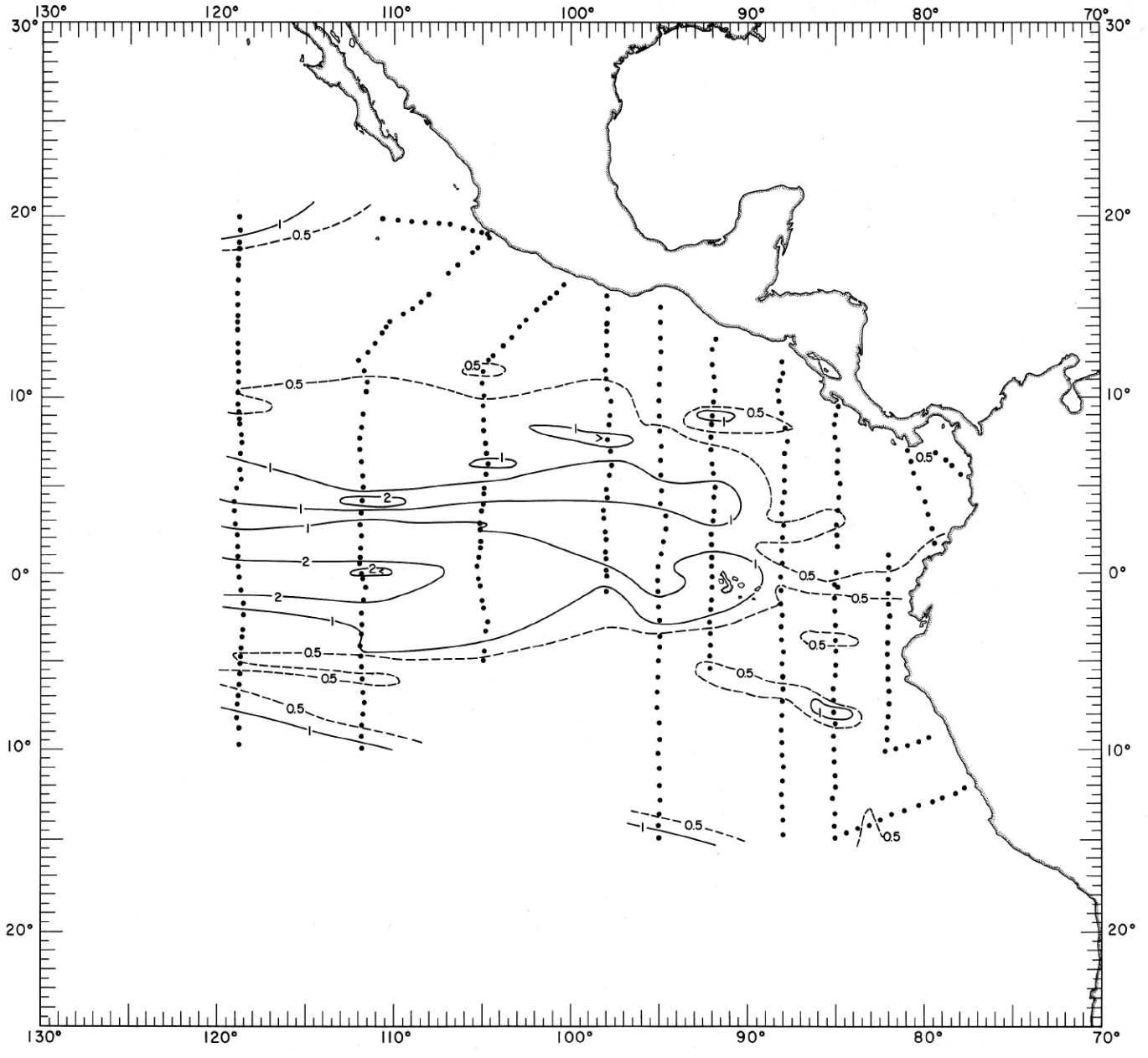

FIGURE 40-O2-δ160.—Oxygen (ml./l.) on the surface where $\delta_T = 160$ cl./t., August-September 1967.

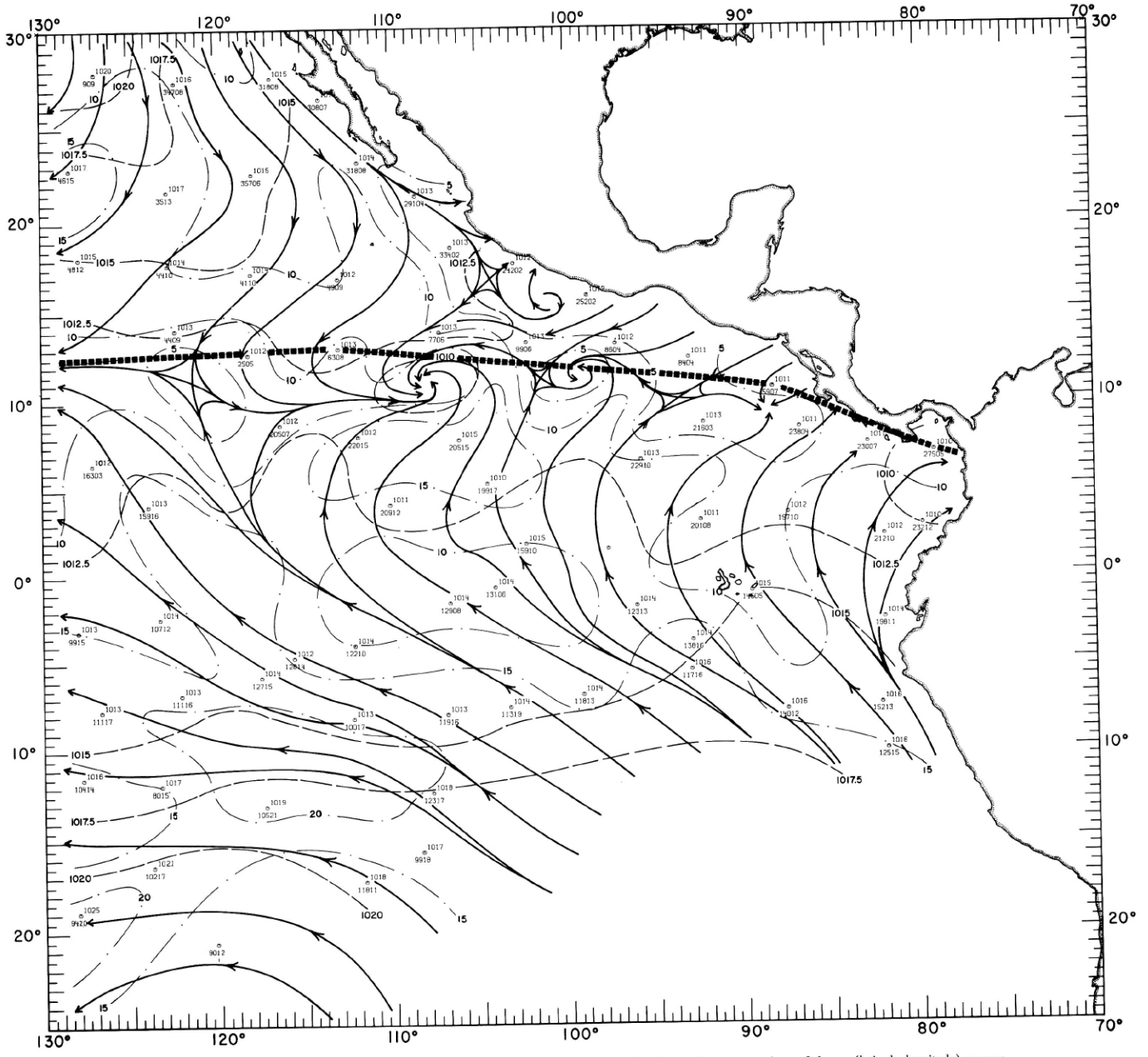

40-MW-1.

FIGURE 40-MW-1.—Analyses of the surface air pressure and surface winds from all available ship observations, averaged over 2-degree (latitude-longitude) squares for the period August 1-12, 1967. Heavy dashed lines are isobars. Solid lines are streamlines showing the mean resultant direction of wind flow. Light dash-dot lines are isotachs indicating mean resultant wind speed (kn.). Pressure (mb.) averaged for 5-degree squares is plotted above the mean position of the square, and resultant wind direction followed by speed (kn.) is plotted below. The monthly climatological position of the intertropical convergence zone is shown by a wide dashed band.

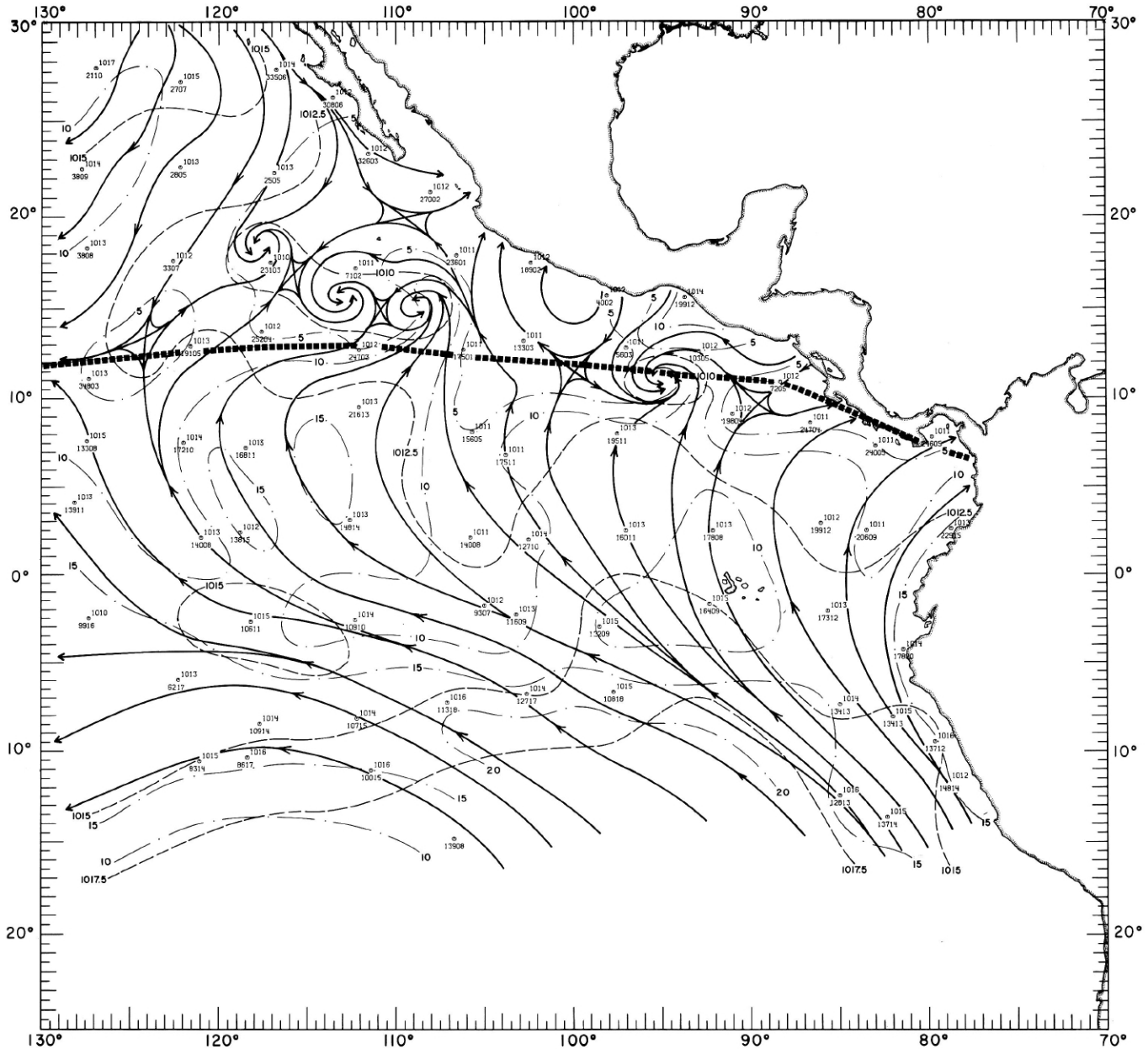

FIGURE 40-MW-2.—Analyses of the surface air pressure and surface winds from all available ship observations, averaged over 2-degree (latitude-longitude) squares for the period August 13-26, 1967. Heavy dashed lines are isobars. Solid lines are streamlines showing the mean resultant direction of wind flow. Light dash-dot lines are isotachs indicating mean resultant wind speed (kn.). Pressure (mb.) averaged for 5-degree squares is plotted above the mean position of the square, and resultant wind direction followed by speed (kn.) is plotted below. The monthly climatological position of the intertropical convergence zone is shown by a wide dashed band.

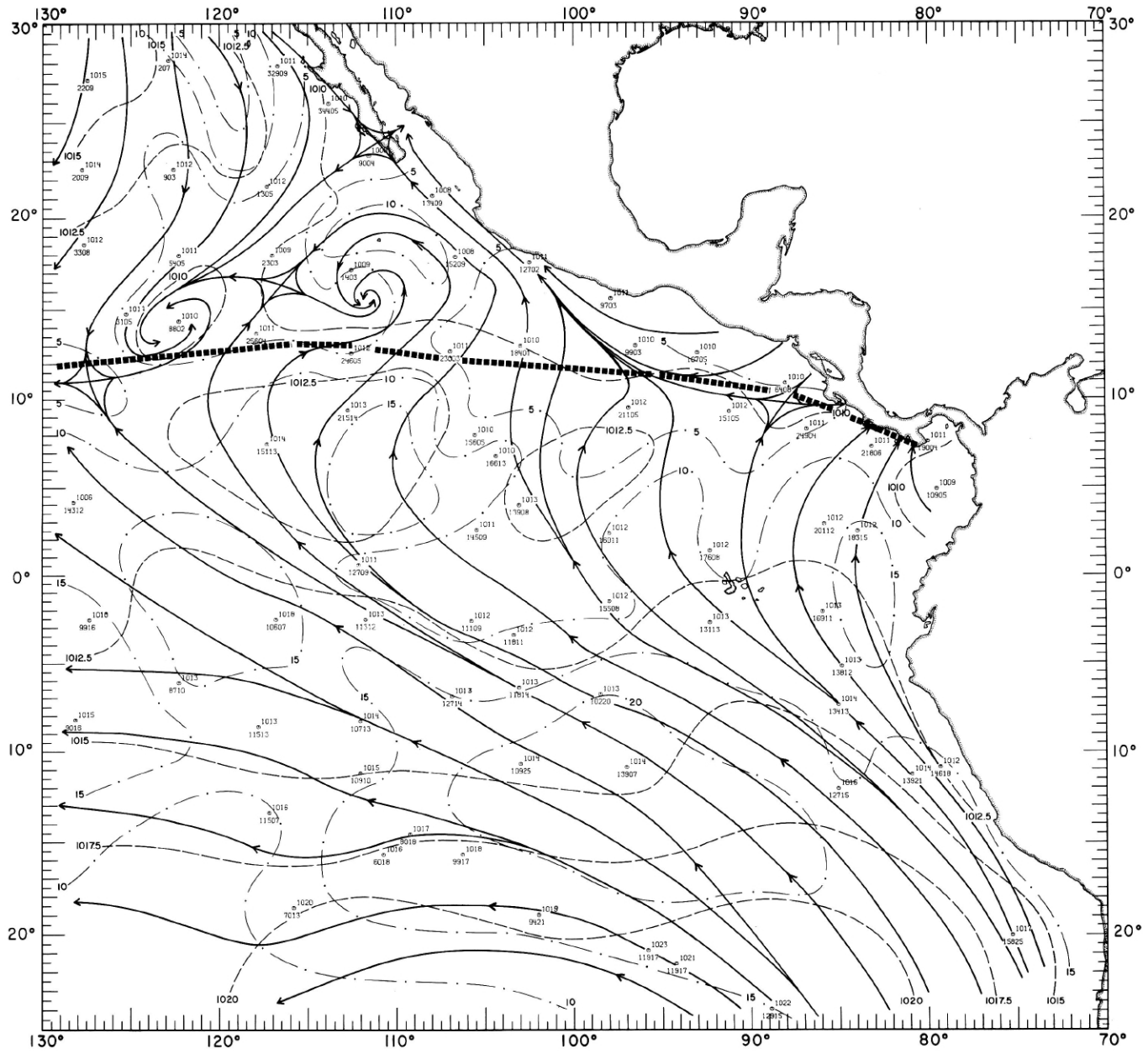

40-MW-3.

FIGURE 40-MW-3.—Analyses of the surface air pressure and surface winds from all available ship observations, averaged over 2-degree (latitude-longitude) squares for the period August 20-31, 1967. Heavy dashed lines are isobars. Solid lines are streamlines showing the mean resultant direction of wind flow. Light dash-dot lines are isotachs indicating mean resultant wind speed (kn.). Pressure (mb.) averaged for 5-degree squares is plotted above the mean position of the square, and resultant wind direction followed by speed (kn.) is plotted below. The monthly climatological position of the intertropical convergence zone is shown by a wide dashed band.

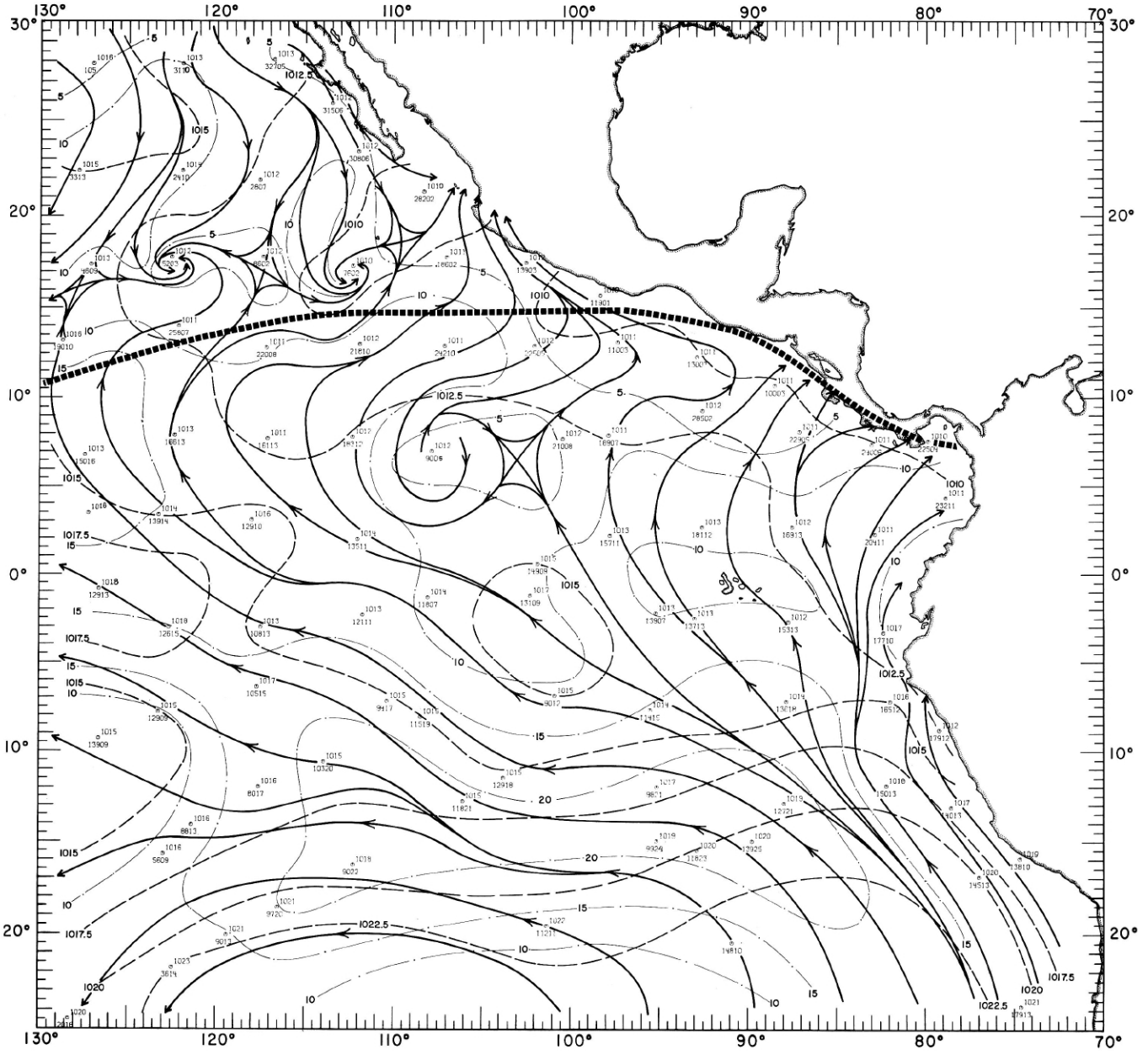

FIGURE 40-MW-4.—Analyses of the surface air pressure and surface winds from all available ship observations, averaged over 2-degree (latitude-longitude) squares for the period September 1-16, 1967. Heavy dashed lines are isobars. Solid lines are streamlines showing the mean resultant direction of wind flow. Light dash-dot lines are isotachs indicating mean resultant wind speed (kn.). Pressure (mb.) averaged for 5-degree squares is plotted above the mean position of the square, and resultant wind direction followed by speed (kn.) is plotted below. The monthly climatological position of the intertropical convergence zone is shown by a wide dashed band.

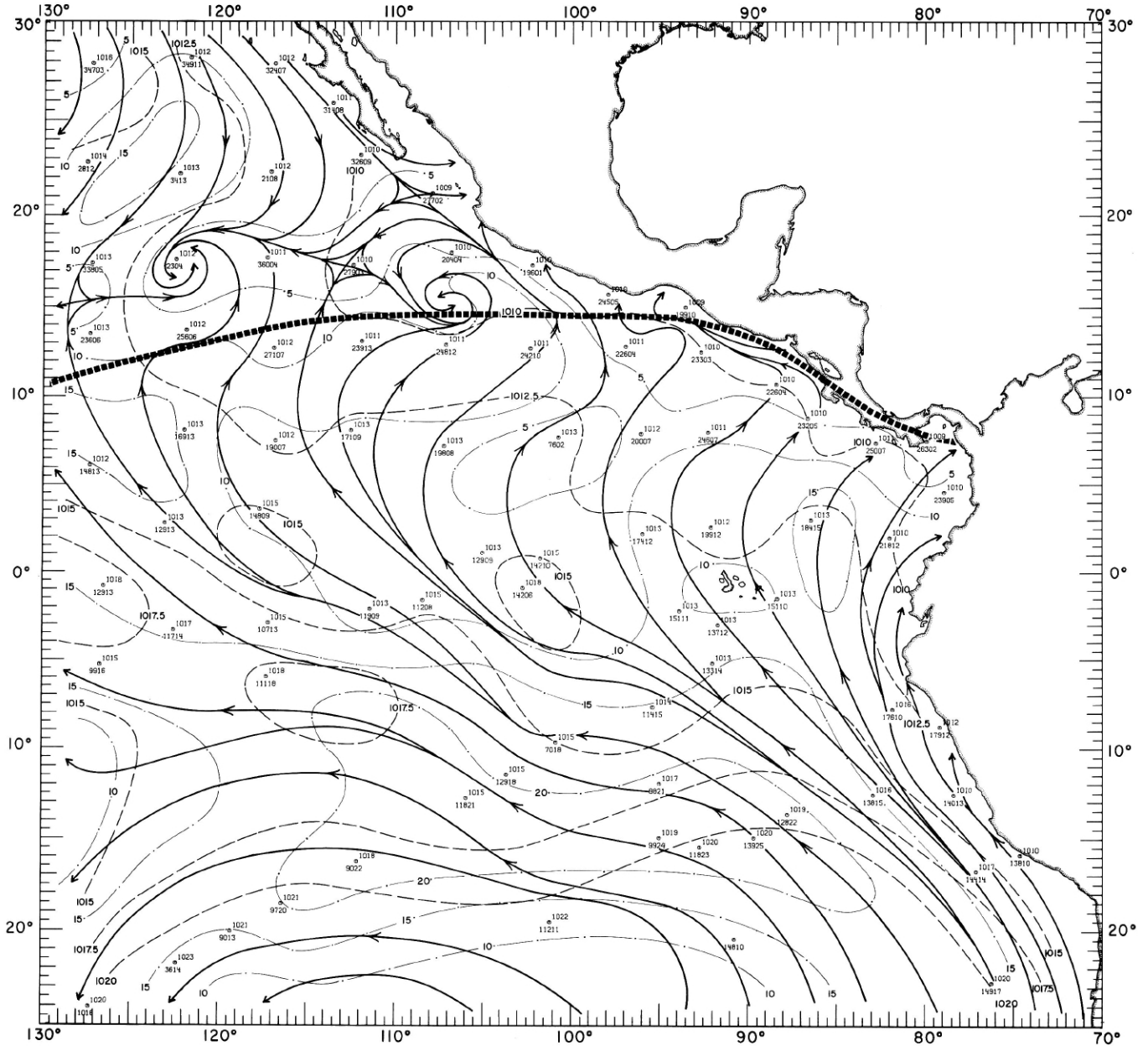

40-MW-5.

FIGURE 40-MW-5.—Analyses of the surface air pressure and surface winds from all available ship observations, averaged over 2-degree (latitude-longitude) squares for the period September 10-23, 1967. Heavy dashed lines are isobars. Solid lines are streamlines showing the mean resultant direction of wind flow. Light dash-dot lines are isotachs indicating mean resultant wind speed (kn.). Pressure (mb.) averaged for 5-degree squares is plotted above the mean position of the square, and resultant wind direction followed by speed (kn.) is plotted below. The monthly climatological position of the intertropical convergence zone is shown by a wide dashed band.

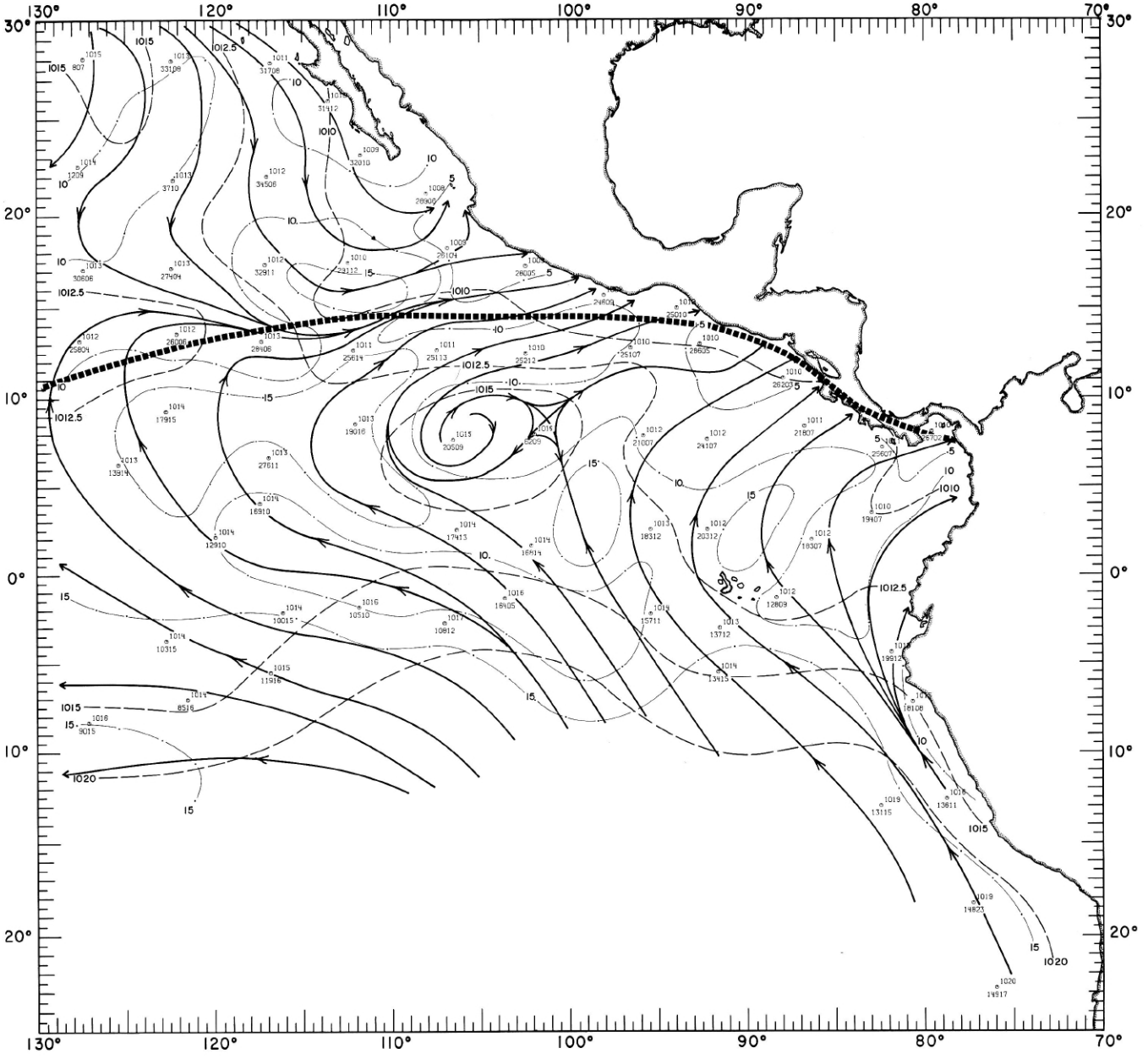

40-MW-6.

FIGURE 40-MW-6.—Analyses of the surface air pressure and surface winds from all available ship observations, averaged over 2-degree (latitude-longitude) squares for the period September 17-30, 1967. Heavy dashed lines are isobars. Solid lines are streamlines showing the mean resultant direction of wind flow. Light dash-dot lines are isotachs indicating mean resultant wind speed (kn.). Pressure (mb.) averaged for 5-degree squares is plotted above the mean position of the square, and resultant wind direction followed by speed (kn.) is plotted below. The monthly climatological position of the intertropical convergence zone is shown by a wide dashed band.

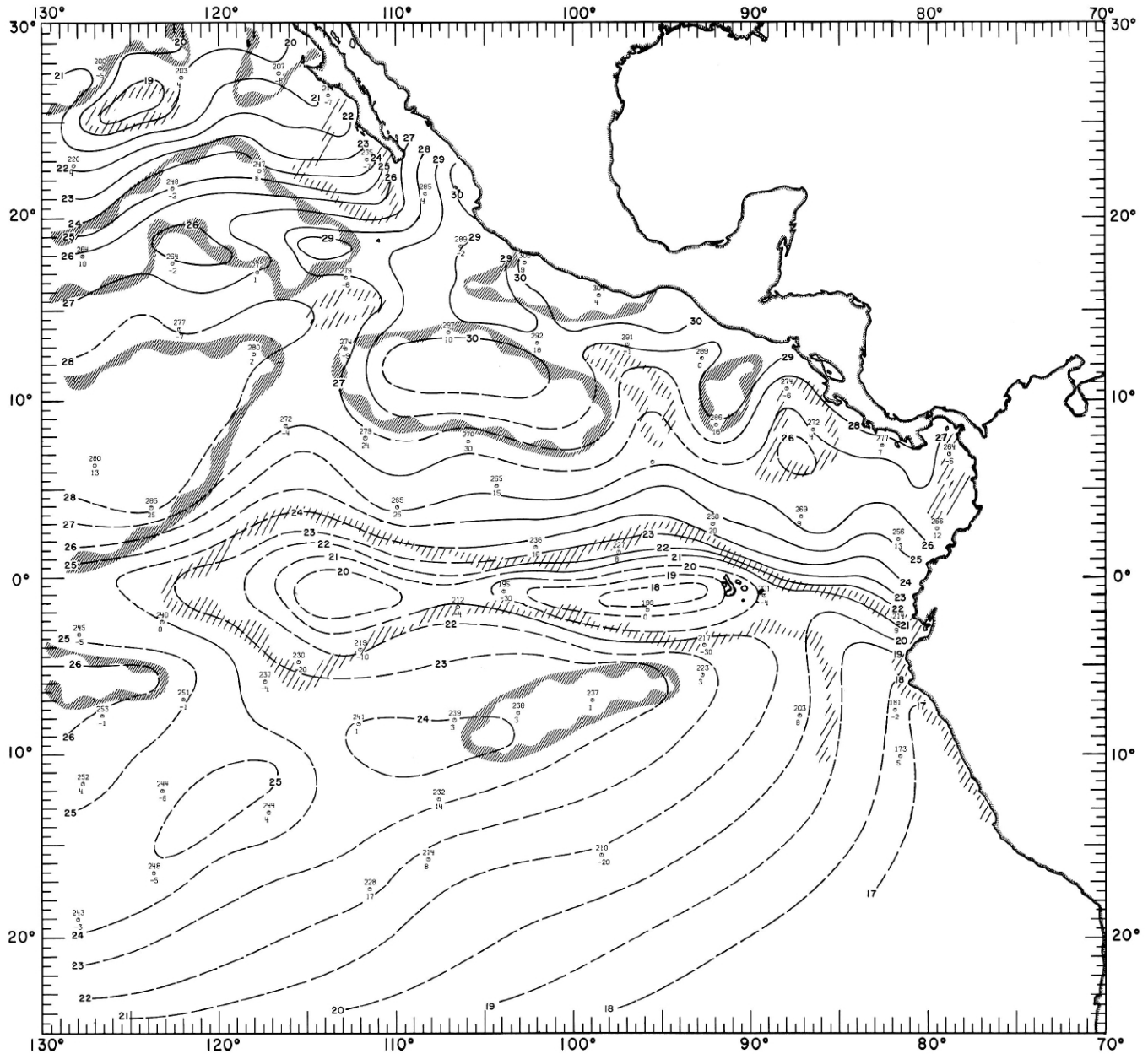

40-MT-1.

FIGURE 40-MT-1.—Analysis of sea surface temperatures based on averages for 2-degree (latitude-longitude) squares from all available ship observations for the period August 1-12, 1967. Solid lines are sea surface isotherms (° C.); the isotherms are dashed where data are sparse. Dark hatching outlines areas with positive temperature anomalies (computed from mean sea surface temperatures averaged over 22 years) greater than 1° C.; light hatching shows areas with negative anomalies greater than 1° C. Sea surface temperature (° C. x 10) averaged for 5-degree squares is plotted above the mean position of the square; sea temperature minus air temperature difference (° C. x 10) is plotted below the symbol.

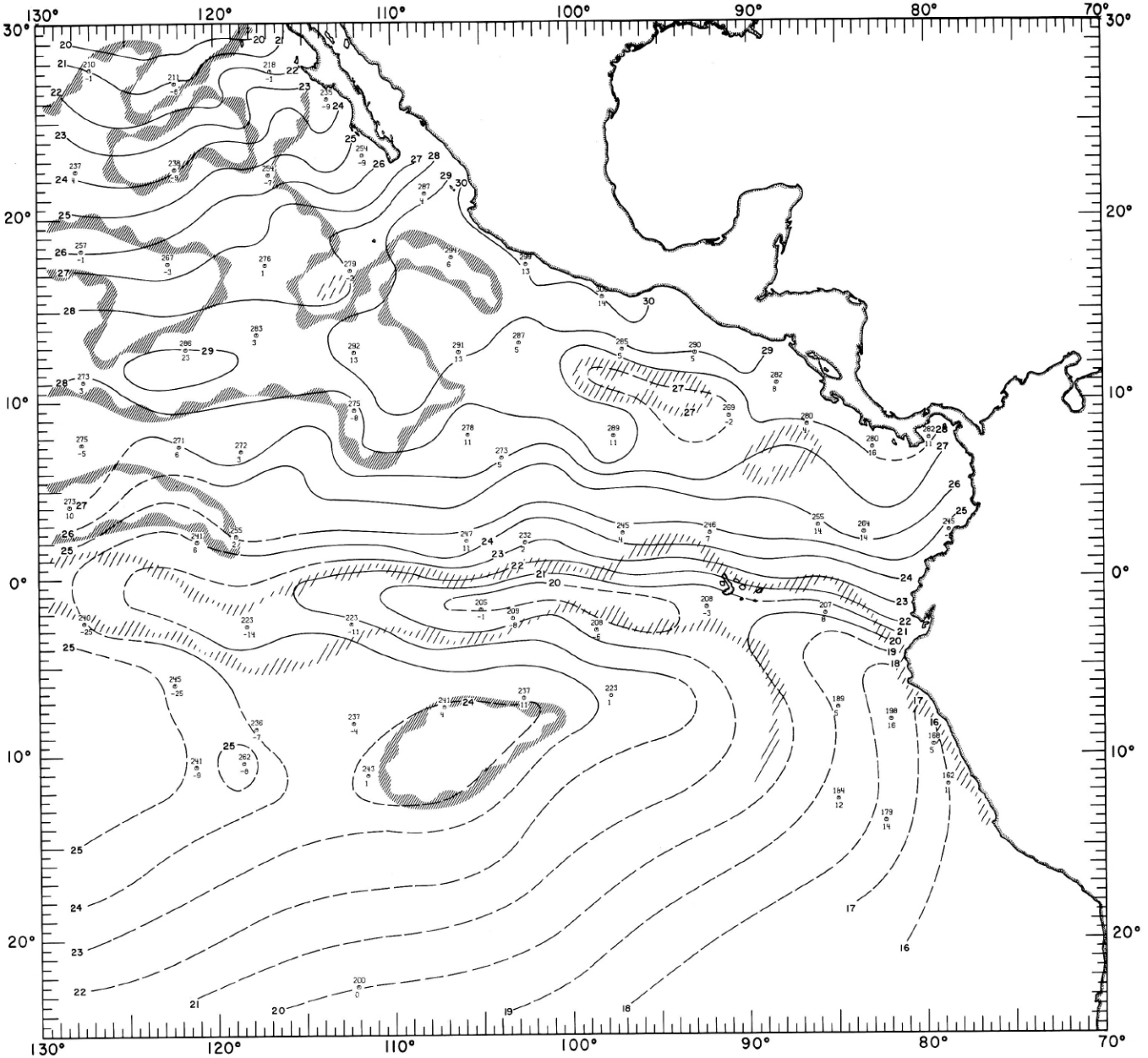

FIGURE 40-MT-2.—Analysis of sea surface temperatures based on averages for 2-degree (latitude-longitude) squares from all available ship observations for the period August 13-26, 1967. Solid lines are sea surface isotherms (° C.); the isotherms are dashed where data are sparse. Dark hatching outlines areas with positive temperature anomalies (computed from mean sea surface temperatures averaged over 22 years) greater than 1° C.; light hatching shows areas with negative anomalies greater than 1° C. Sea surface temperature (° C. x 10) averaged for 5-degree squares is plotted above the mean position of the square; sea temperature minus air temperature difference (° C. x 10) is plotted below the symbol.

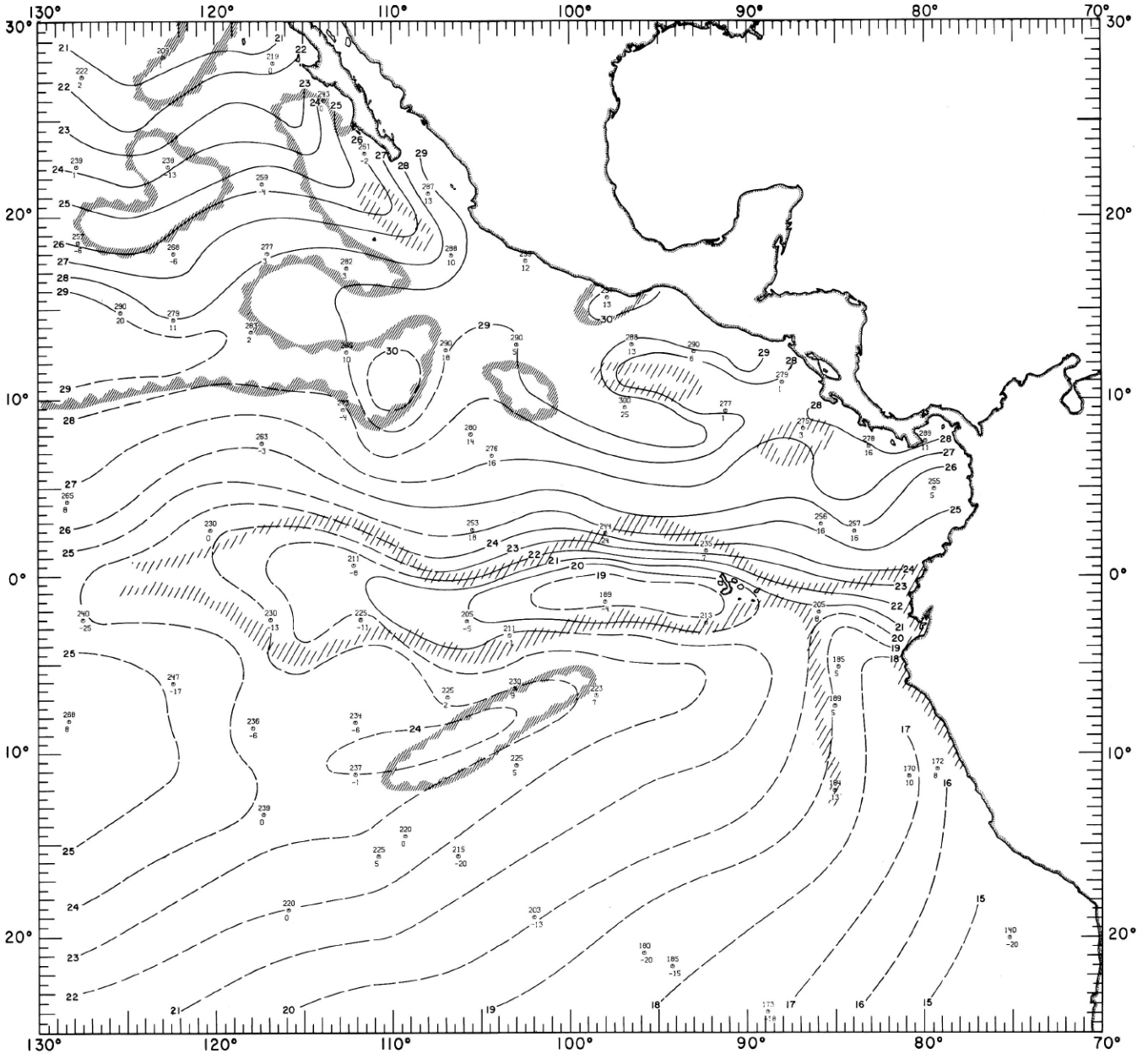

40-MT-3.

FIGURE 40-MT-3.—Analysis of sea surface temperatures based on averages for 2-degree (latitude-longitude) squares from all available ship observations for the period August 20-31, 1967. Solid lines are sea surface isotherms (° C.); the isotherms are dashed where data are sparse. Dark hatching outlines areas with positive temperature anomalies (computed from mean sea surface temperatures averaged over 22 years) greater than 1° C.; light hatching shows areas with negative anomalies greater than 1° C. Sea surface temperature (° C. x 10) averaged for 5-degree squares is plotted above the mean position of the square; sea temperature minus air temperature difference (° C. x 10) is plotted below the symbol.

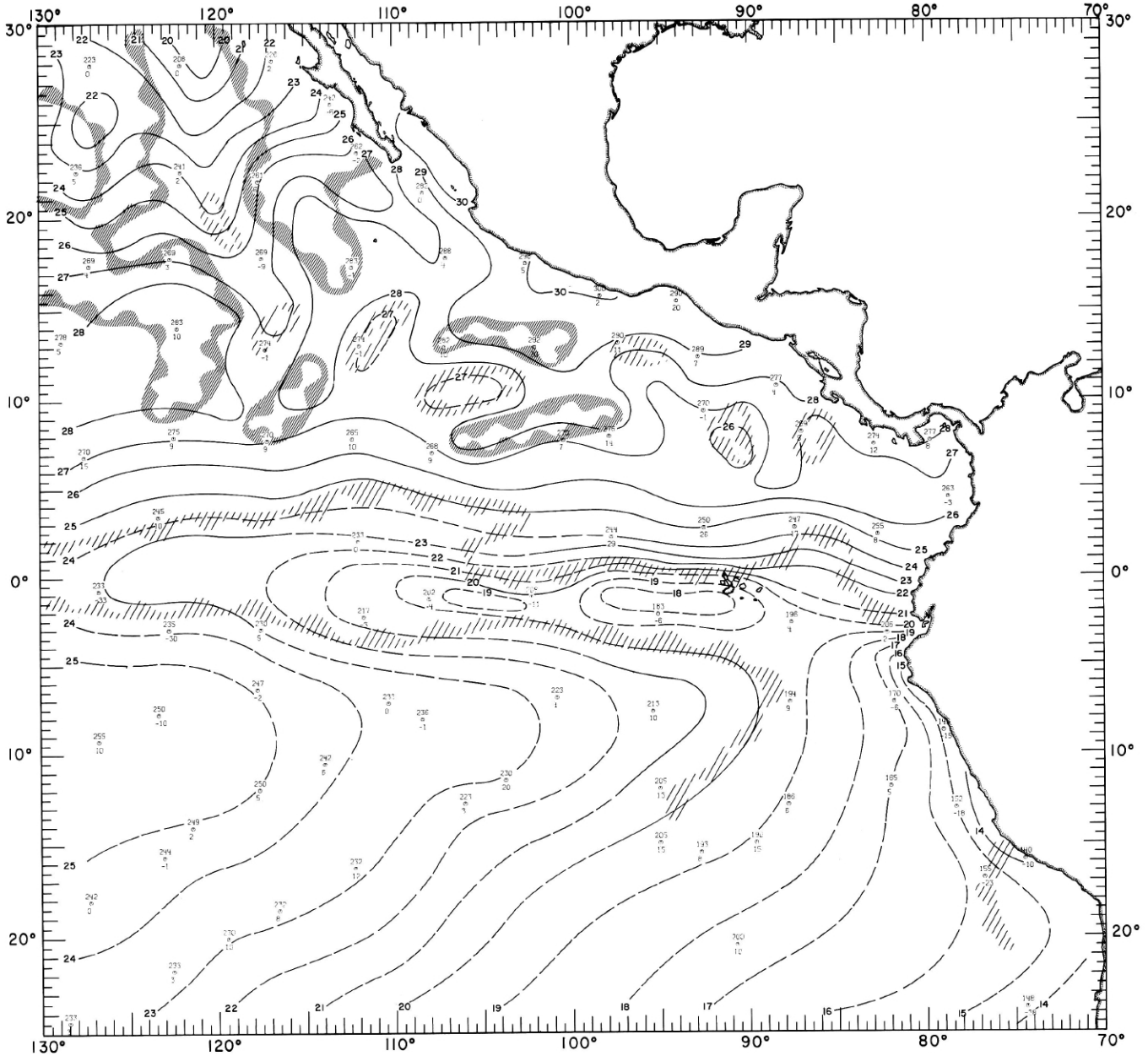

40-MT-4.

FIGURE 40-MT-4.—Analysis of sea surface temperatures based on averages for 2-degree (latitude-longitude) squares from all available ship observations for the period September 1-16, 1967. Solid lines are sea surface isotherms (° C.); the isotherms are dashed where data are sparse. Dark hatching outlines areas with positive temperature anomalies (computed from mean sea surface temperatures averaged over 22 years) greater than 1° C.; light hatching shows areas with negative anomalies greater than 1° C. Sea surface temperature (° C. x 10) averaged for 5-degree squares is plotted above the mean position of the square; sea temperature minus air temperature difference (° C. x 10) is plotted below the symbol.

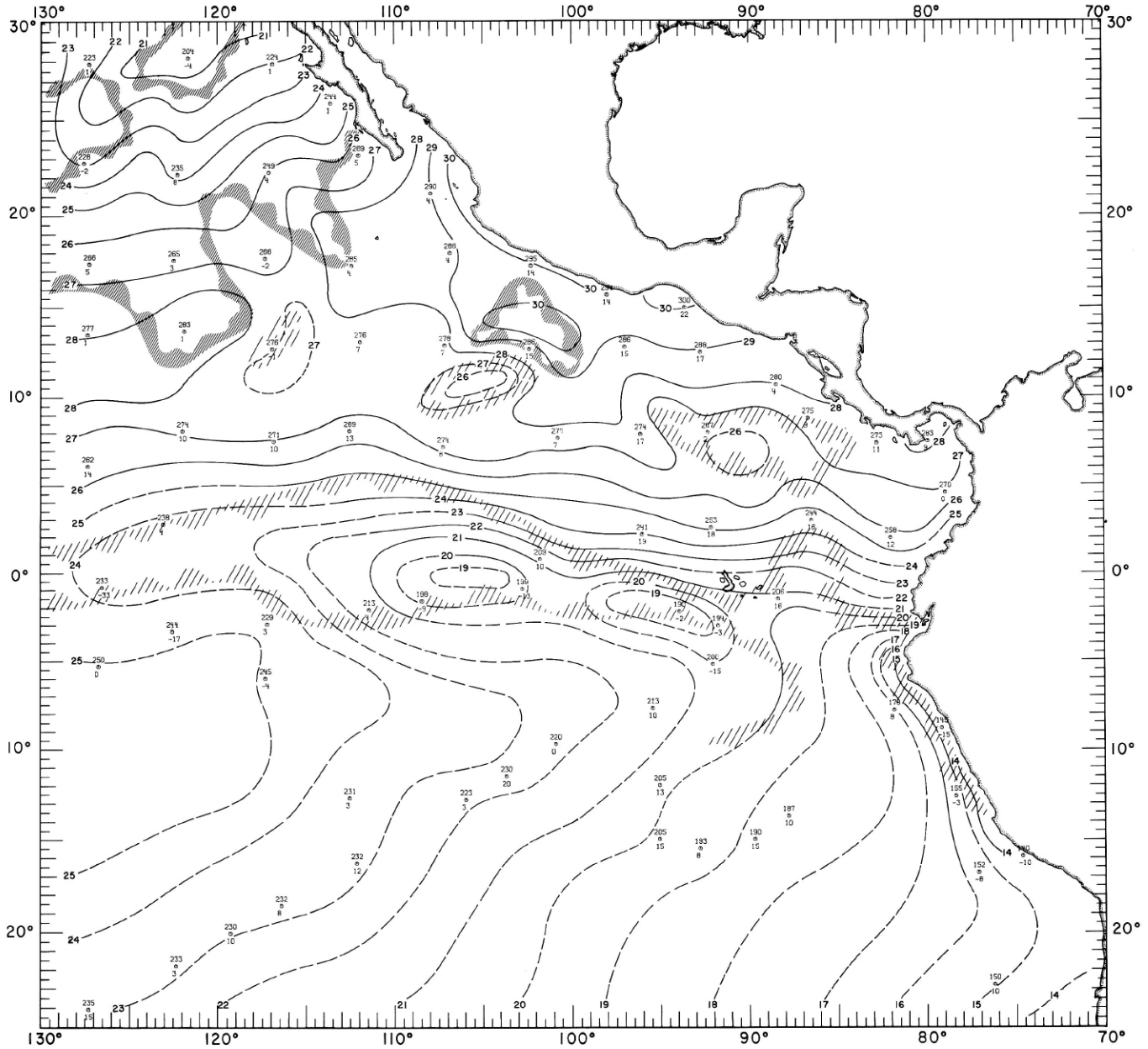

40-MT-5.

FIGURE 40-MT-5.—Analysis of sea surface temperatures based on averages for 2-degree (latitude-longitude) squares from all available ship observations for the period September 10-23, 1967. Solid lines are sea surface isotherms (° C.); the isotherms are dashed where data are sparse. Dark hatching outlines areas with positive temperature anomalies (computed from mean sea surface temperatures averaged over 22 years) greater than 1° C.; light hatching shows areas with negative anomalies greater than 1° C. Sea surface temperature (° C. x 10) averaged for 5-degree squares is plotted above the mean position of the square; sea temperature minus air temperature difference (° C. x 10) is plotted below the symbol.

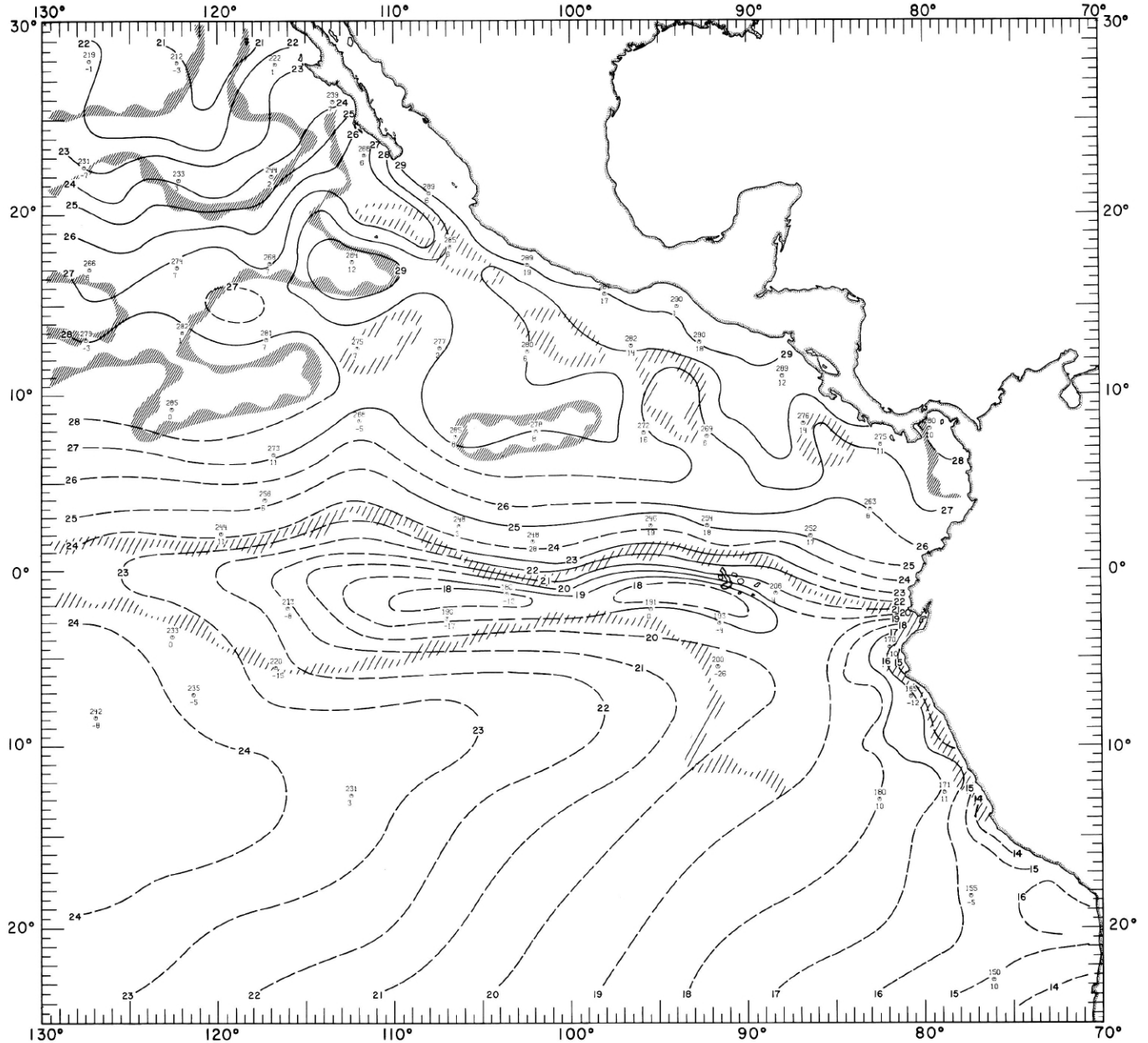

FIGURE 40-MT-6.—Analysis of sea surface temperatures based on averages for 2-degree (latitude-longitude) squares from all available ship observations for the period September 17-30, 1967. Solid lines are sea surface isotherms (° C.); the isotherms are dashed where data are sparse. Dark hatching outlines areas with positive temperature anomalies (computed from mean sea surface temperatures averaged over 22 years) greater than 1° C.; light hatching shows areas with negative anomalies greater than 1° C. Sea surface temperature (° C. x 10) averaged for 5-degree squares is plotted above the mean position of the square; sea temperature minus air temperature difference (° C. x 10) is plotted below the symbol.

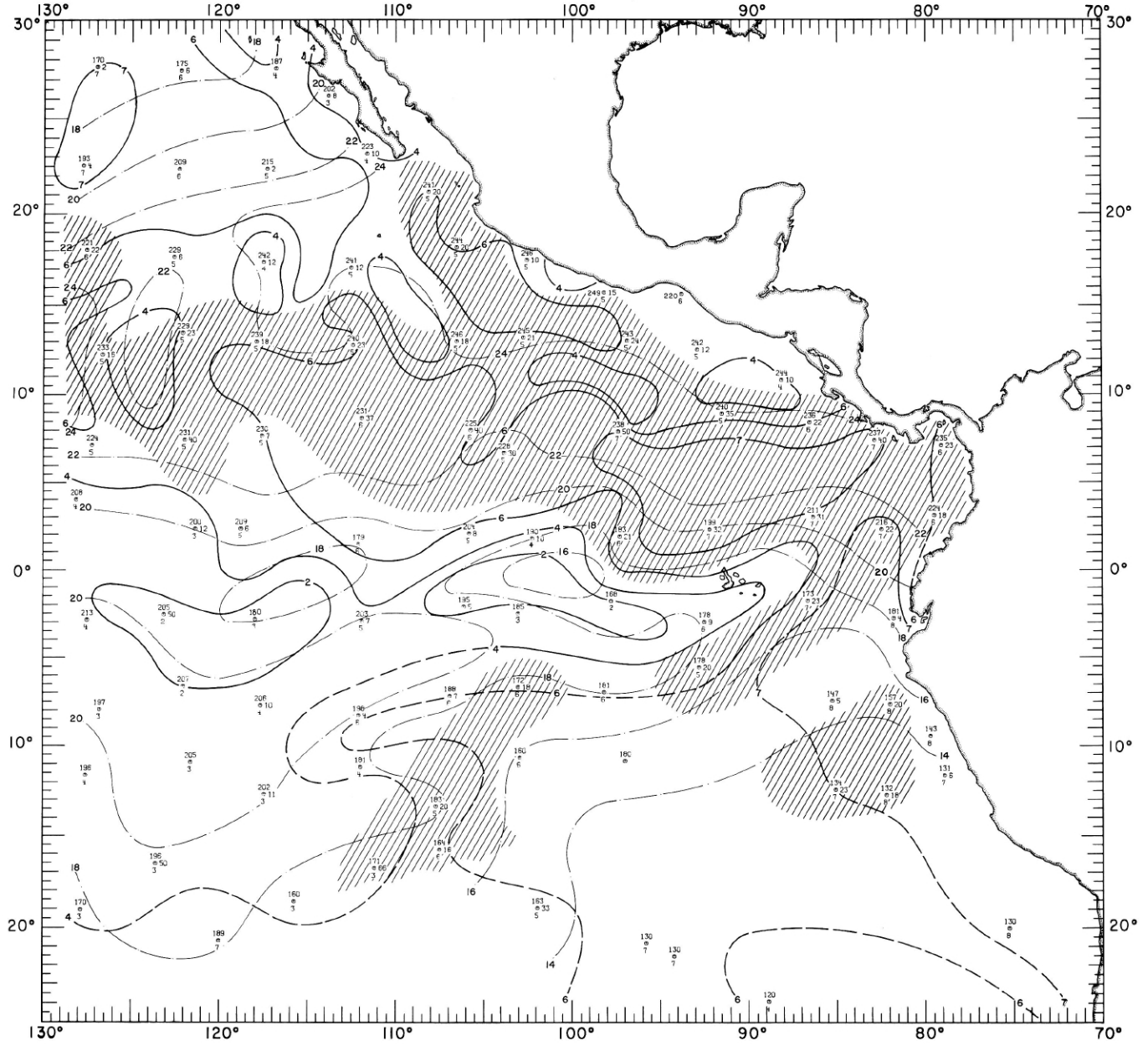

40-MC-1.

FIGURE 40-MC-1.—Analyses of the surface dew-point temperature of the air and total cloud cover based on 2-degree (latitude-longitude) averages from all available ship observations for the month of August 1967. Solid lines depict the monthly mean total cloud cover in oktas; the lines are dashed where data are sparse. Dash-dot lines are isotherms of the mean monthly dew-point temperature at 2-degree (C.) intervals. Areas where 15 percent or more of the ships reported rain of any type at or within sight of the ship are shaded. Dew-point temperature (°C. x 10) averaged for 5-degree squares is plotted above the mean position of the square, with total cloud cover (oktas) below and rainfall frequency (%) to the right of the symbol.

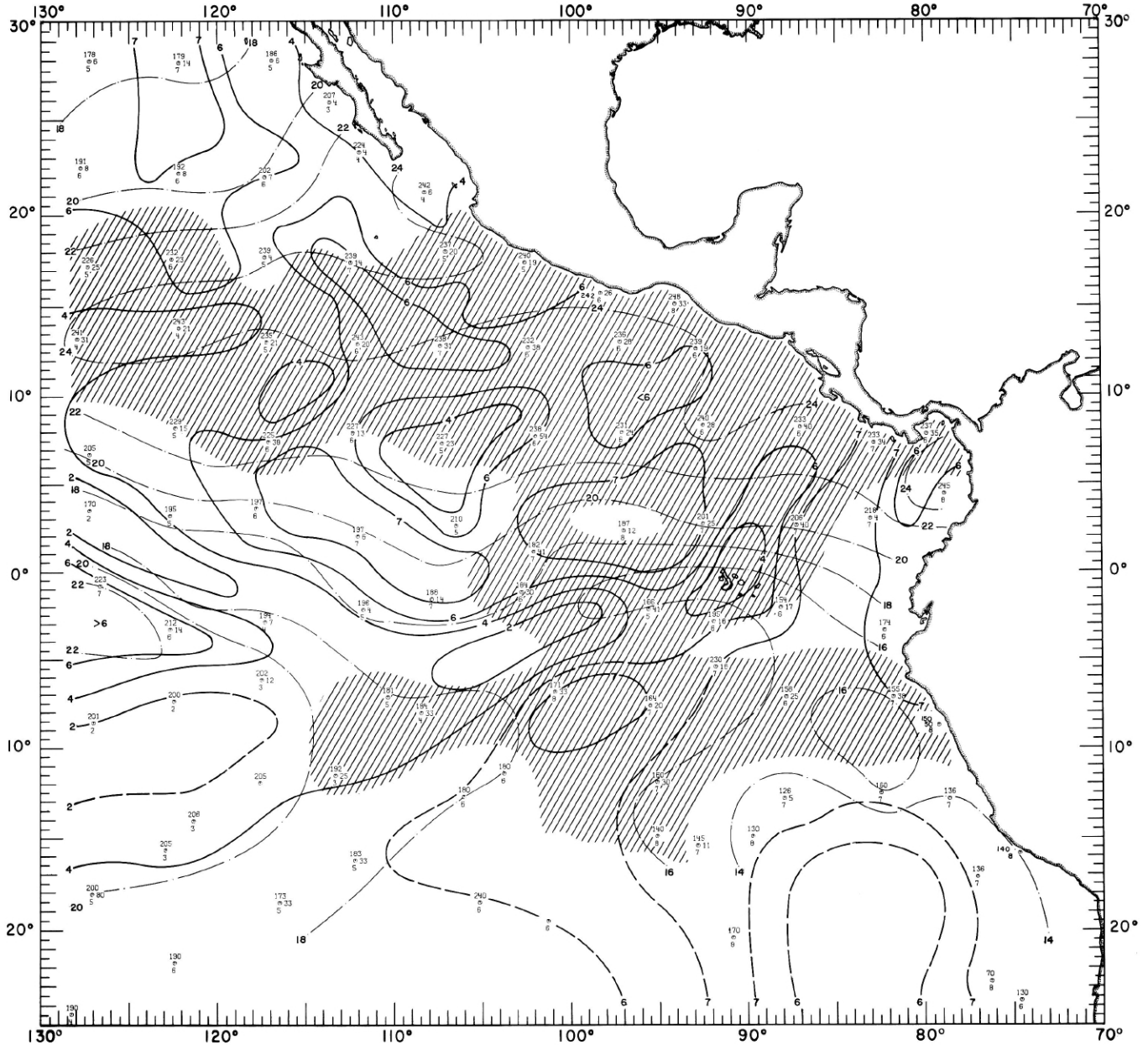

40-MC-2.

FIGURE 40-MC-2.—Analyses of the surface dew-point temperature of the air and total cloud cover based on 2-degree (latitude-longitude) averages from all available ship observations for the month of September 1967. Solid lines depict the monthly mean total cloud cover in oktas; the lines are dashed where data are sparse. Dash-dot lines are isotherms of the mean monthly dew-point temperature at 2-degree (C.) intervals. Areas where 15 percent or more of the ships reported rain of any type at or within sight of the ship are shaded. Dew-point temperature (°C. x 10) averaged for 5-degree squares is plotted above the mean position of the square, with total cloud cover (oktas) below and rainfall frequency (%) to the right of the symbol.

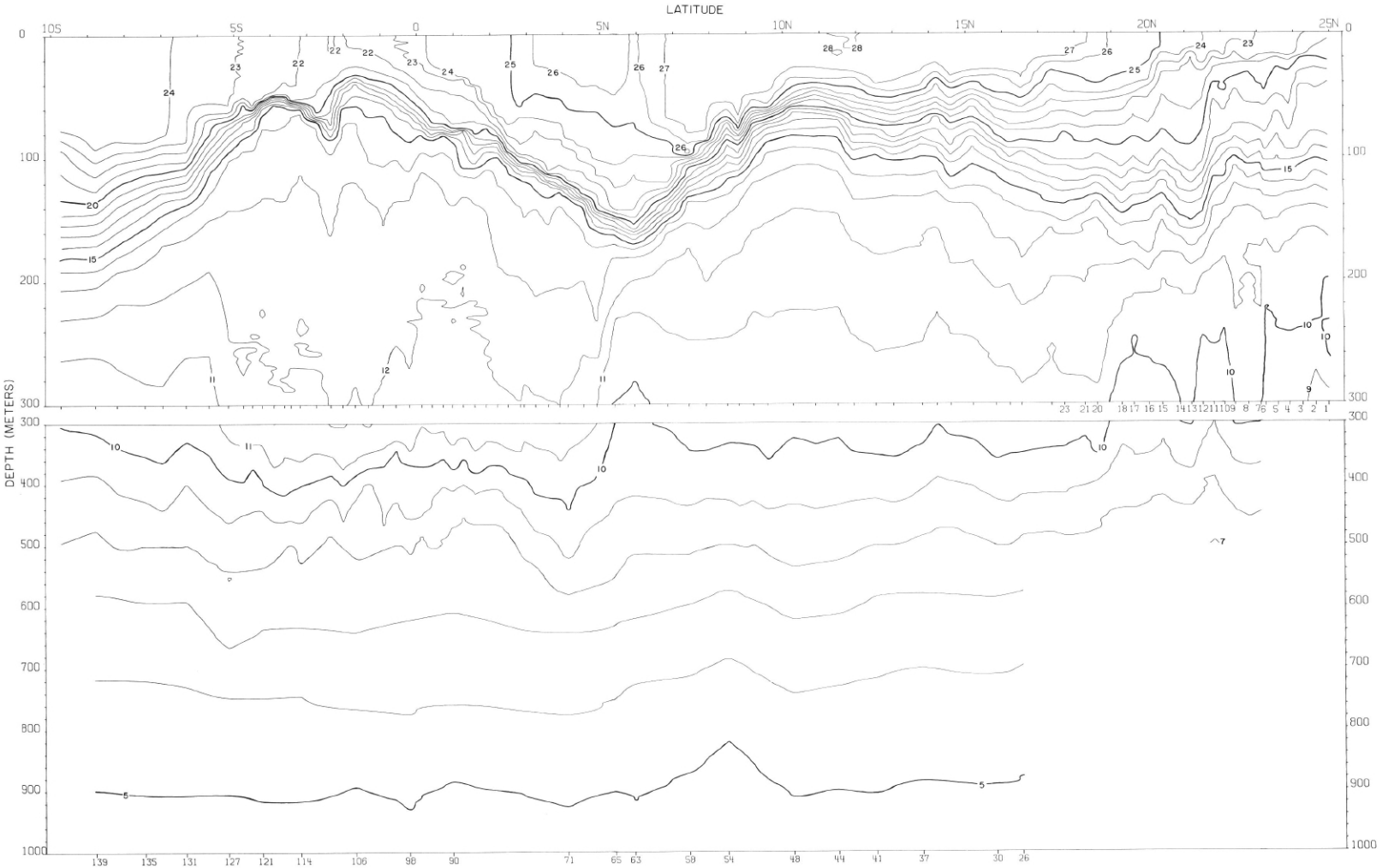

FIGURE 45-T-v1.—Vertical distribution of temperature (°C.) along 119° W., August 3-21, 1967. The data from Stations 1-15 were not calibrated against Nansen cast data.

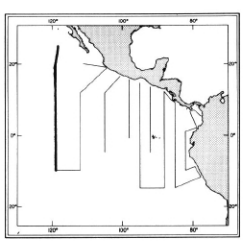

45-T-v1.

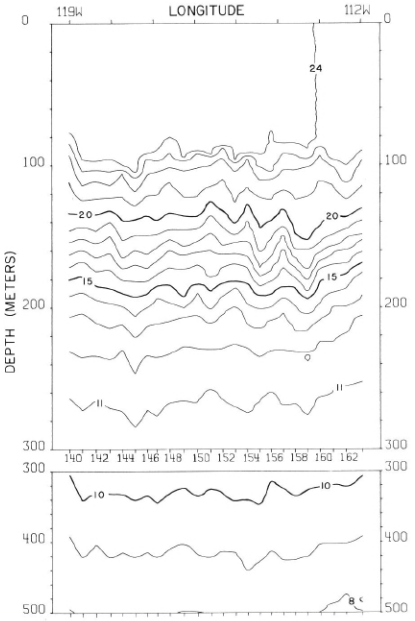

FIGURE 45-T-v2.—Vertical distribution of temperature (°C.) along 10° S., August 21-23, 1967.

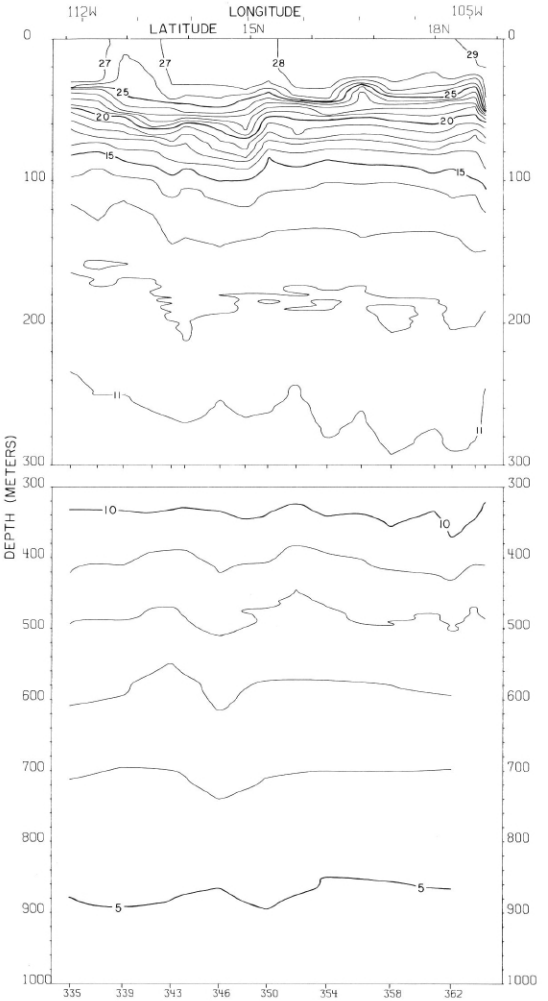

FIGURE 45-T-v5.—Vertical distribution of temperature (°C.) along a section from 12° N., 112° W. to Manzanillo, September 7-10, 1967.

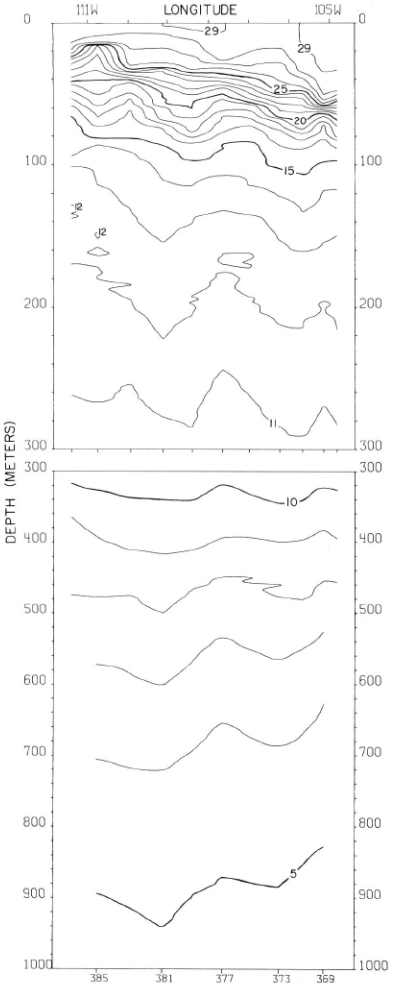

FIGURE 45-T-v6.—Vertical distribution of temperature (°C.) along 19°30′ N. from Manzanillo to 111°25′ W., September 13-15, 1967.

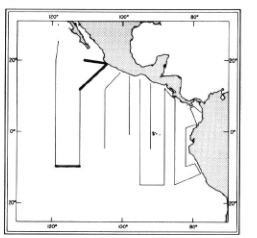

45-T-v2.

45-T-v5.

45-T-v6.

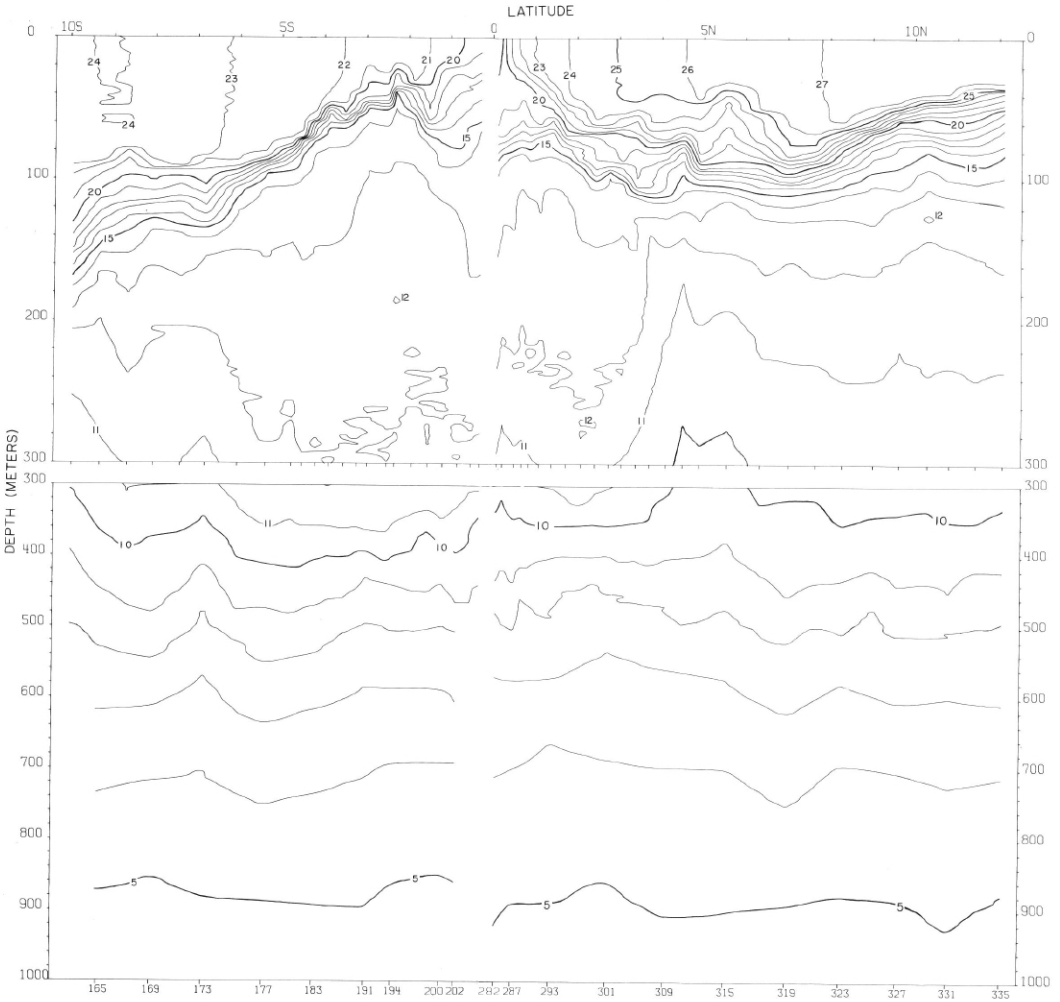

FIGURE 45-T-v3.—Vertical distribution of temperature (°C.) along 112° W., August 23-September 7, 1967. The interruption in the contours indicates a 4-day interval between Stations 206 and 282 in the upper (0-500 m.) portion of the section, or between Stations 202 and 282 in the lower portion.

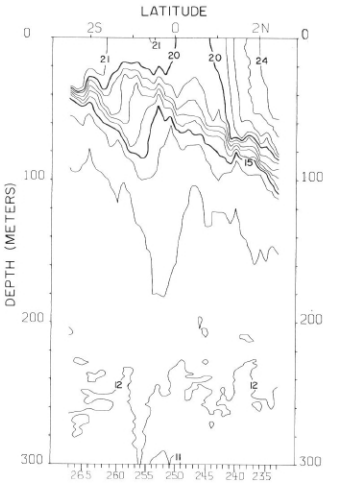

FIGURE 45-T-v4.—Vertical distribution of temperature (°C.) along 112° W. from 2°27′ N. to 2°29′ S., August 30-September 1, 1967. These data are part of a special series of observations made during the time interval indicated by the interrupted contours on figure 45-T-v3.

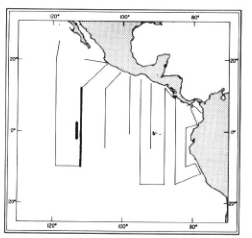

45-T-v3.

45-T-v4.

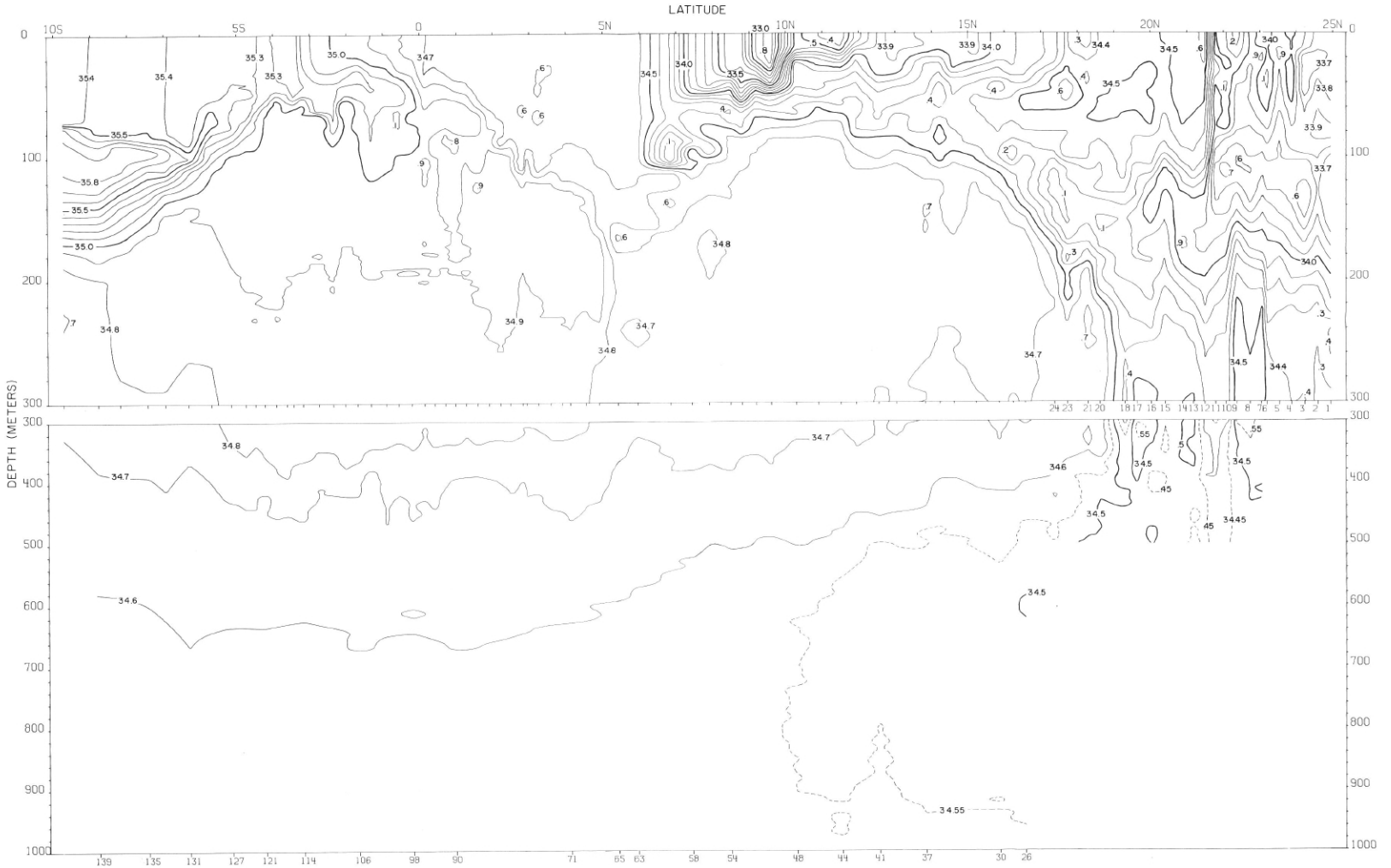

FIGURE 45-S-v1.—Vertical distribution of salinity (‰) along 119° W., August 3-21, 1967. The data from Stations 1-15 were not calibrated against Nansen cast data.

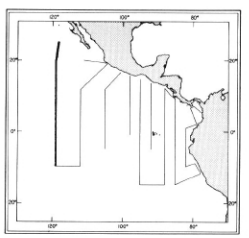

45-S-v1.

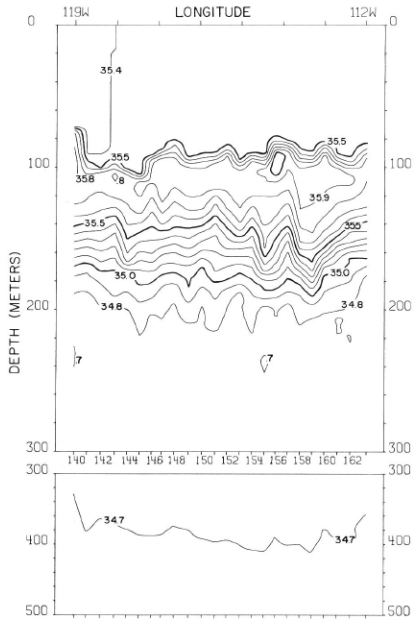

FIGURE 45-S-v2.—Vertical distribution of salinity (‰) along 10° S., August 21-23, 1967.

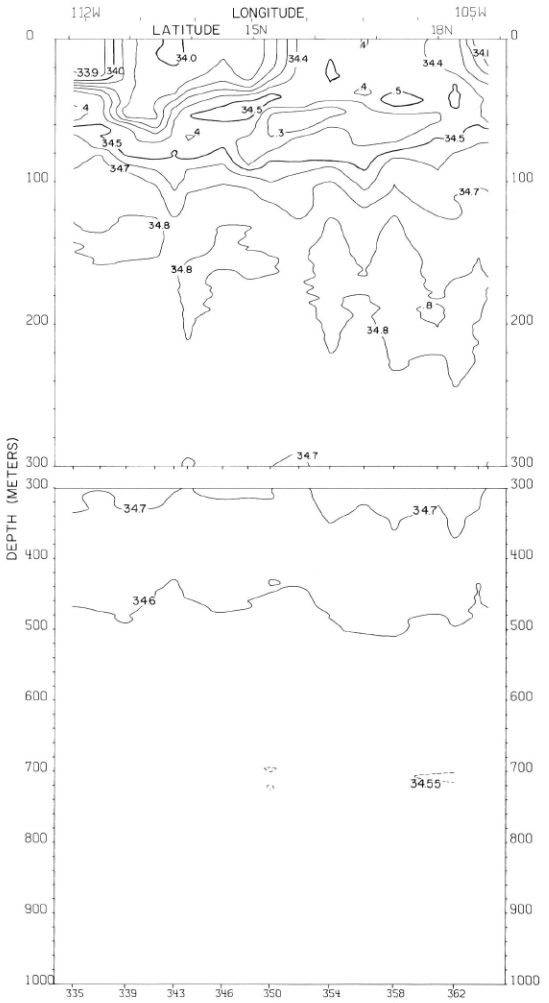

FIGURE 45-S-v5.—Vertical distribution of salinity (‰) along a section from 12° N., to 112° W. to Manzanillo, September 7-10, 1967.

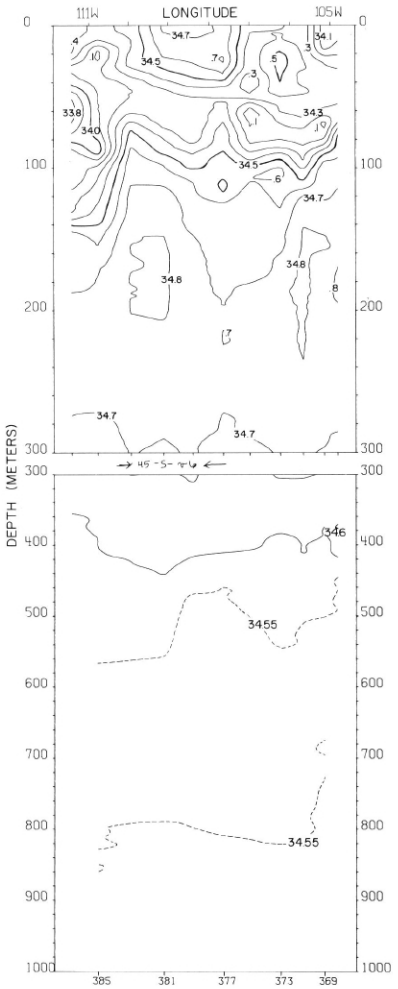

FIGURE 45-S-v6.—Vertical distribution of salinity (‰) along 19°30′ N. from Manzanillo to 111°25′ W., September 13-15, 1967.

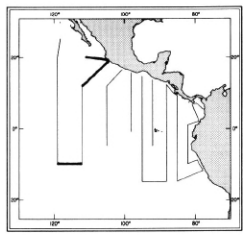

45-S-v2.

45-S-v5.

45-S-v6.

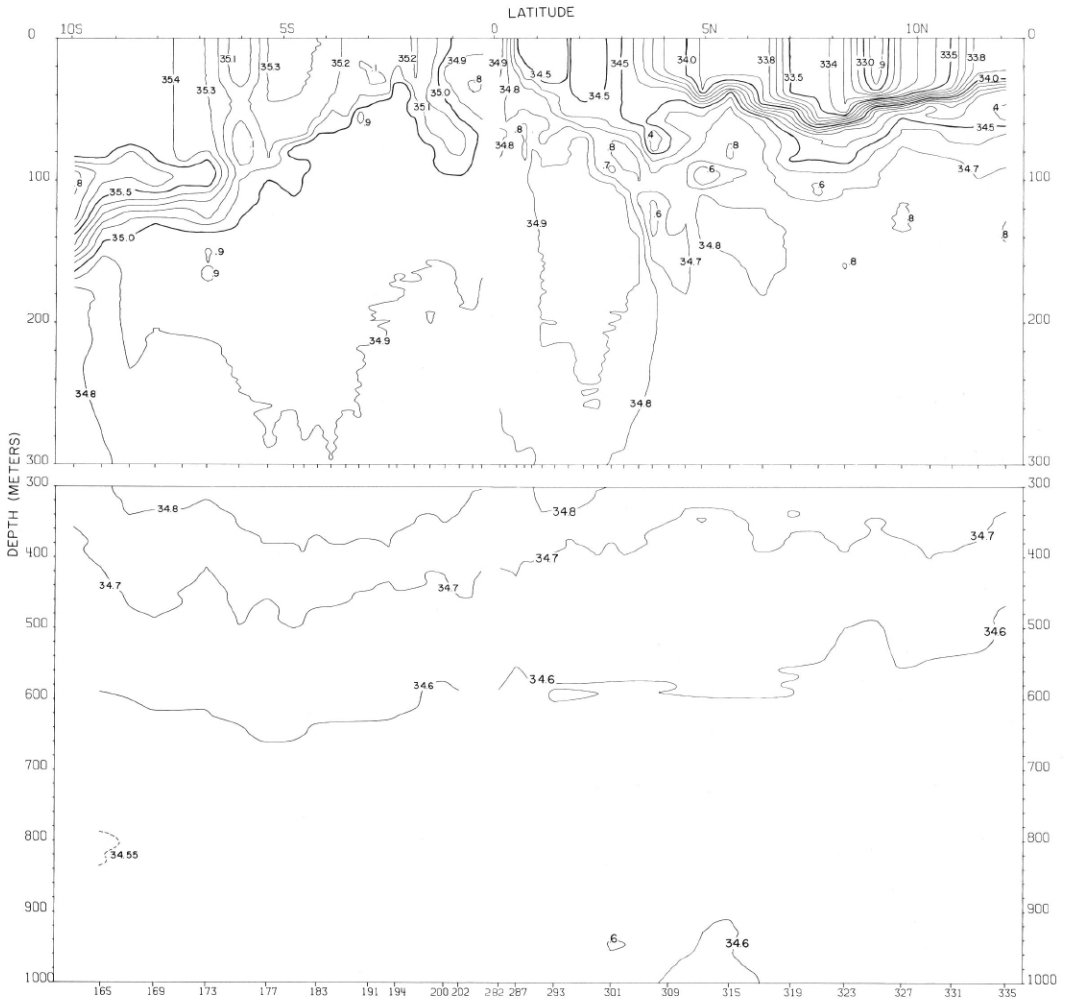

FIGURE 45-S-v3.—Vertical distribution of salinity (‰) along 112° W., August 23-September 7, 1967. The interruption in the contours indicates a 4-day interval between Stations 206 and 282 in the upper (0-500 m.) portion of the section, or between Stations 202 and 282 in the lower portion.

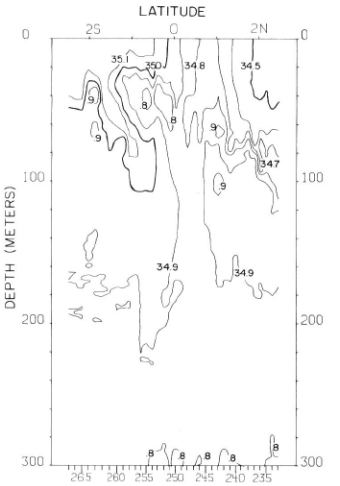

FIGURE 45-S-v4.—Vertical distribution of salinity (‰) along 112° W. from 2°27′ N. to 2°29′ S., August 30-September 1, 1967. These data are part of a special series of observations made during the time interval indicated by the interrupted contours on figure 45-S-v3.

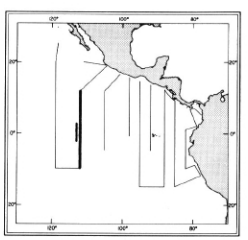

45-S-v3.

45-S-v4.

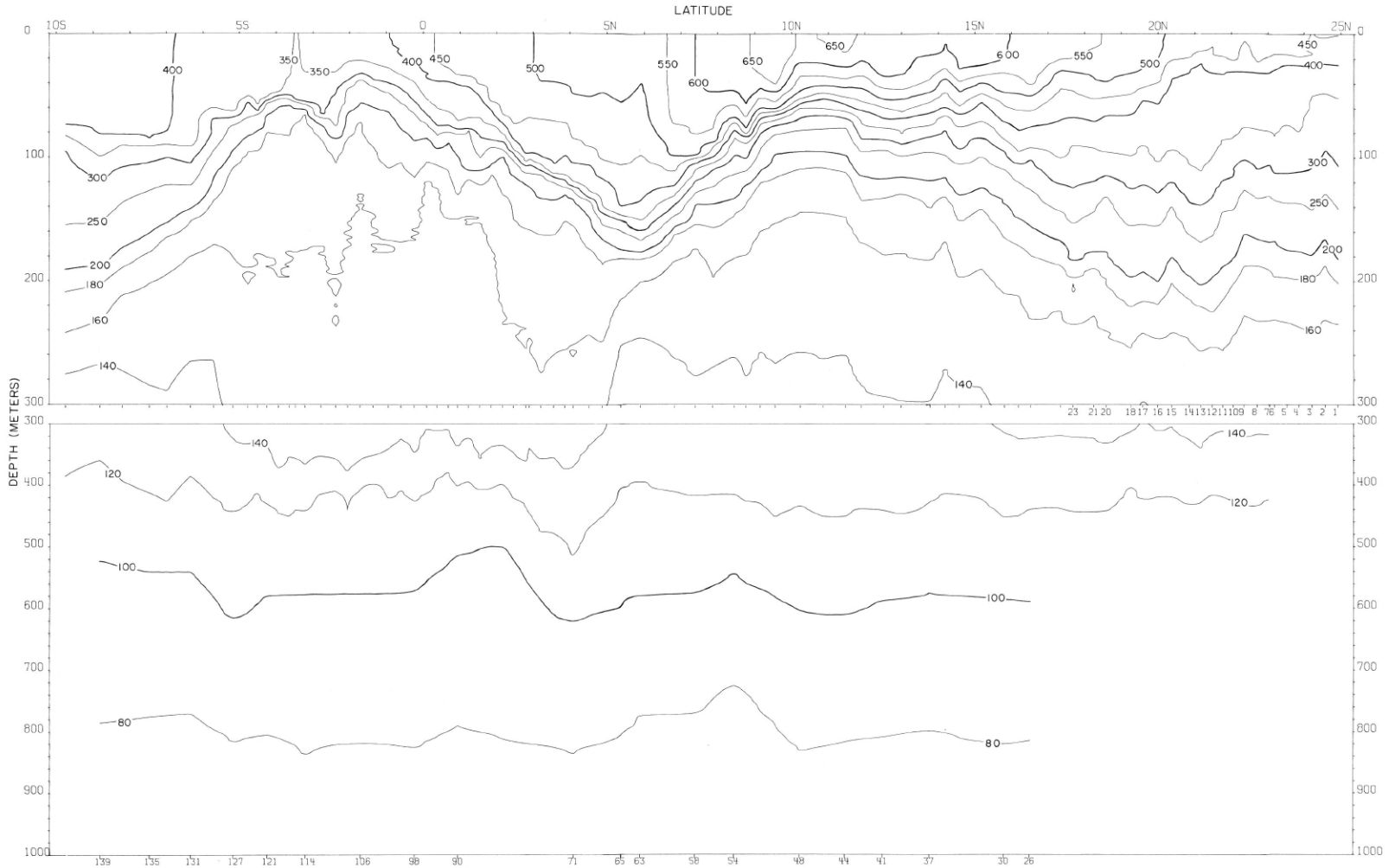

FIGURE 45-δ-v1.—Vertical distribution of thermosteric anomaly, δ_T, (cl./t.) along 119° W., August 3-21, 1967. The temperature and salinity data from Stations 1-15 were not calibrated against Nansen cast data.

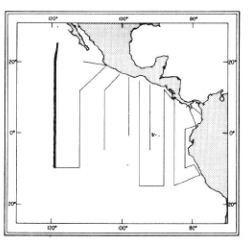

45-δ-v1.

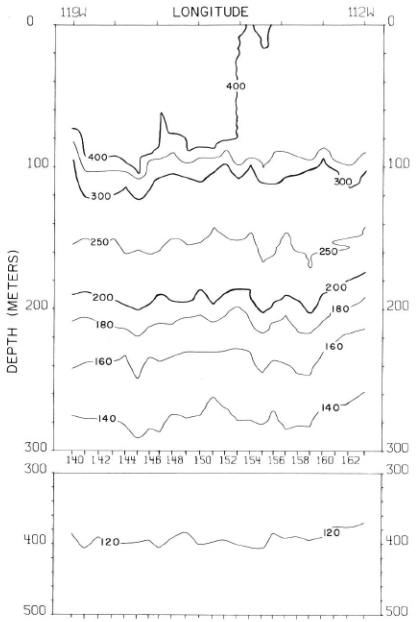

FIGURE 45-δ-v2.—Vertical distribution of thermosteric anomaly, δ_T, (cl./t.) along 10° S., August 21-23, 1967.

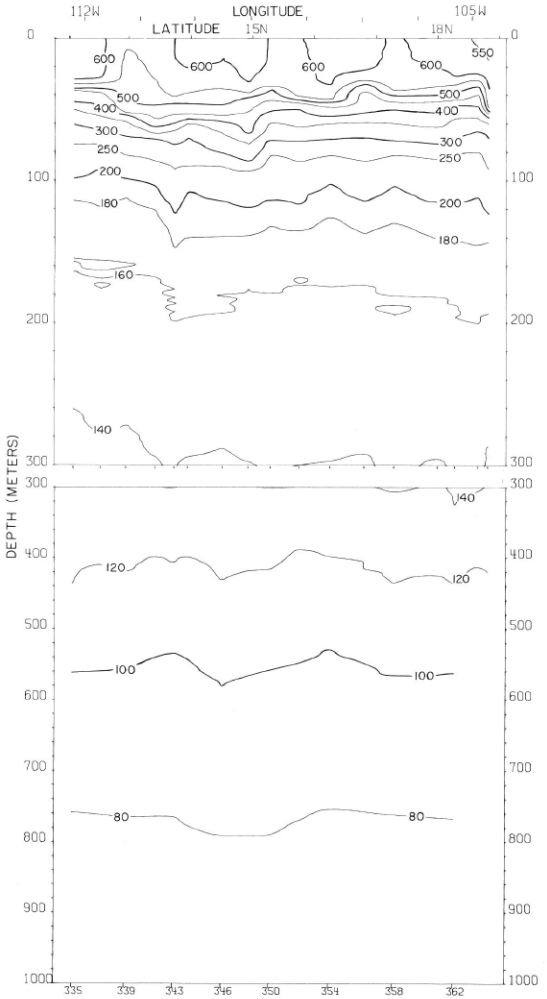

FIGURE 45-δ-v5.—Vertical distribution of thermosteric anomaly, δ_T, (cl./t.) along a section from 12° N., 112° W. to Manzanillo, September 7-10, 1967.

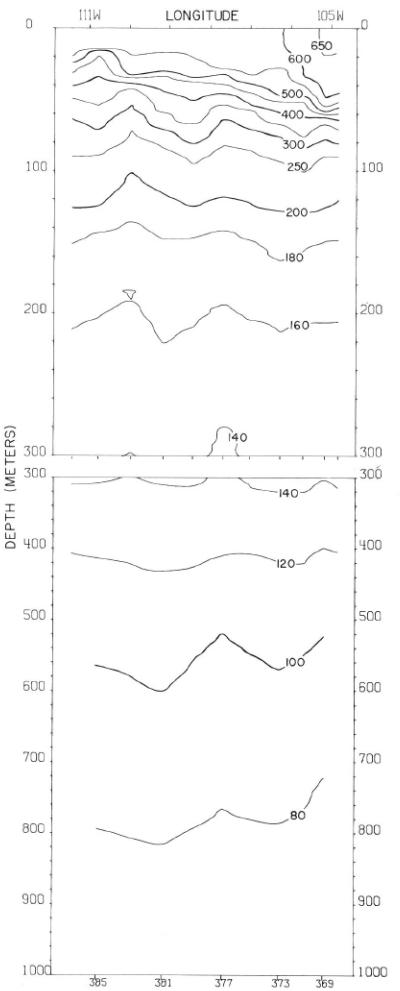

FIGURE 45-δ-v6.—Vertical distribution of thermosteric anomaly, δ_T, (cl./t.) along 19°30′ N. from Manzanillo to 111°25′ W., September 13-15, 1967.

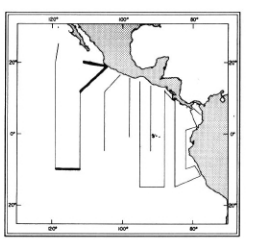

45-δ-v2.

45-δ-v5.

45-δ-v6.

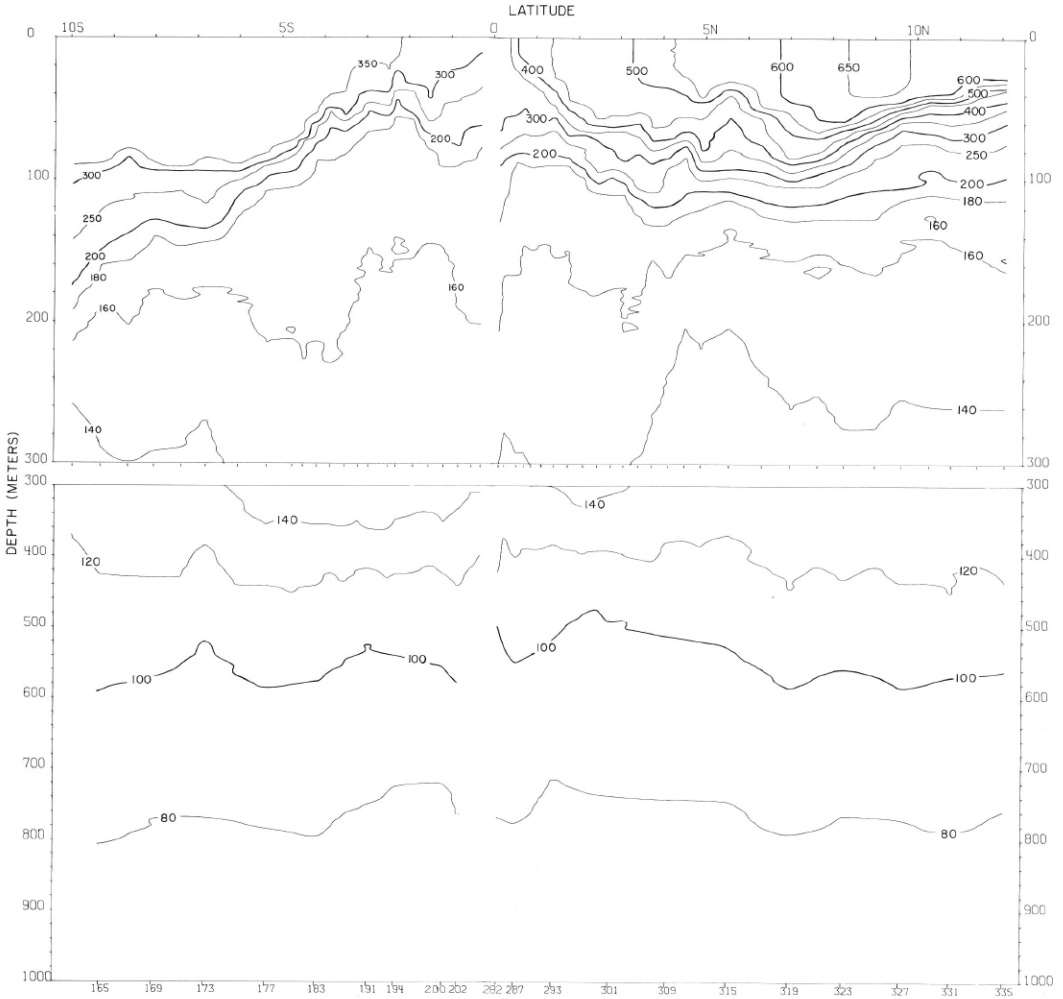

FIGURE 45-δ-v3.—Vertical distribution of thermosteric anomaly, δ_T, (cl./t.) along 112° W., August 23-September 7, 1967. The interruption in the contours indicates a 4-day interval between Stations 206 and 282 in the upper (0-500 m.) portion of the section, or between Stations 202 and 282 in the lower portion.

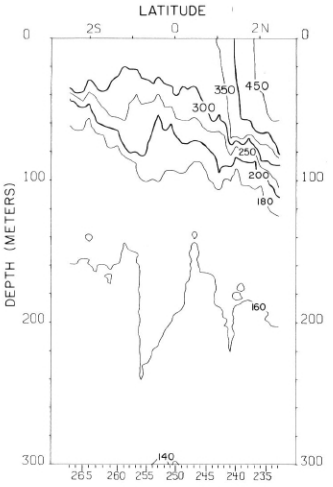

FIGURE 45-δ-v4.—Vertical distribution of thermosteric anomaly, δ_T, (cl./t.) along 112° W. from 2°27′ N. to 2°29′ S., August 30-September 1, 1967. These data are part of a special series of observations made during the time interval indicated by the interrupted contours on figure 45-δ-v3.

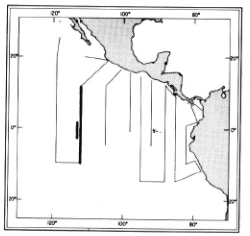

45-δ-v3.

45-δ-v4.

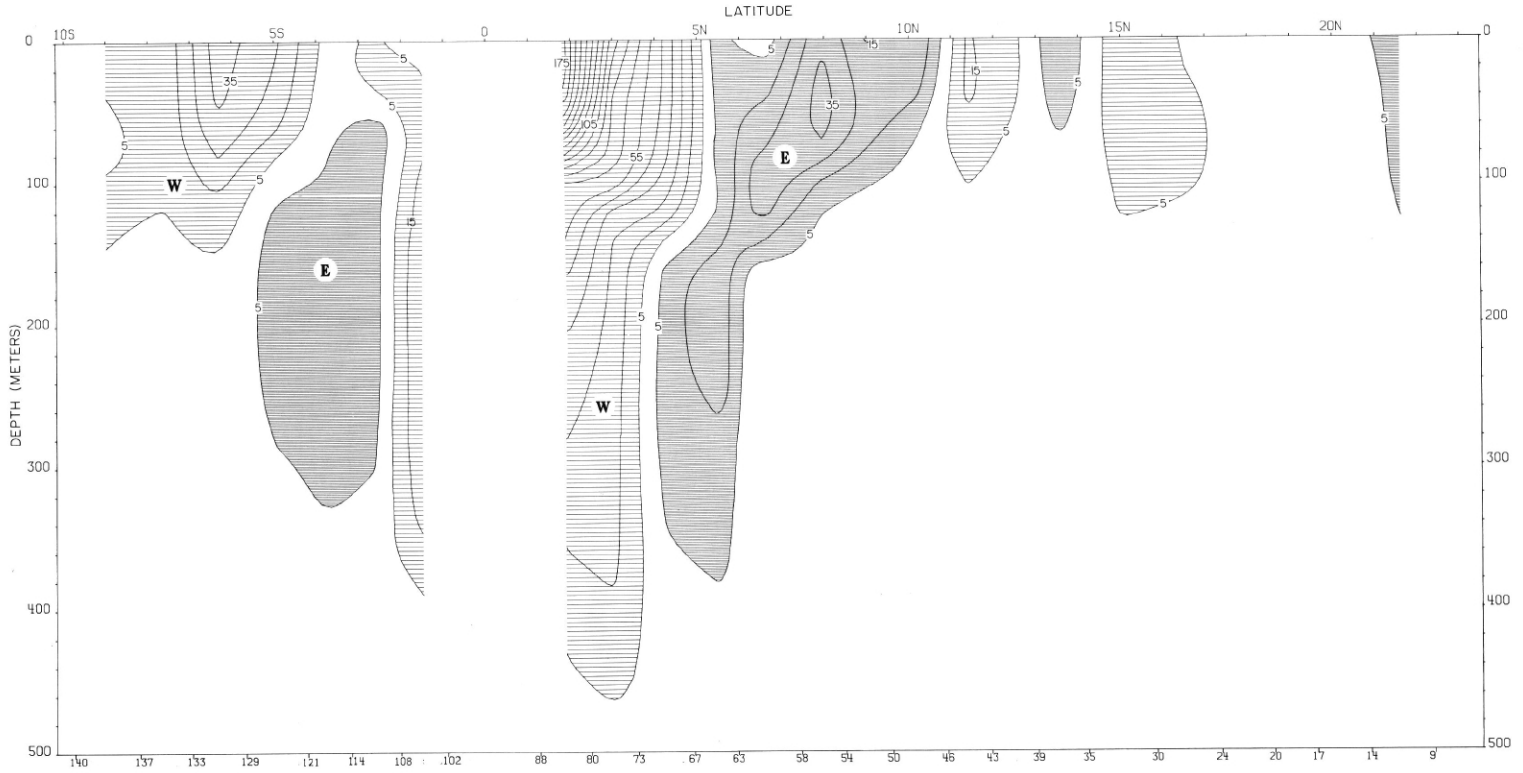

FIGURE 45-G-v1.—Vertical distribution of the zonal component of geostrophic velocity (cm./sec.), relative to 500 db., along 119° W., August 3-21, 1967. Dark shading indicates eastward flow with a velocity greater than 5 cm./sec.; light shading indicates westward flow with a velocity greater than 5 cm./sec.

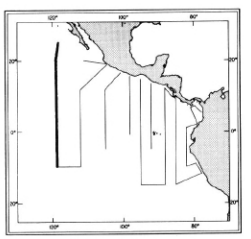

45-G-v1.

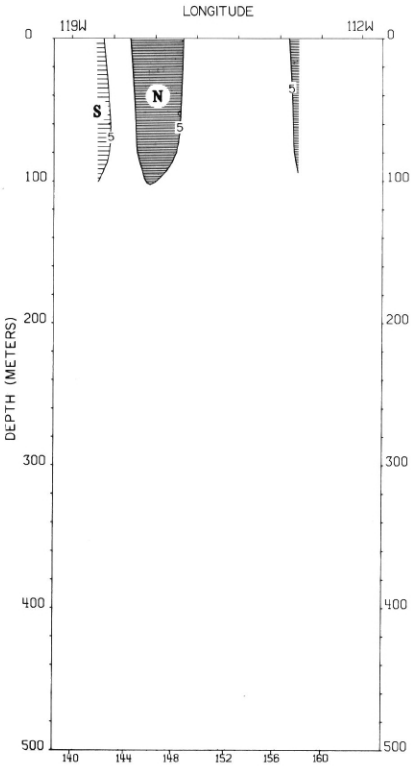

FIGURE 45-G-v2.—Vertical distribution of the meridional component of geostrophic velocity (cm./sec.), relative to 500 db., along 10° S., August 21-23, 1967. Dark shading indicates northward flow with a velocity greater than 5 cm./sec.; light shading indicates southward flow with a velocity greater than 5 cm./sec.

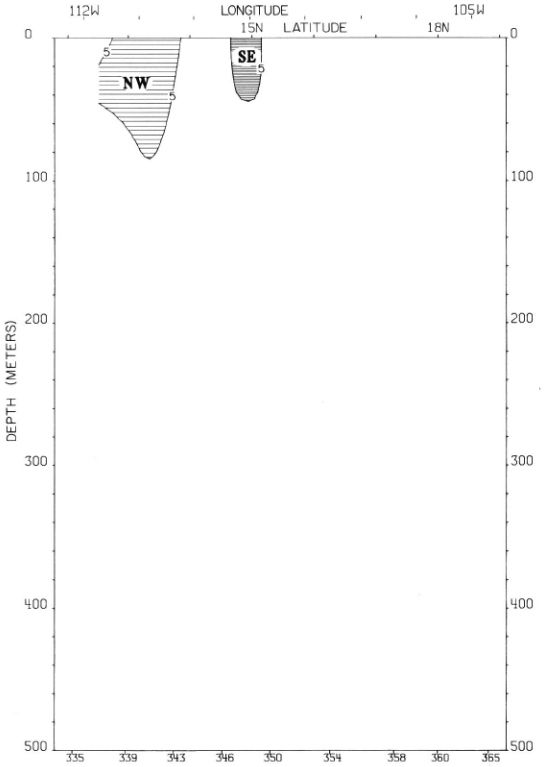

FIGURE 45-G-v5.—Vertical distribution of the component of geostrophic velocity (cm./sec.), relative to 500 db., normal to a section from 12° N., 112° W. to Manzanillo, September 7-10, 1967. Dark shading indicates flow toward the southeast with a velocity greater than 5 cm./sec.; light shading indicates flow toward the northwest with a velocity greater than 5 cm./sec.

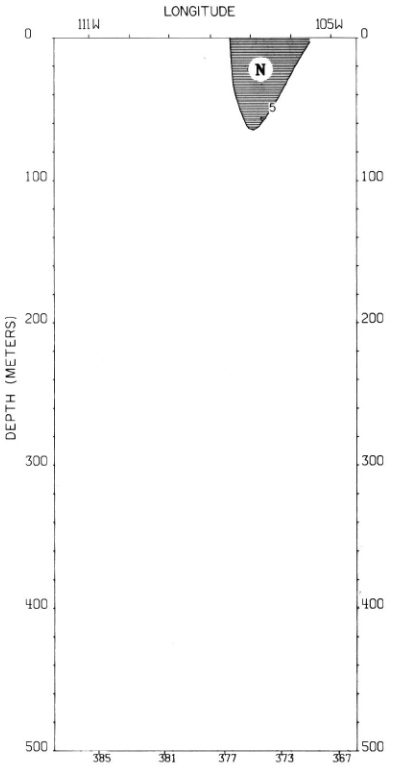

FIGURE 45-G-v6.—Vertical distribution of the meridional component of geostrophic velocity (cm./sec.), relative to 500 db., along 19°30′ N. from Manzanillo to 111°25′ W., September 13-15, 1967. The dark shading indicates northward flow with a velocity greater than 5 cm./sec.

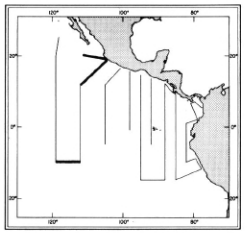

45-G-v2.

45-G-v5.

45-G-v6.

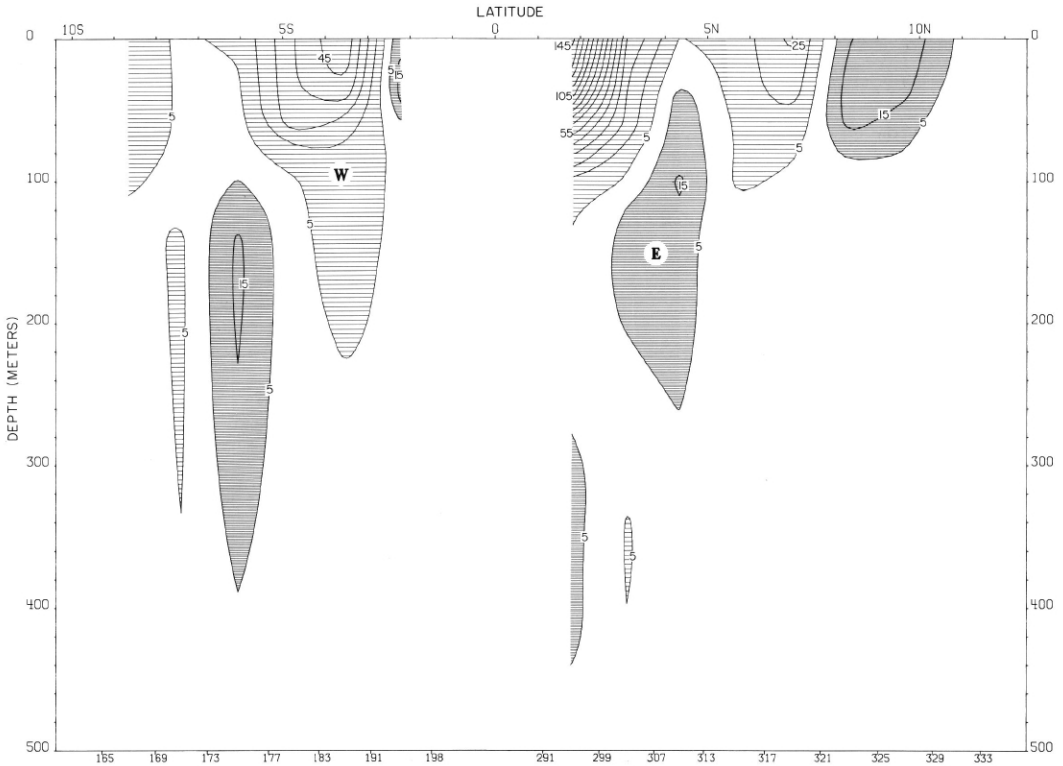

FIGURE 45-G-v3.—Vertical distribution of the zonal component of geostrophic velocity (cm./sec.), relative to 500 db., along 112° W., August 23-September 7, 1967. Dark shading indicates eastward flow with a velocity greater than 5 cm./sec.; light shading indicates westward flow with a velocity greater than 5 cm./sec.

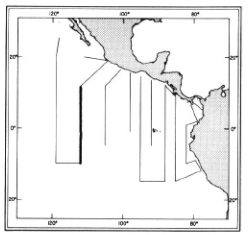

45-G-v3.

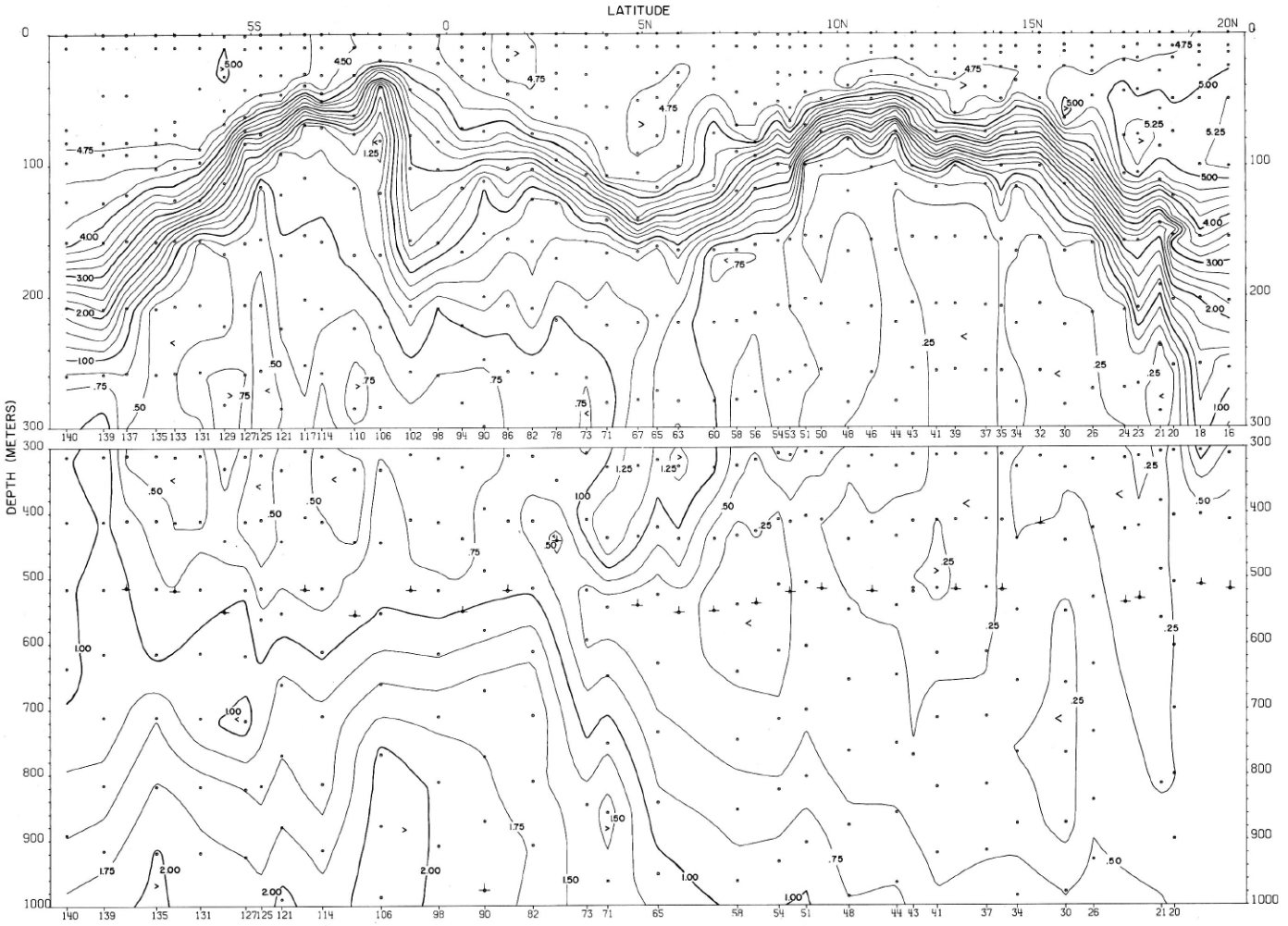

FIGURE 45-O₂-v1.—Vertical distribution of oxygen (ml./l.) along 119° W., August 7-21, 1967.

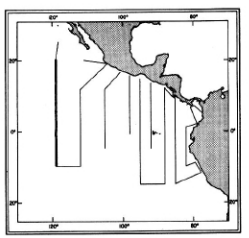

45-O₂-v1.

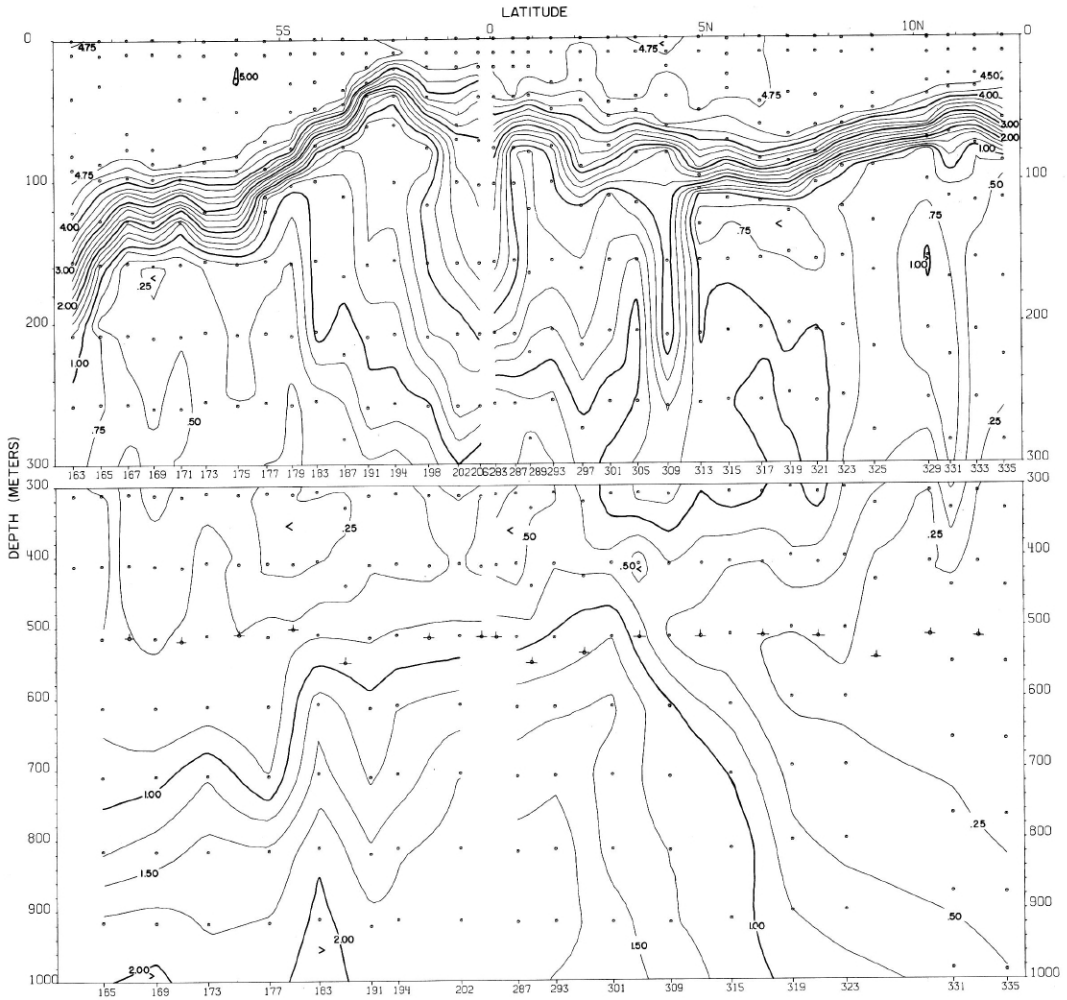

FIGURE 45-O₂-v3.—Vertical distribution of oxygen (ml./l.) along 112° W., August 23-September 7, 1967. The interruption in the contours indicates a 5-day interval between Stations 206 and 283 in the upper (0-500 m.) portion of the section, or between Stations 202 and 287 in the lower portion.

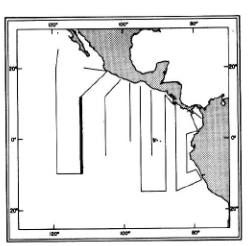

45-O₂-v3.

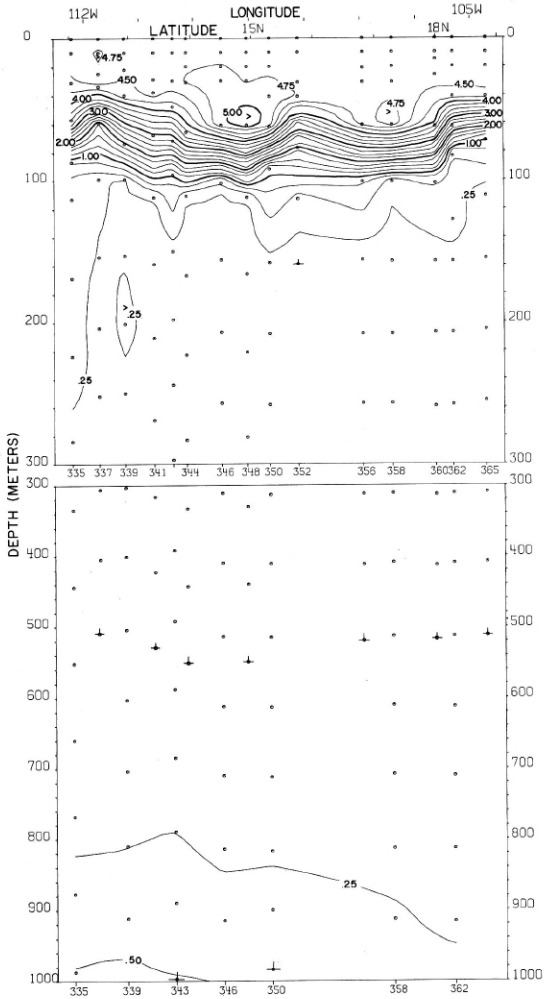

FIGURE 45-O₂-v5.—Vertical distribution of oxygen (ml./l.) along a section from 12° N., 112° W. to Manzanillo, September 7-10, 1967.

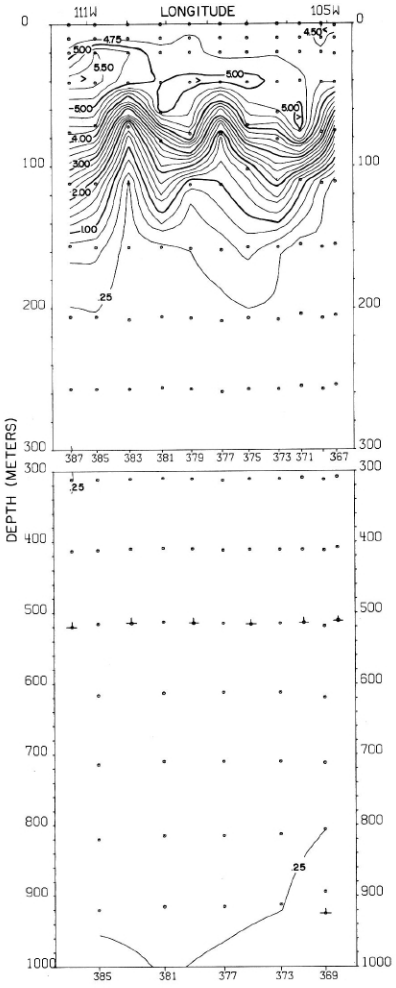

FIGURE 45-O₂-v6.—Vertical distribution of oxygen (ml./l.) along 19°30′ N. from Manzanillo to 111°25′ W., September 13-15, 1967.

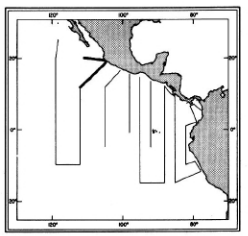

45-O₂-v5.

45-O₂-v6.

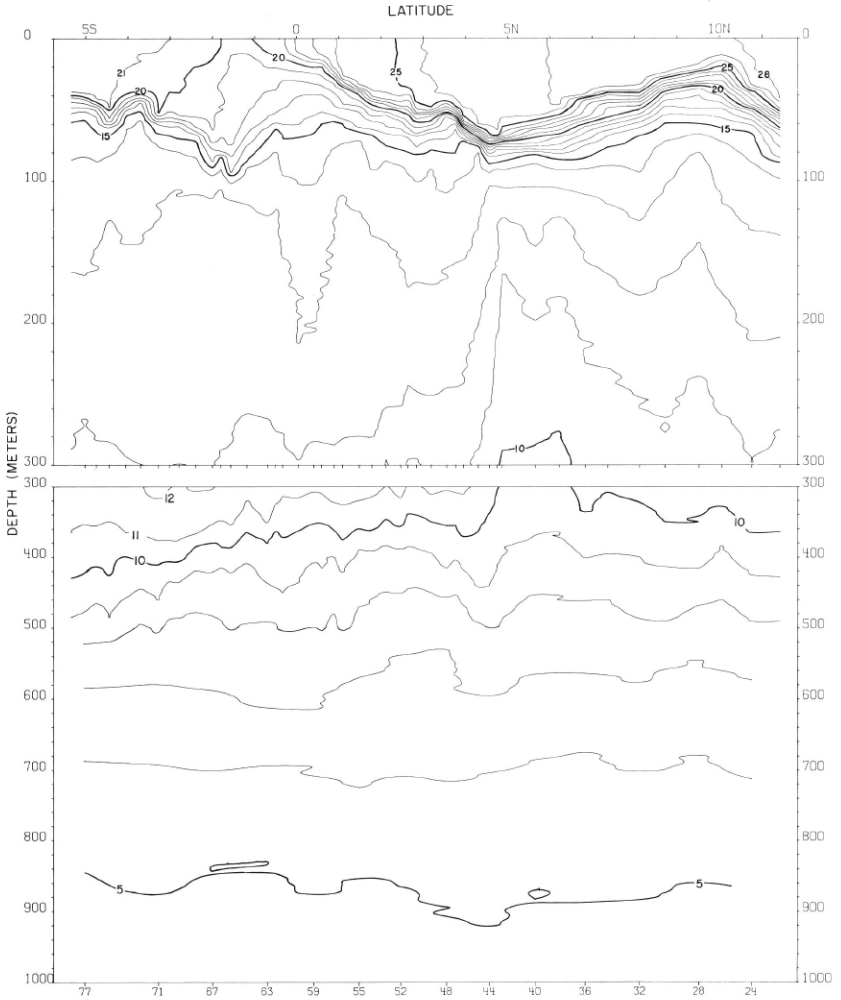

FIGURE 46-T-v2.—Vertical distribution of temperature (° C.) along 105° W., August 19-28, 1967.

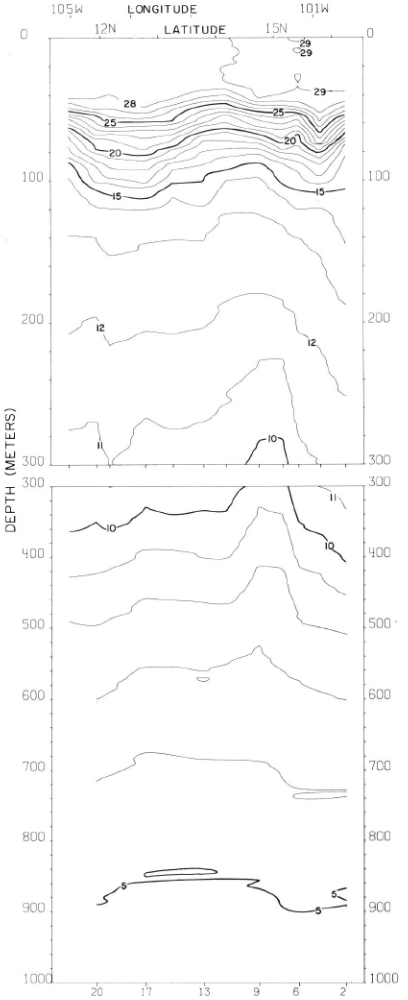

FIGURE 46-T-v1.—Vertical distribution of temperature (° C.) along a section from Acapulco to 12° N., 105° W., August 16-19, 1967.

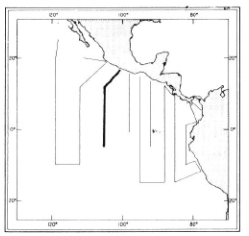

46-T-v1.

46-T-v2.

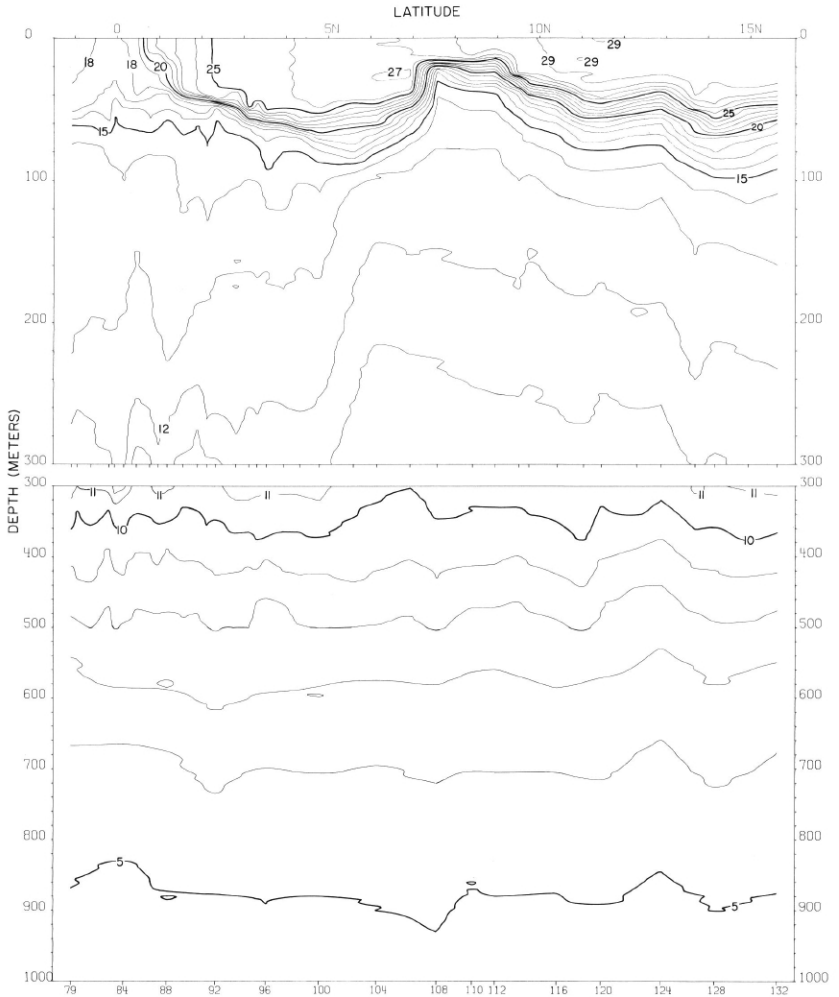

FIGURE 46-T-v3.—Vertical distribution of temperature (° C.) along 98° W., August 31-September 6, 1967.

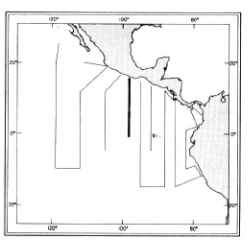

46-T-v3.

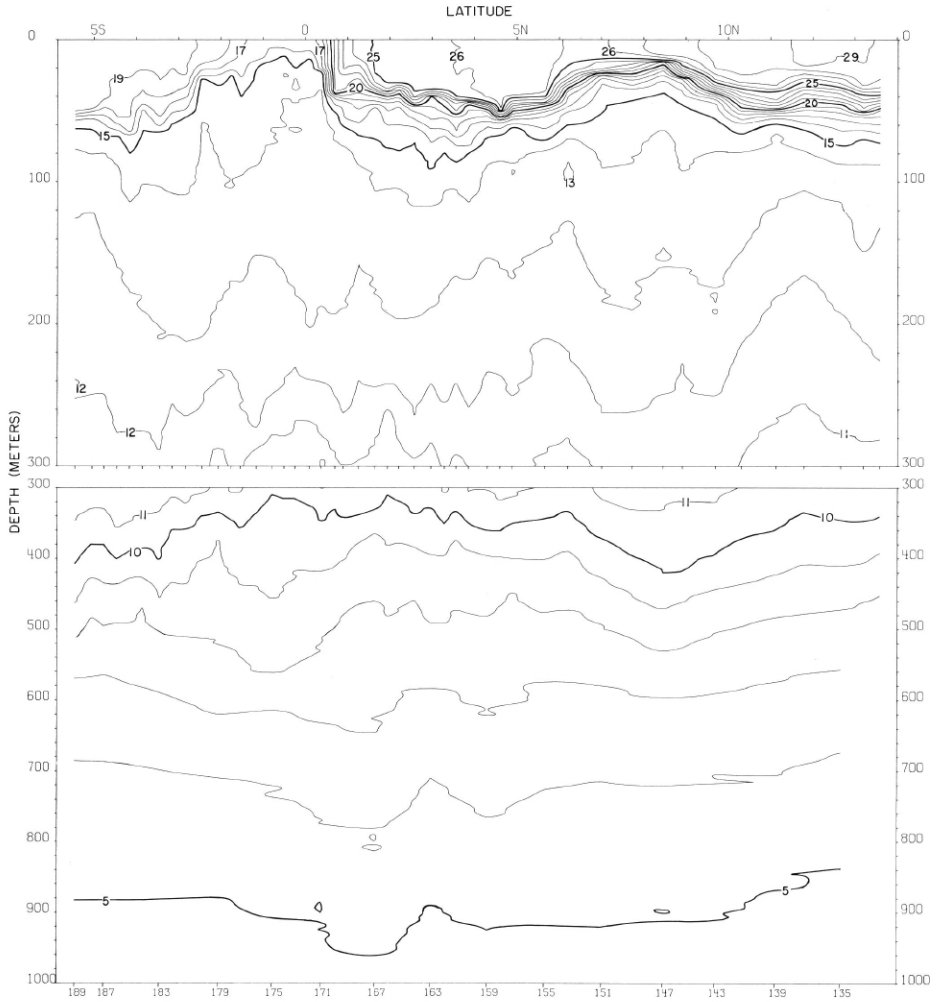

FIGURE 46-T-v4.—Vertical distribution of temperature (° C.) along 92° W., September 15-22, 1967.

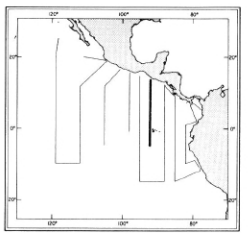

46-T-v4.

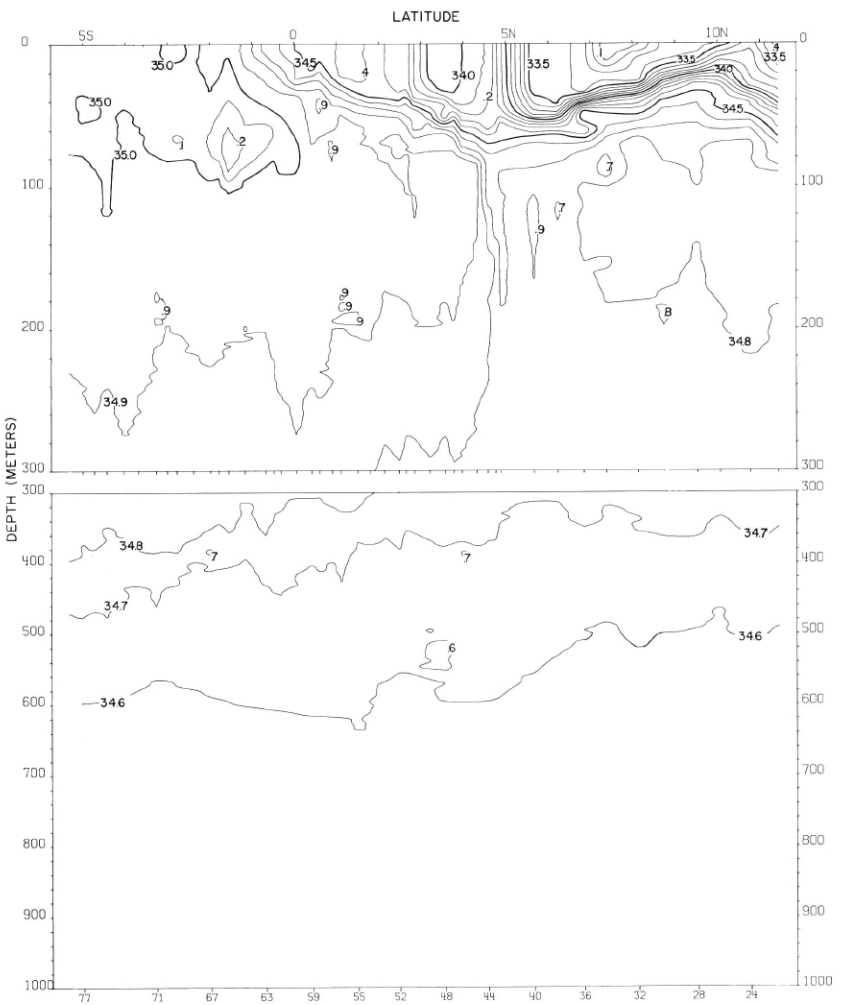

FIGURE 46-S-v2.—Vertical distribution of salinity (‰) along 105° W., August 19-28, 1967.

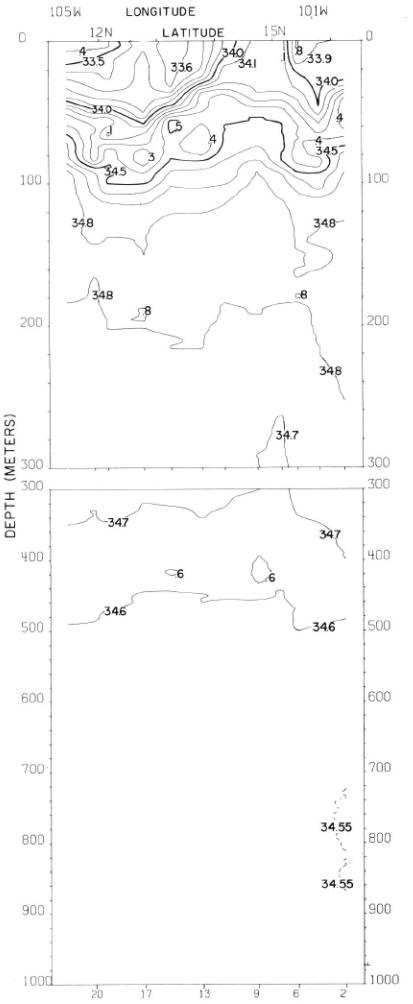

FIGURE 46-S-v1.—Vertical distribution of salinity (‰) along a section from Acapulco to 12° N., 105° W., August 16-19, 1967.

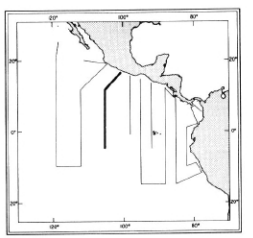

46-S-v1.

46-S-v2.

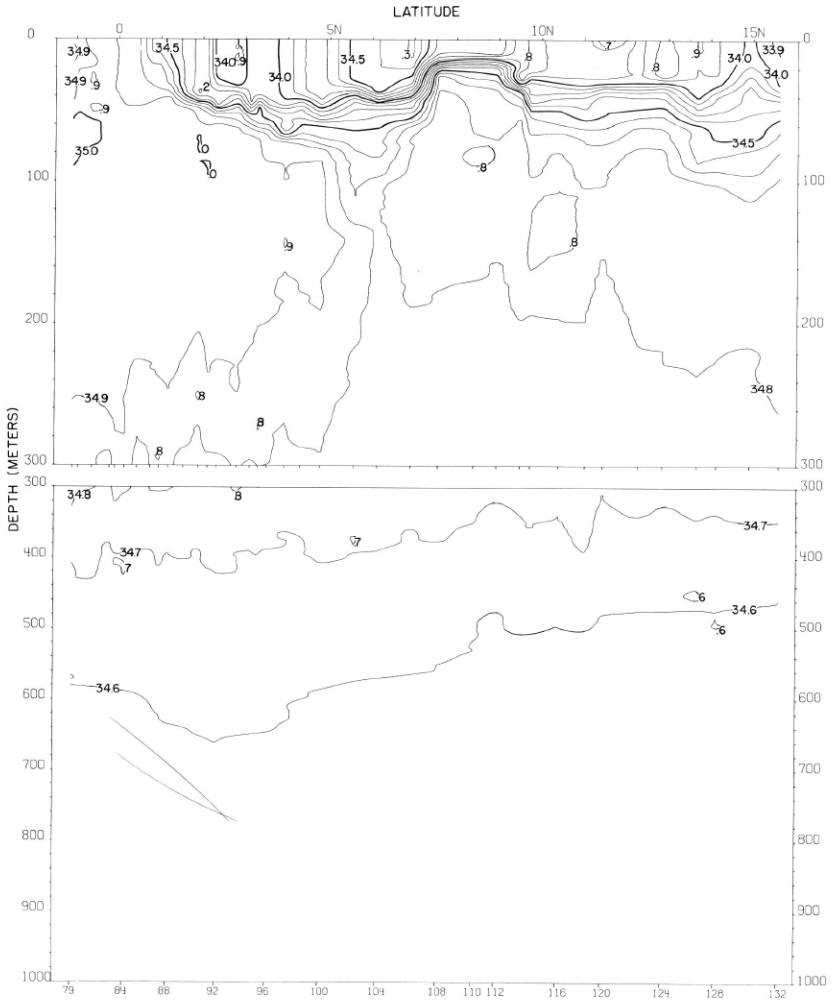

FIGURE 46-S-v3.—Vertical distribution of salinity (‰) along 98° W., August 31-September 6, 1967.

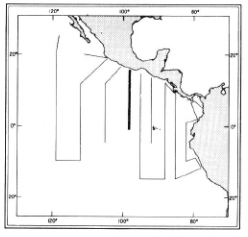

46-S-v3.

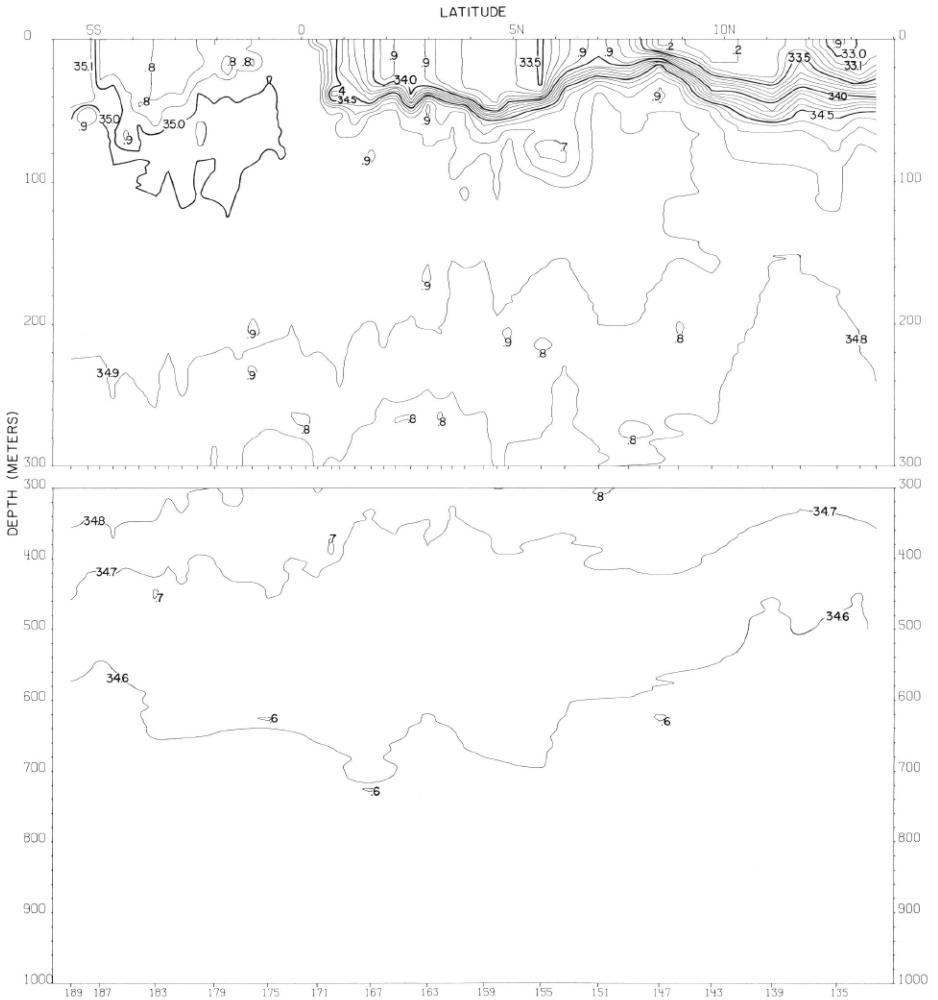

FIGURE 46-S-v4.—Vertical distribution of salinity (‰) along 92° W., September 15-22, 1967.

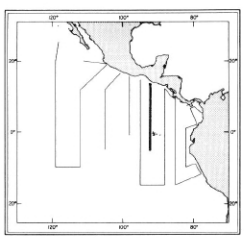

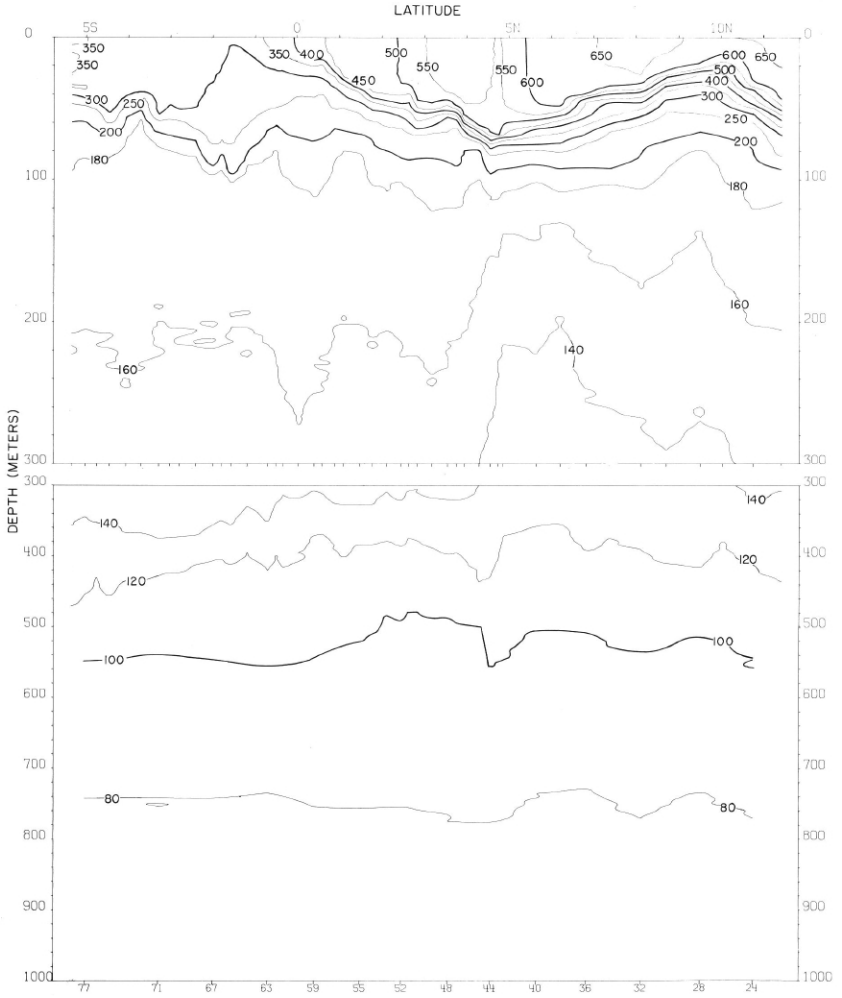

FIGURE 46-δ-v2.—Vertical distribution of thermosteric anomaly, δ_T, (cl./t.) along 105° W., August 19-28, 1967.

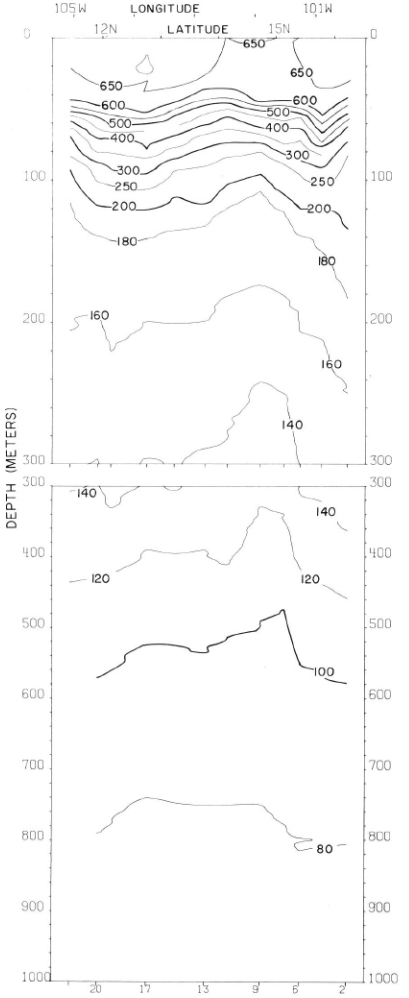

FIGURE 46-δ-v1.—Vertical distribution of thermosteric anomaly, δ_T, (cl./t.) along a section from Acapulco to 12° N., 105° W., August 16-19, 1967.

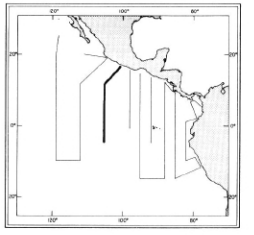

46-δ-v1.

46-δ-v2.

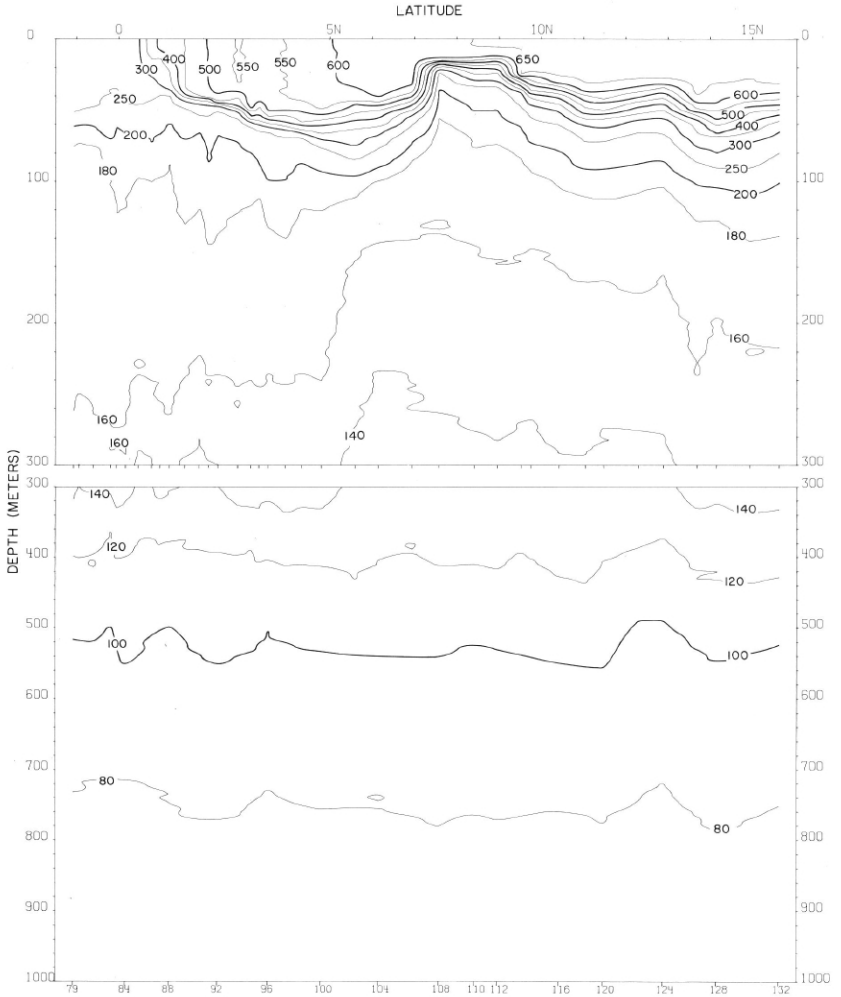

FIGURE 46-δ-v3.—Vertical distribution of thermosteric anomaly, δ_T, (cl./t.) along 98° W., August 31-September 6, 1967.

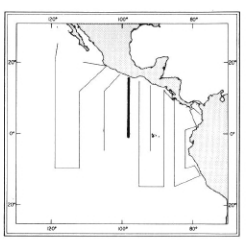

46-δ-v3.

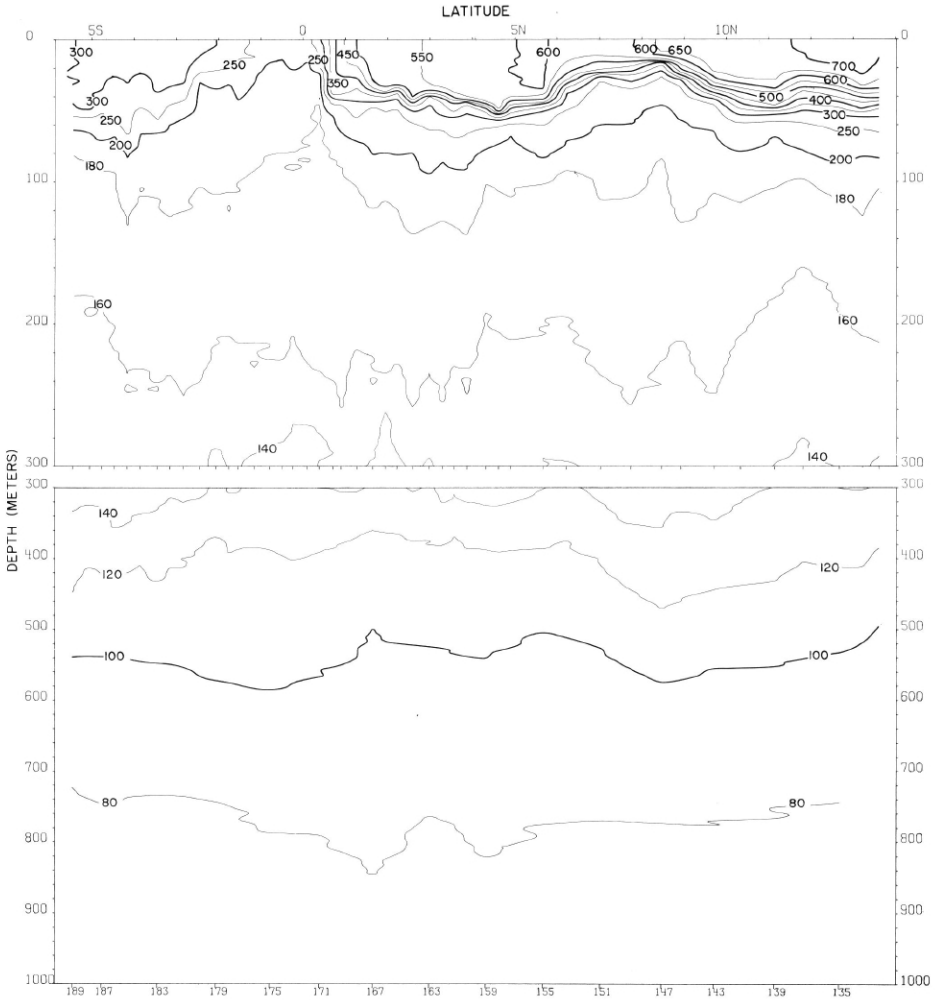

FIGURE 46-δ-v4.—Vertical distribution of thermosteric anomaly, δ_T, (cl./t.) along 92° W., September 15-22, 1967.

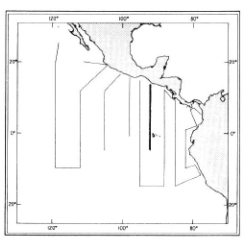

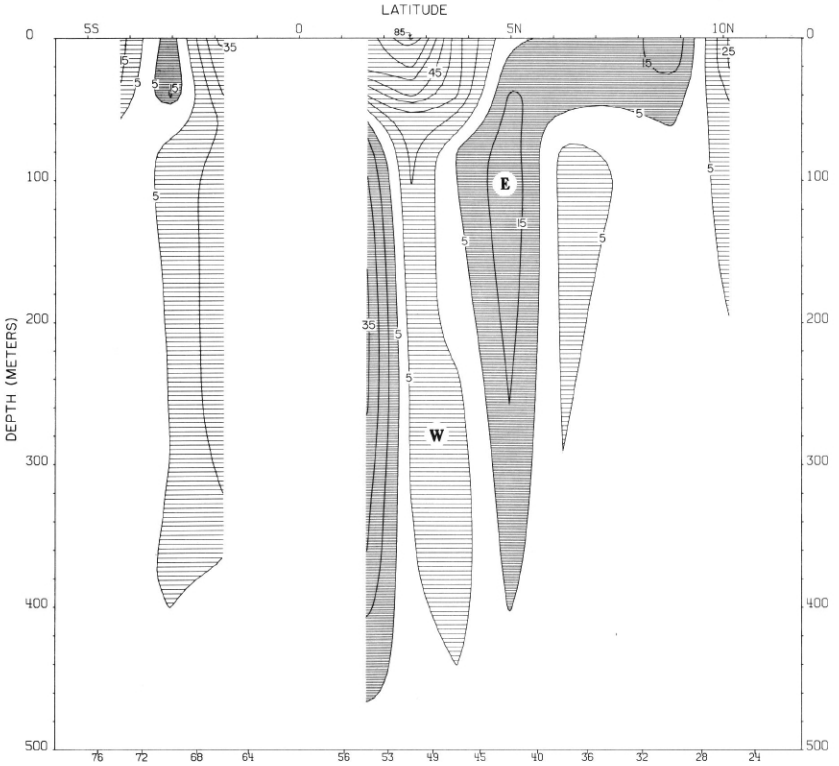

FIGURE 46-G-v2.—Vertical distribution of the zonal component of geostrophic velocity (cm./sec.), relative to 500 db., along 105° W., August 19-28, 1967. Dark shading indicates eastward flow with a velocity greater than 5 cm./sec.; light shading indicates westward flow with a velocity greater than 5 cm./sec.

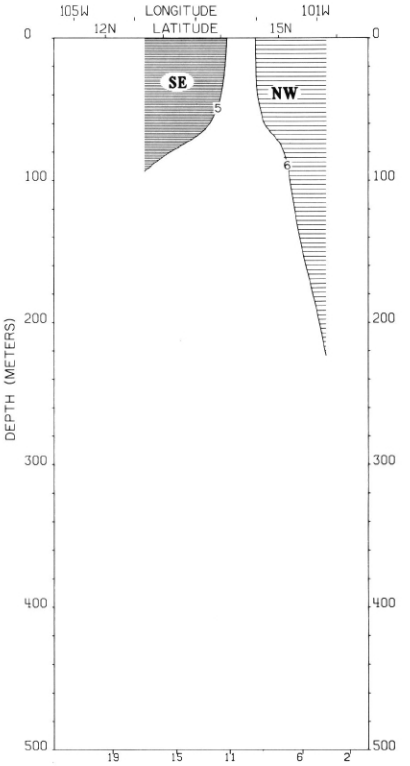

FIGURE 46-G-v1.—Vertical distribution of the component of geostrophic velocity (cm./sec.), relative to 500 db., normal to a section from Acapulco to 12° N., 105° W., August 16-19, 1967. Dark shading indicates flow toward the southeast with a velocity greater than 5 cm./sec.; light shading indicates flow toward the northwest with a velocity greater than 5 cm./sec.

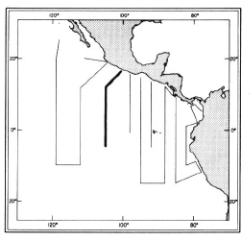

46-G-v1.

46-G-v2.

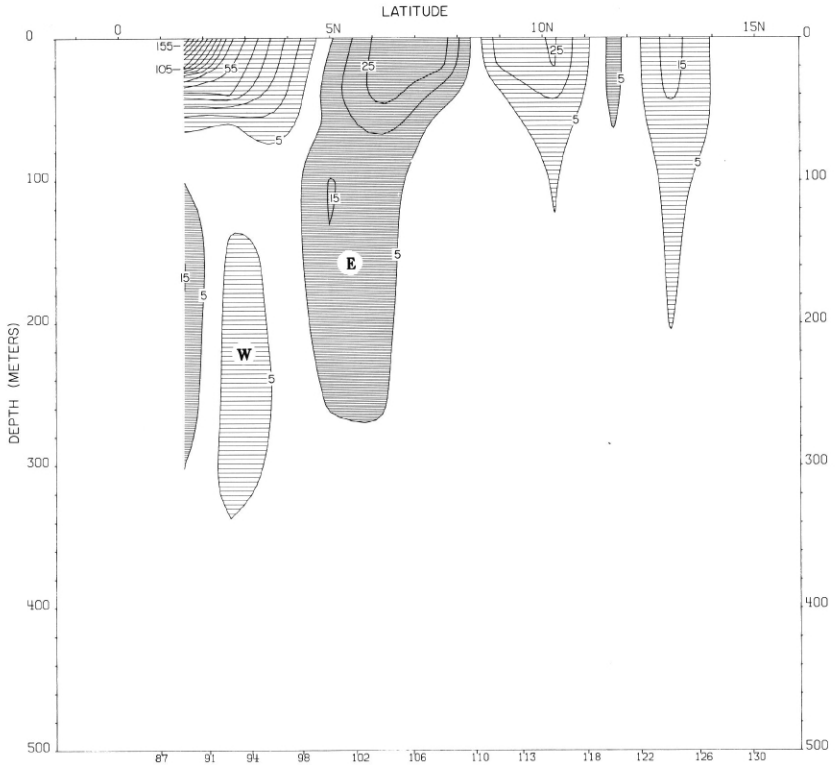

FIGURE 46-G-v3.—Vertical distribution of the zonal component of geostrophic velocity (cm./sec.), relative to 500 db., along 98° W., August 31-September 6, 1967. Dark shading indicates eastward flow with a velocity greater than 5 cm./sec.; light shading indicates westward flow with a velocity greater than 5 cm./sec.

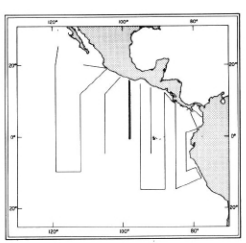

46-G-v3.

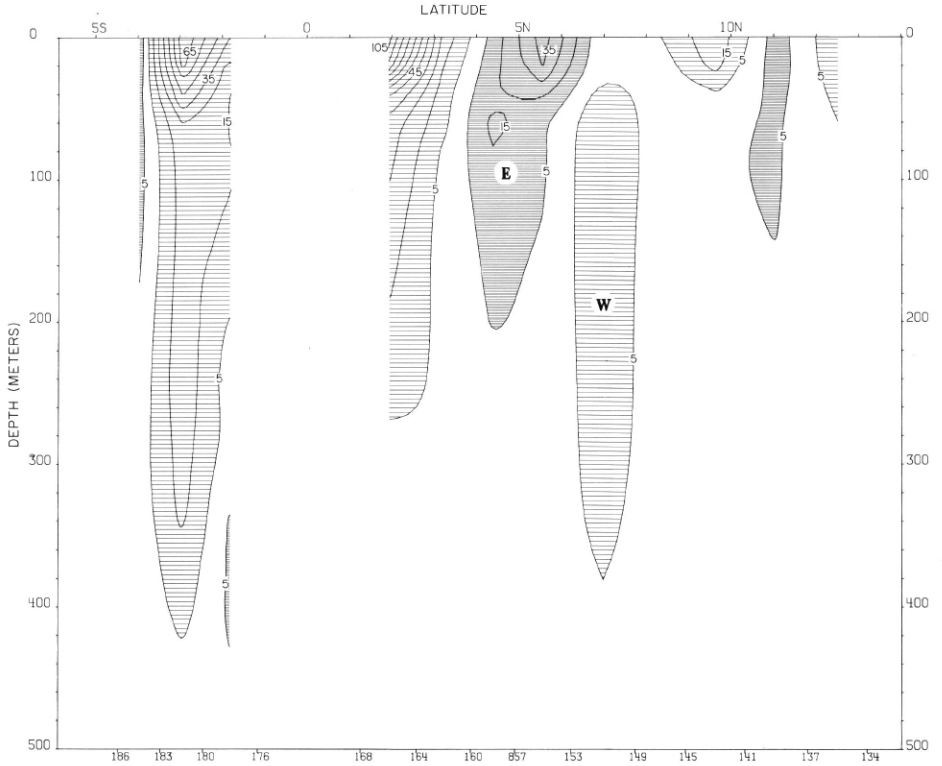

FIGURE 46-G-v4.—Vertical distribution of the zonal component of geostrophic velocity (cm./sec.), relative to 500 db., along 92° W., September 15-22, 1967. Dark shading indicates eastward flow with a velocity greater than 5 cm./sec.; light shading indicates westward flow with a velocity greater than 5 cm./sec.

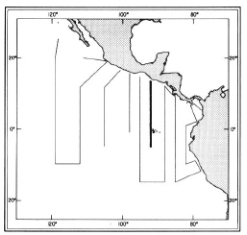

46-G-v4.

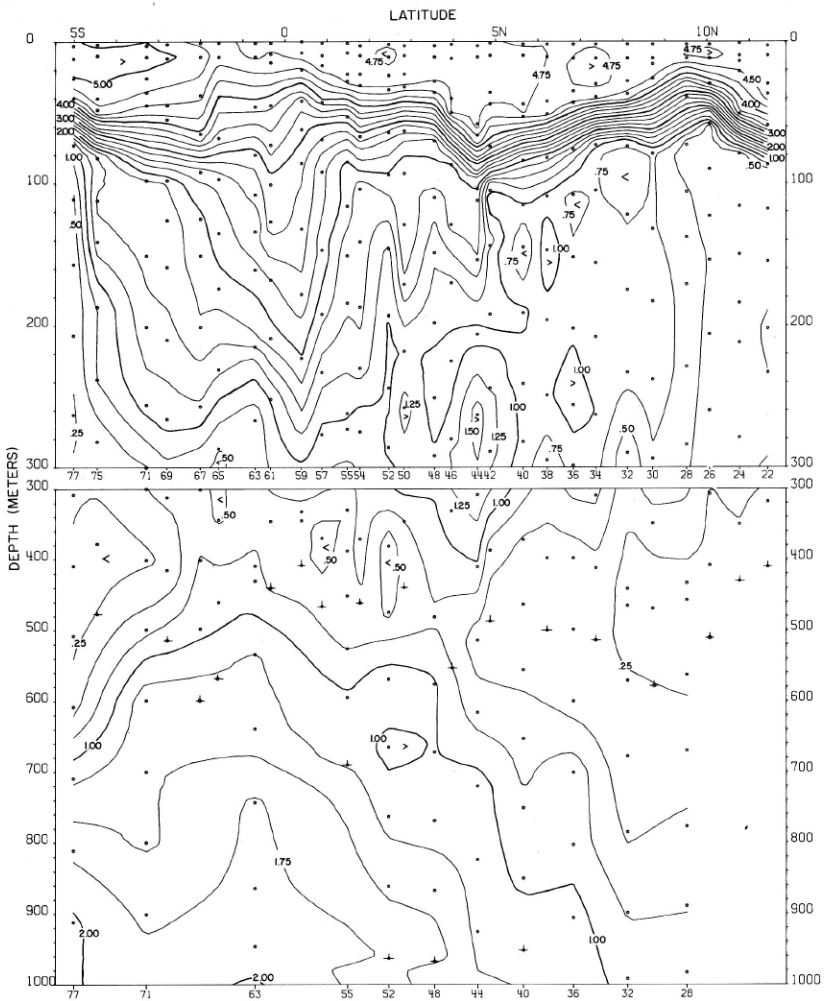

FIGURE 46-O_2-v2.—Vertical distribution of oxygen (ml./l.) along 105° W., August 19-28, 1967.

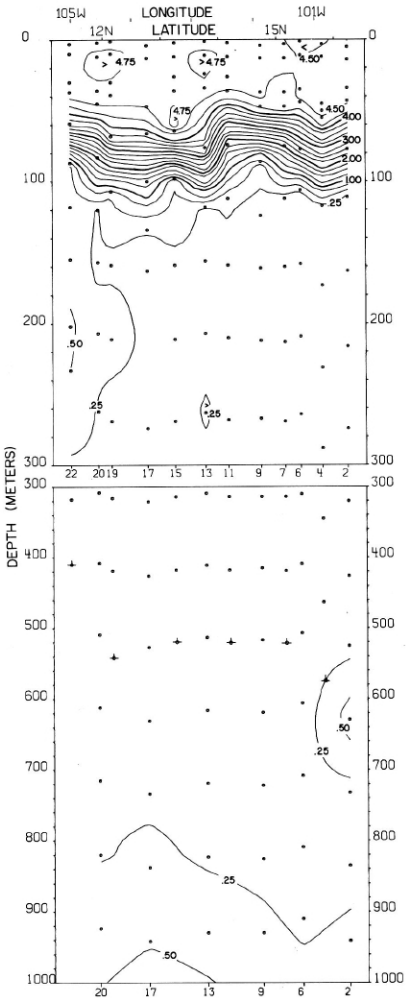

FIGURE 46-O_2-v1.—Vertical distribution of oxygen (ml./l.) along a section from Acapulco to 12° N., 105° W., August 16-19, 1967.

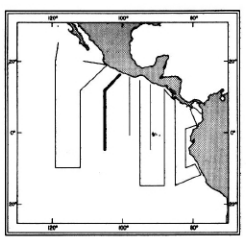

46-O_2-v1.

46-O_2-v2.

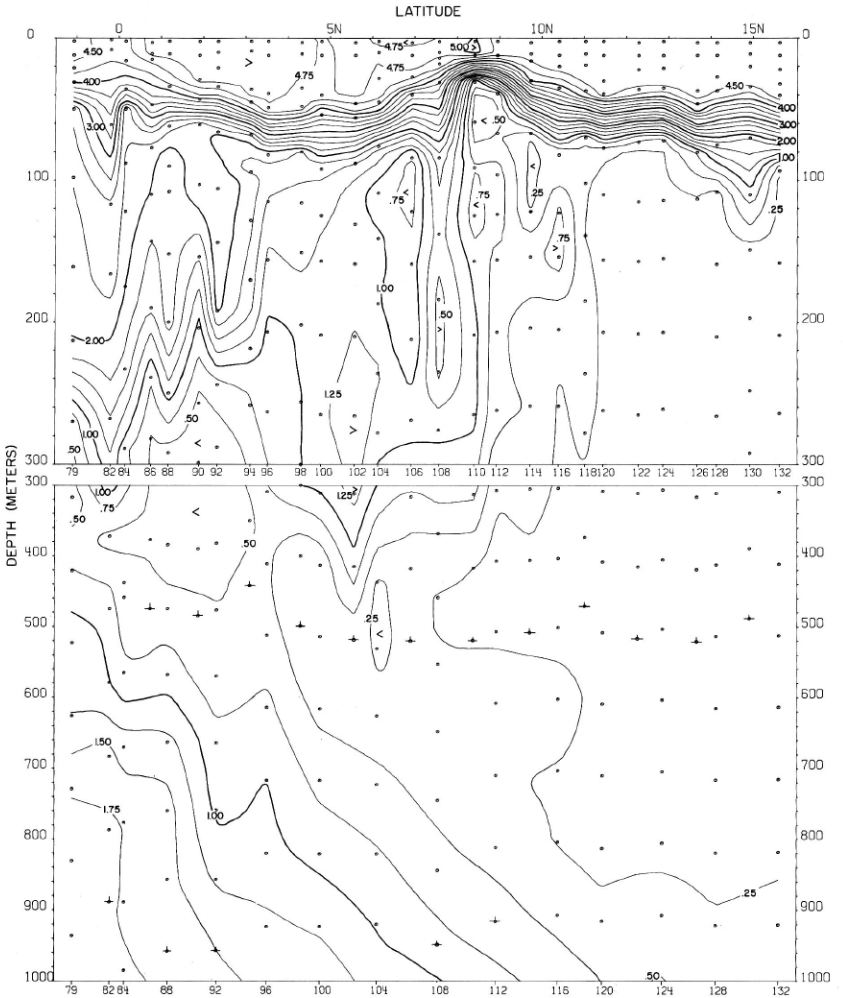

FIGURE 46-O_2-v3.—Vertical distribution of oxygen (ml./l.) along 98° W., August 31-September 6, 1967.

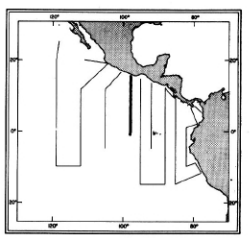

46-O_2-v3.

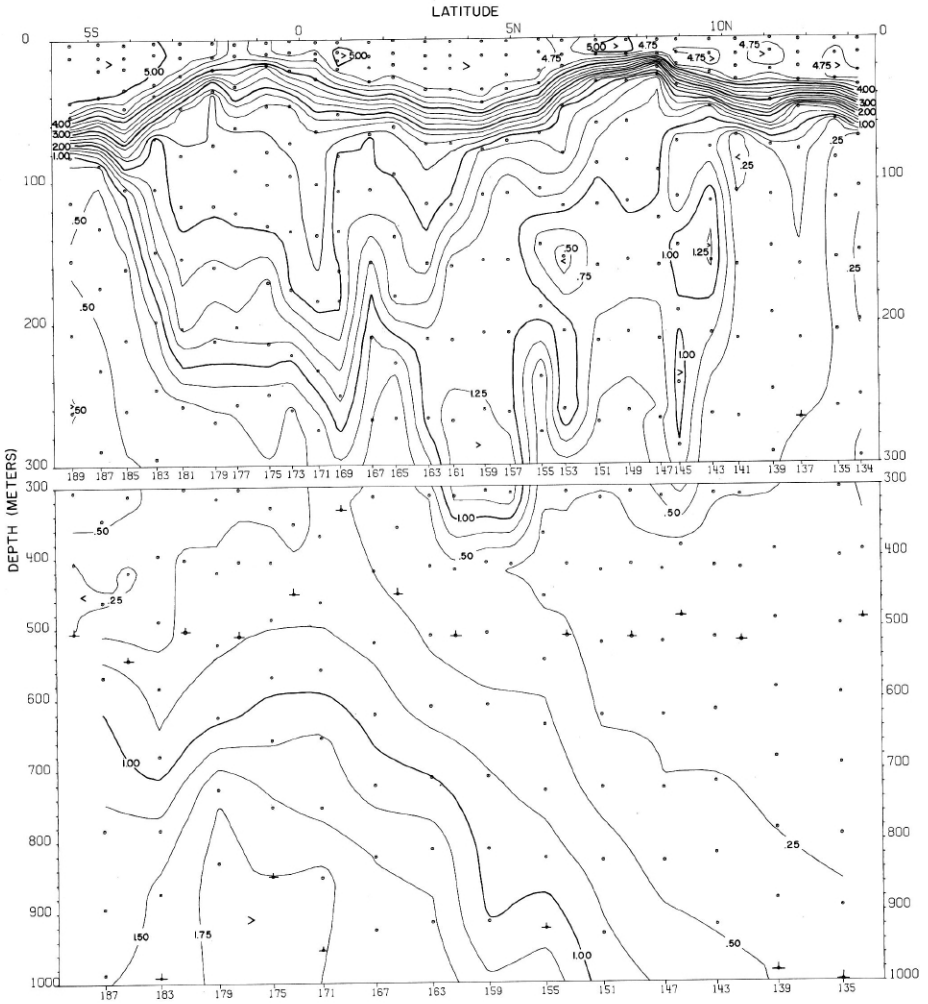

FIGURE 46-O_2-v4.—Vertical distribution of oxygen (ml./l.) along 92° W., September 15-22, 1967.

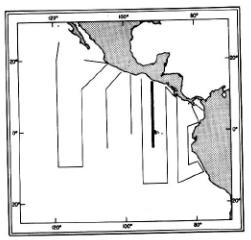

46-O_2-v4.

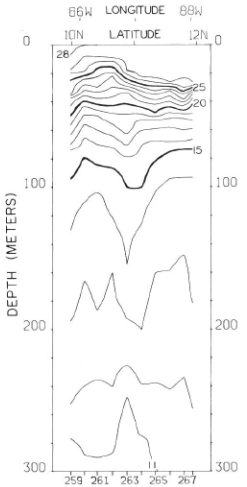

FIGURE 47-T-v9.—Vertical distribution of temperature (°C.) along the coasts of Costa Rica and Nicaragua from 85°52′ W. to 88°02′ W., August 30-31, 1967. These contours are based on STD data read from analog traces.

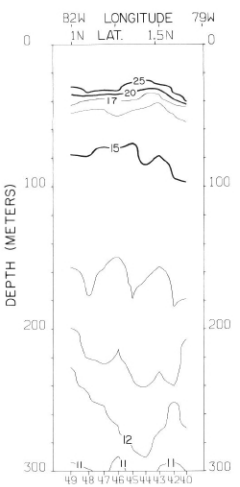

FIGURE 47-T-v3.—Vertical distribution of temperature (°C.) along 1°20′ N. from the coast of Colombia to 82° W., August 5, 1967. These contours are based on STD data read from analog traces.

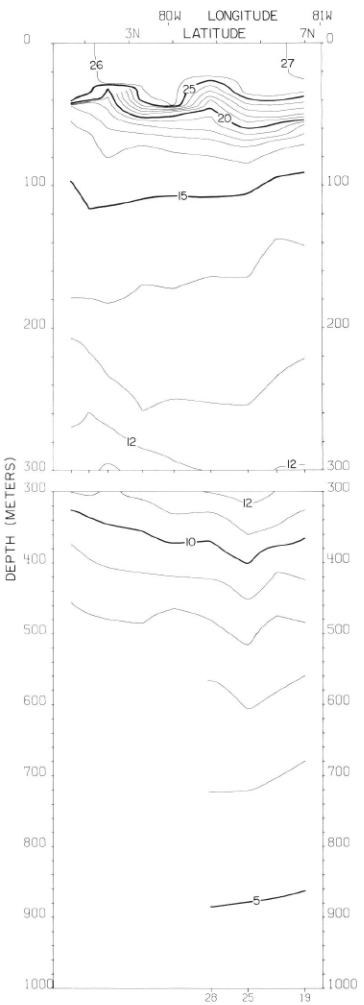

FIGURE 47-T-v2.—Vertical distribution of temperature (°C.) along a northwest-southeast section in the central portion of the Panama Bight from Peninsula de Azuero, Panama, to the coast of Colombia, August 3-5, 1967. These contours are based on STD data read from analog traces.

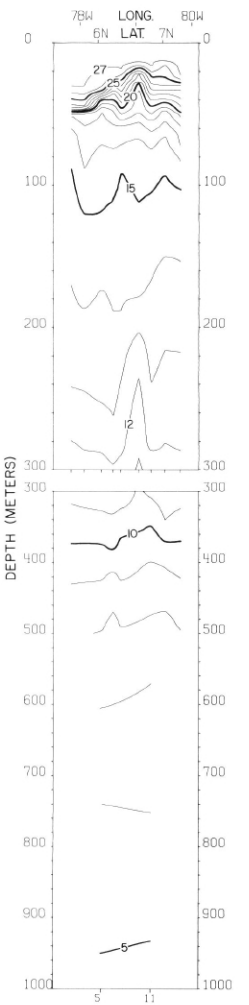

FIGURE 47-T-v1.—Vertical distribution of temperature (°C.) across the northern portion of the Panama Bight from the coast of Colombia to Cabo Mala, Panama, August 1-2, 1967. These contours are based on STD data read from analog traces.

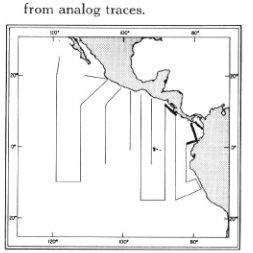

47-T-v1.

47-T-v2.

47-T-v3.

47-T-v9.

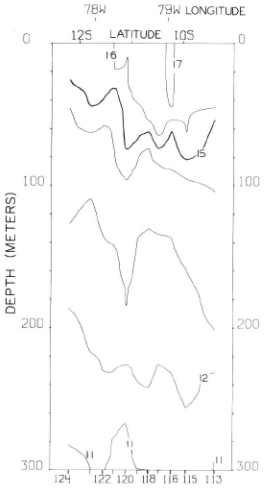

FIGURE 47-T-v6.—Vertical distribution of temperature (°C.) along the coast of Peru from 9°22′ S. to 12°12′ S., August 13-16, 1967. These contours are based on STD data read from analog traces.

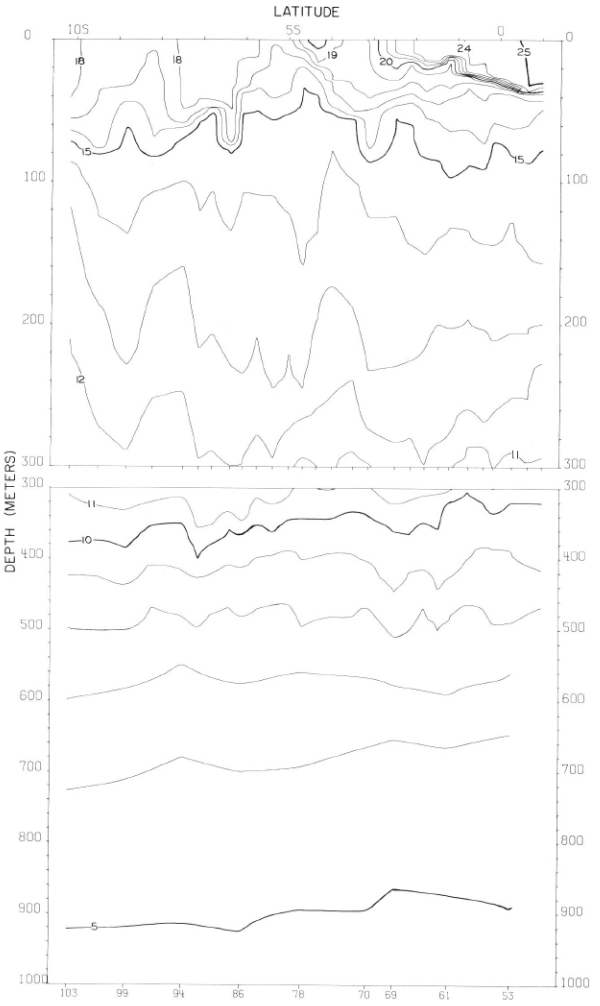

FIGURE 47-T-v4.—Vertical distribution of temperature (°C.) along 82° W., August 5-12, 1967. These contours are based on STD data read from analog traces.

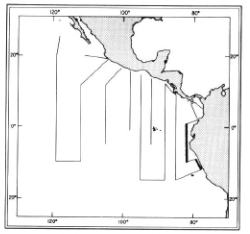

47-T-v4.

47-T-v6.

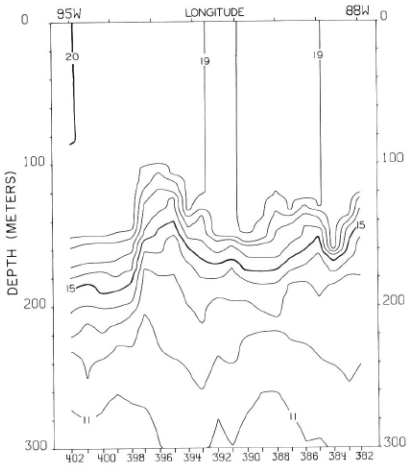

FIGURE 47-T-v11.—Vertical distribution of temperature (°C.) along 15° S., September 10-12, 1967. These contours are based on STD data read from analog traces.

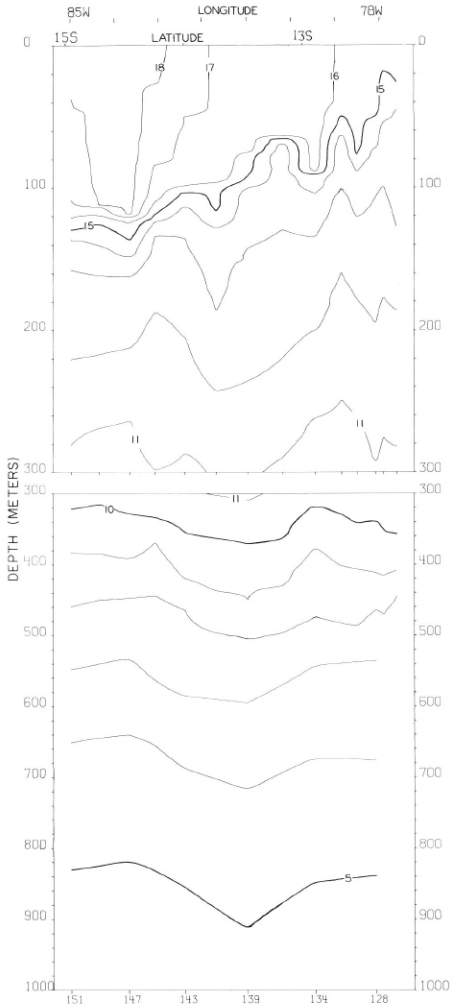

FIGURE 47-T-v7.—Vertical distribution of temperature (°C.) along a northeast-southwest section from the coast of Peru to 15° S., 85° W., August 16-19, 1967. These contours are based on STD data read from analog traces.

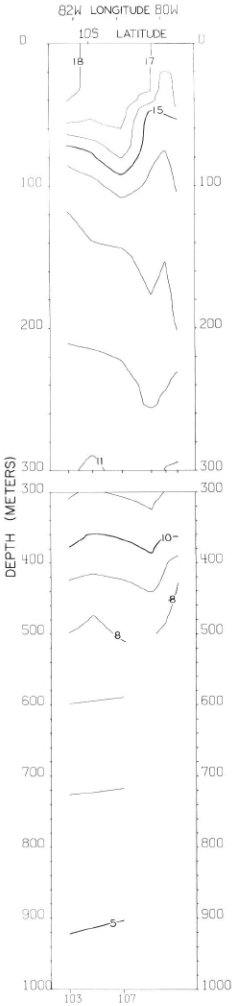

FIGURE 47-T-v5.—Vertical distribution of temperature (°C.) along a southwest-northeast section from 10°09′ S., 82°09′ W. to the coast of Peru, August 12-13, 1967. These contours are based on STD data read from analog traces.

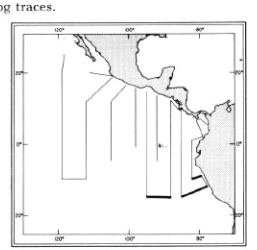

47-T-v5.

47-T-v7.

47-T-v11.

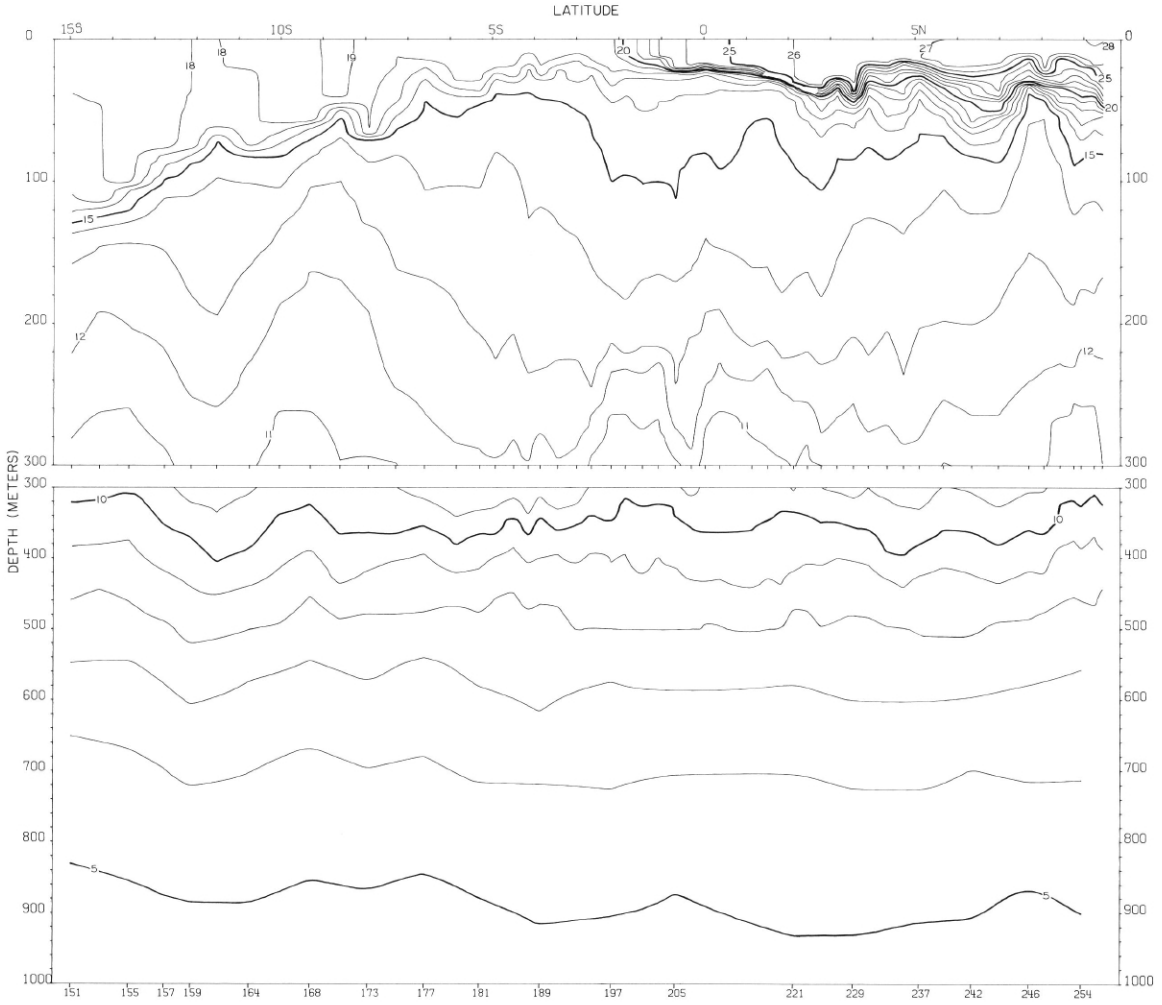

FIGURE 47-T-v8.—Vertical distribution of temperature (°C.) along 85° W., August 19-28, 1967. These contours are based on STD data read from analog traces.

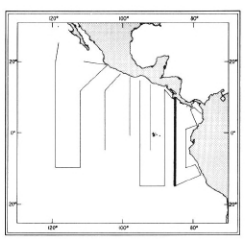

47-T-v8.

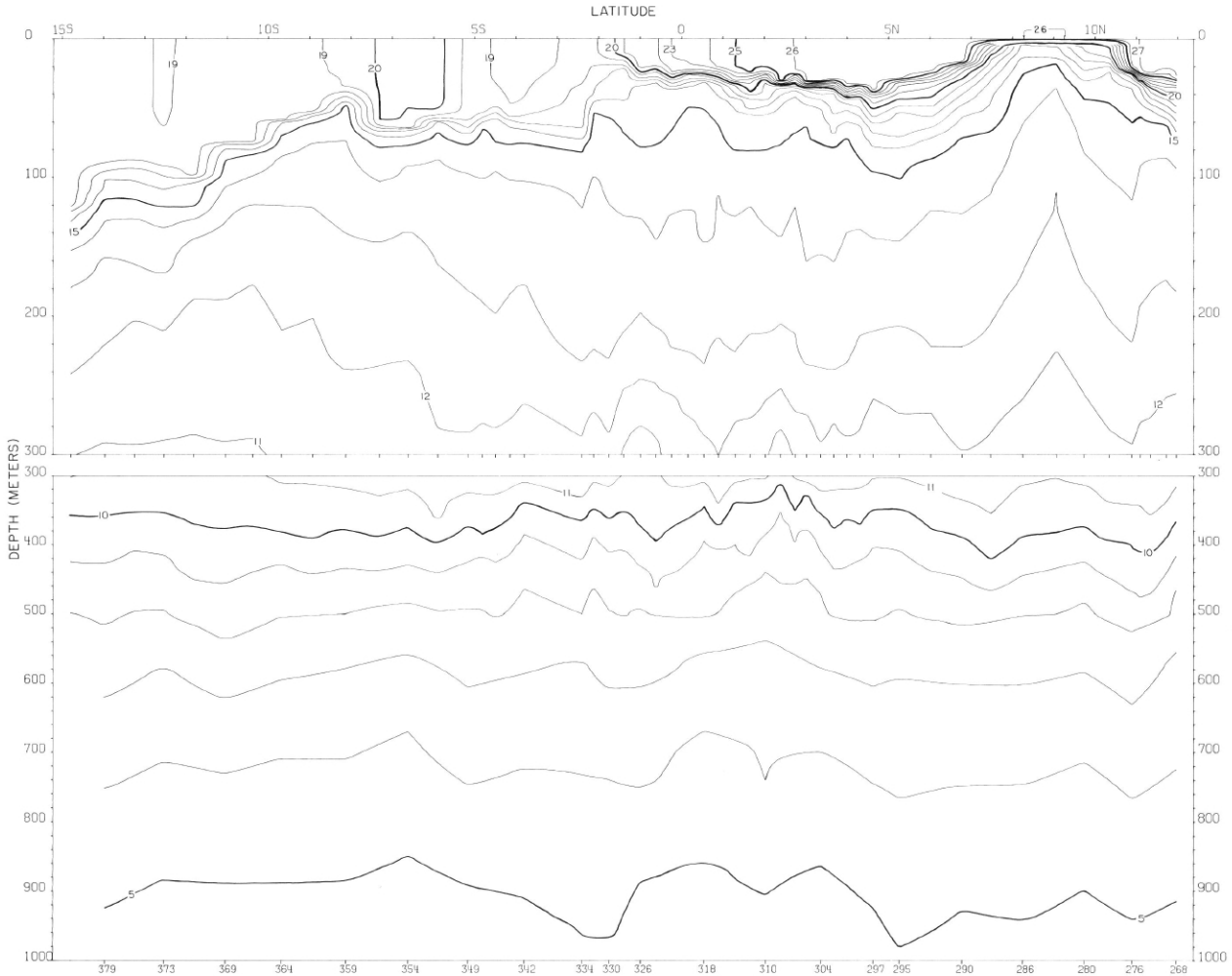

FIGURE 47-T-v10.—Vertical distribution of temperature (°C.) along 88° W., August 31-September 10, 1967. These contours are based on STD data read from analog traces.

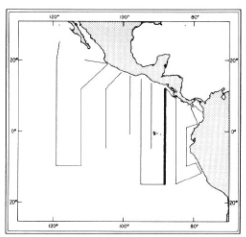

47-T-v10.

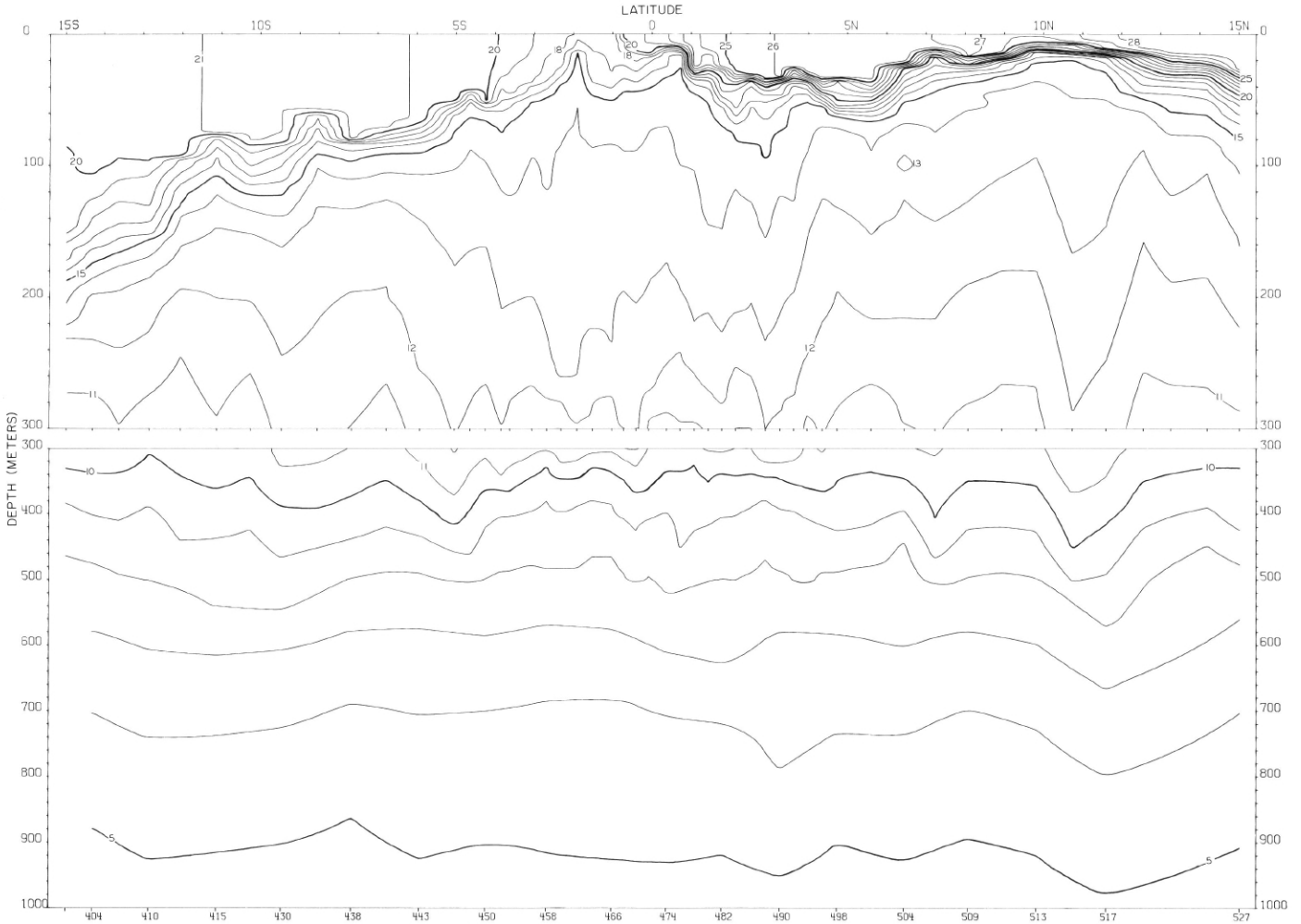

FIGURE 47-T-v12.—Vertical distribution of temperature (°C.) along 95° W., September 12-23, 1967. These contours are based on STD data read from analog traces.

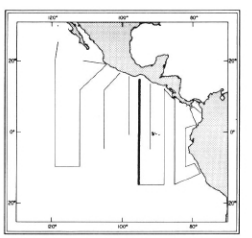

47-T-v12.

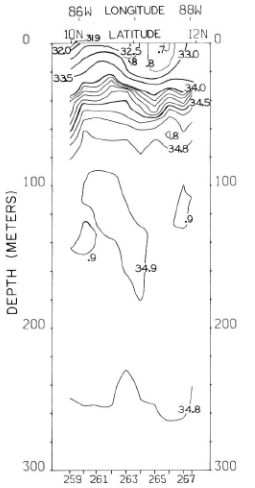

FIGURE 47-S-v9.—Vertical distribution of salinity (‰) along the coasts of Costa Rica and Nicaragua from 85°52′ W. to 88°02′ W., August 30-31, 1967. These contours are based on STD data read from analog traces.

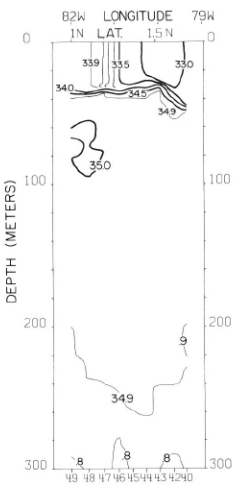

FIGURE 47-S-v3.—Vertical distribution of salinity (‰) along 1°20′ N. from the coast of Colombia to 82° W., August 5, 1967. These contours are based on STD data read from analog traces.

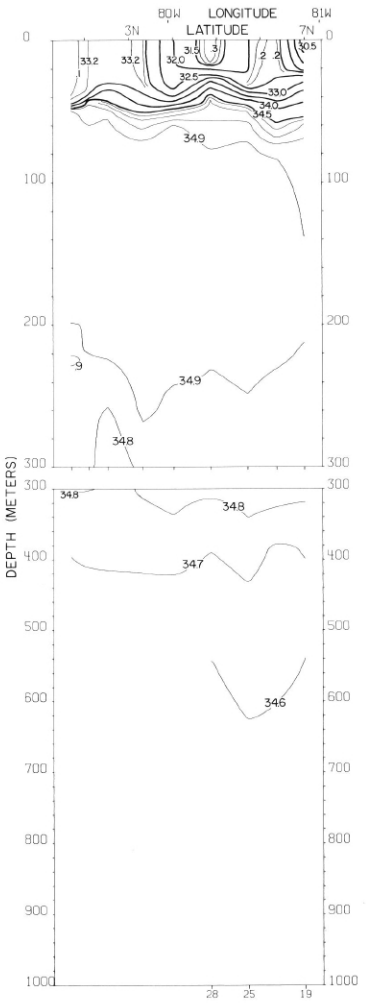

FIGURE 47-S-v2.—Vertical distribution of salinity (‰) along a northwest-southeast section in the central portion of the Panama Bight from Peninsula de Azuero, Panama, to the coast of Colombia, August 3-5, 1967. These contours are based on STD data read from analog traces.

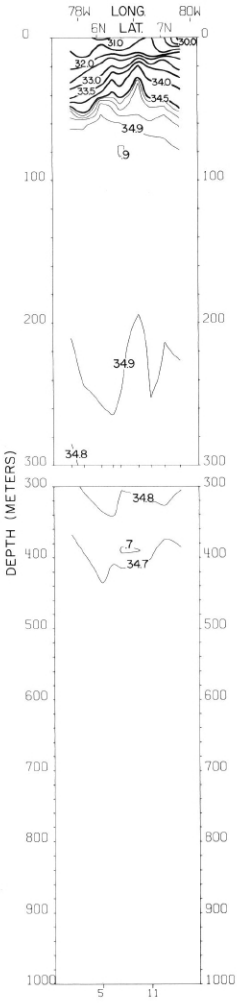

FIGURE 47-S-v1.—Vertical distribution of salinity (‰) across the northern portion of the Panama Bight from the coast of Colombia to Cabo Mala, Panama, August 1-2, 1967. These contours are based on STD data read from analog traces.

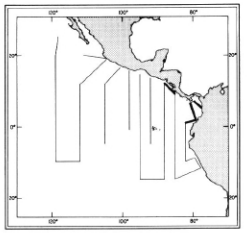

47-S-v1.

47-S-v2.

47-S-v3.

47-S-v9.

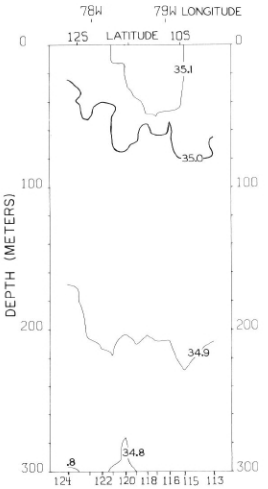

FIGURE 47-S-v6.—Vertical distribution of salinity (‰) along the coast of Peru from 9°22′ S. to 12°12′ S., August 13-16, 1967. These contours are based on STD data read from analog traces.

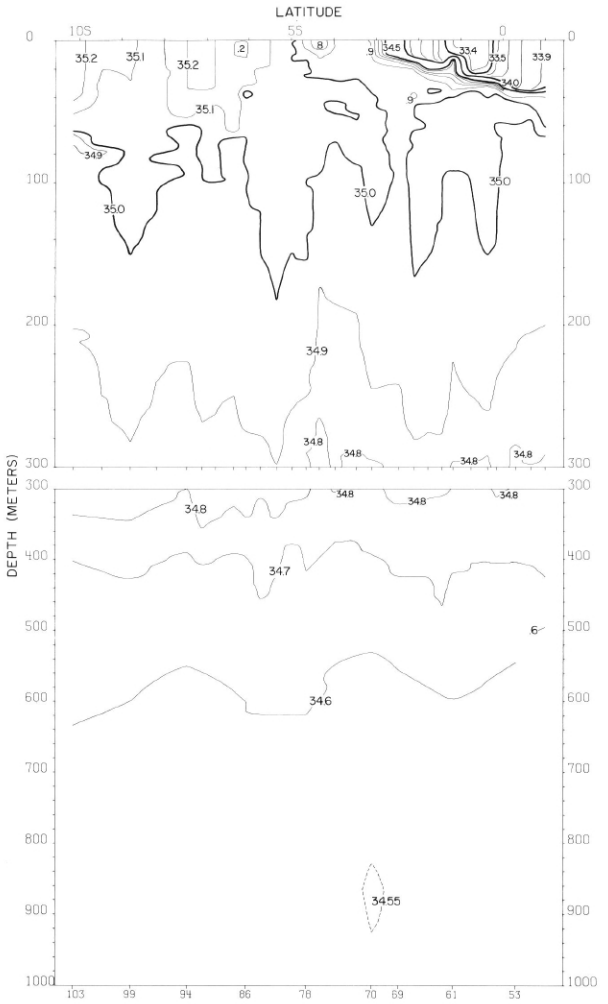

FIGURE 47-S-v4.—Vertical distribution of salinity (‰) along 82° W., August 5-12, 1967. These contours are based on STD data read from analog traces.

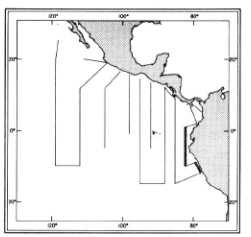

47-S-v4.

47-S-v6.

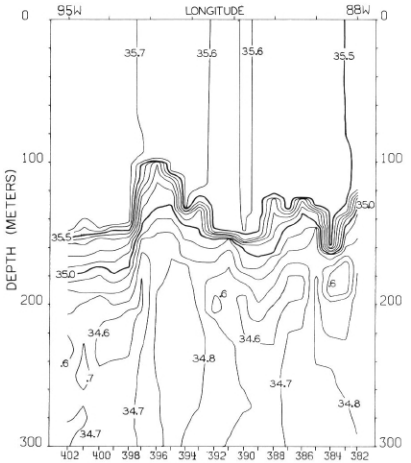

FIGURE 47-S-v11.—Vertical distribution of salinity (‰) along 15° S., September 10-12, 1967. These costours are based on STD data read from analog traces.

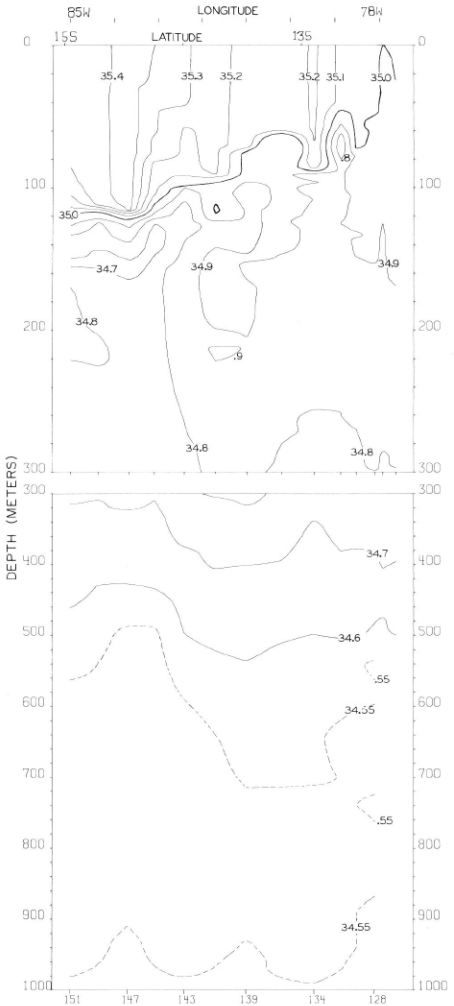

FIGURE 47-S-v7.—Vertical distribution of salinity (‰) along a northeast-southwest section from the coast of Peru to 15° S., 85° W., August 16-19, 1967. These contours are based on STD data read from analog traces.

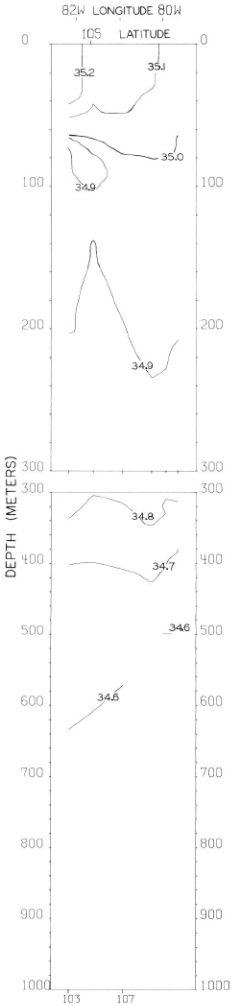

FIGURE 47-S-v5.—Vertical distribution of salinity (‰) along a southwest-northeast section from 10°09′ S., 82°09′ W. to the coast of Peru, August 12-13, 1967. These contours are based on STD data read from analog traces.

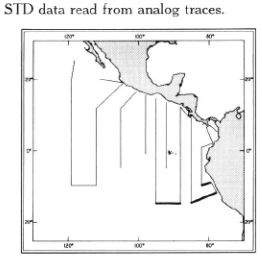

47-S-v5.

47-S-v7.

47-S-v11.

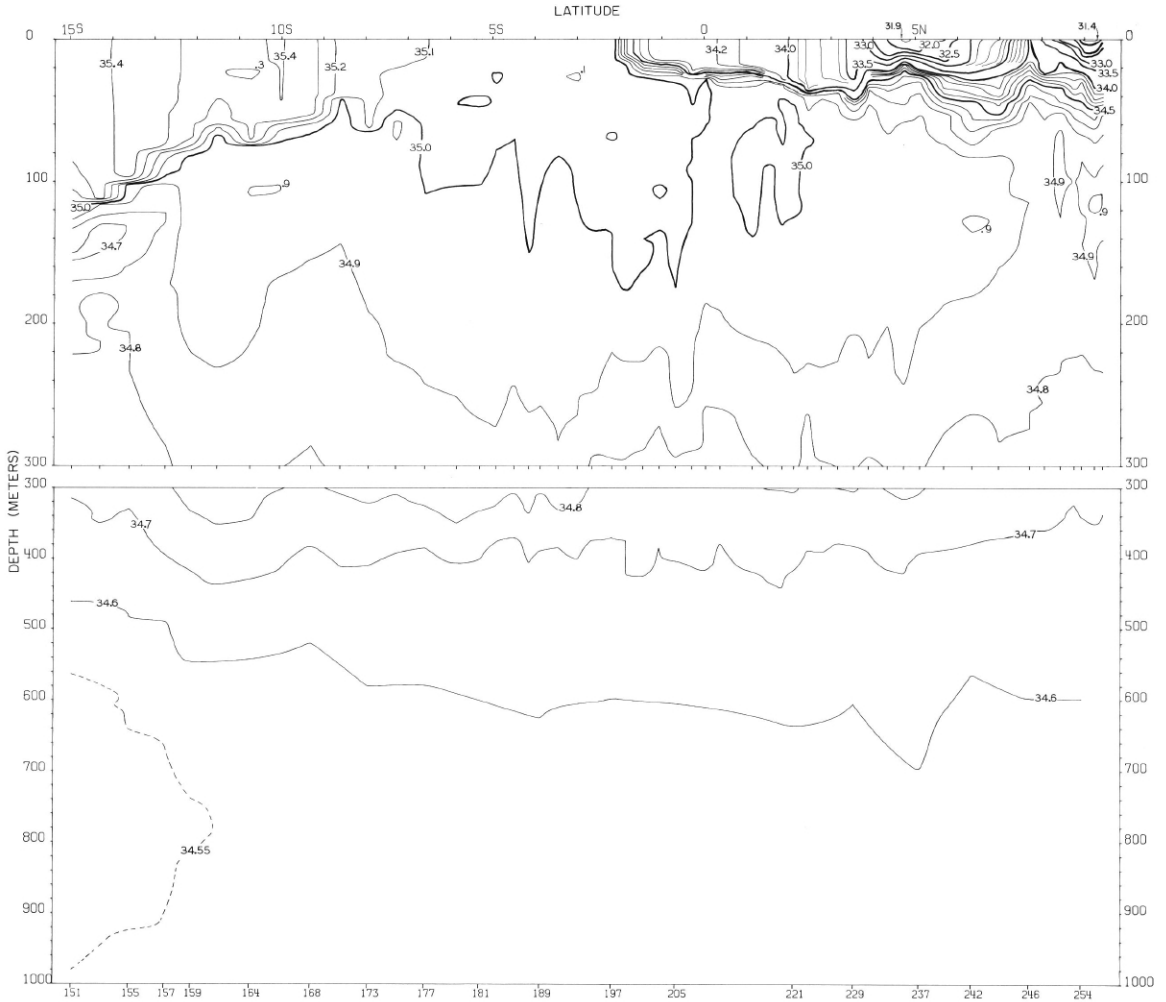

FIGURE 47-S-v8.—Vertical distribution of salinity (‰) along 85° W., August 19-28, 1967. These contours are based on STD data read from analog traces.

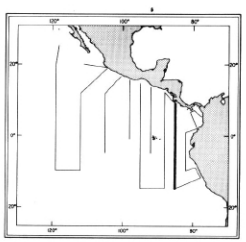

47-S-v8.

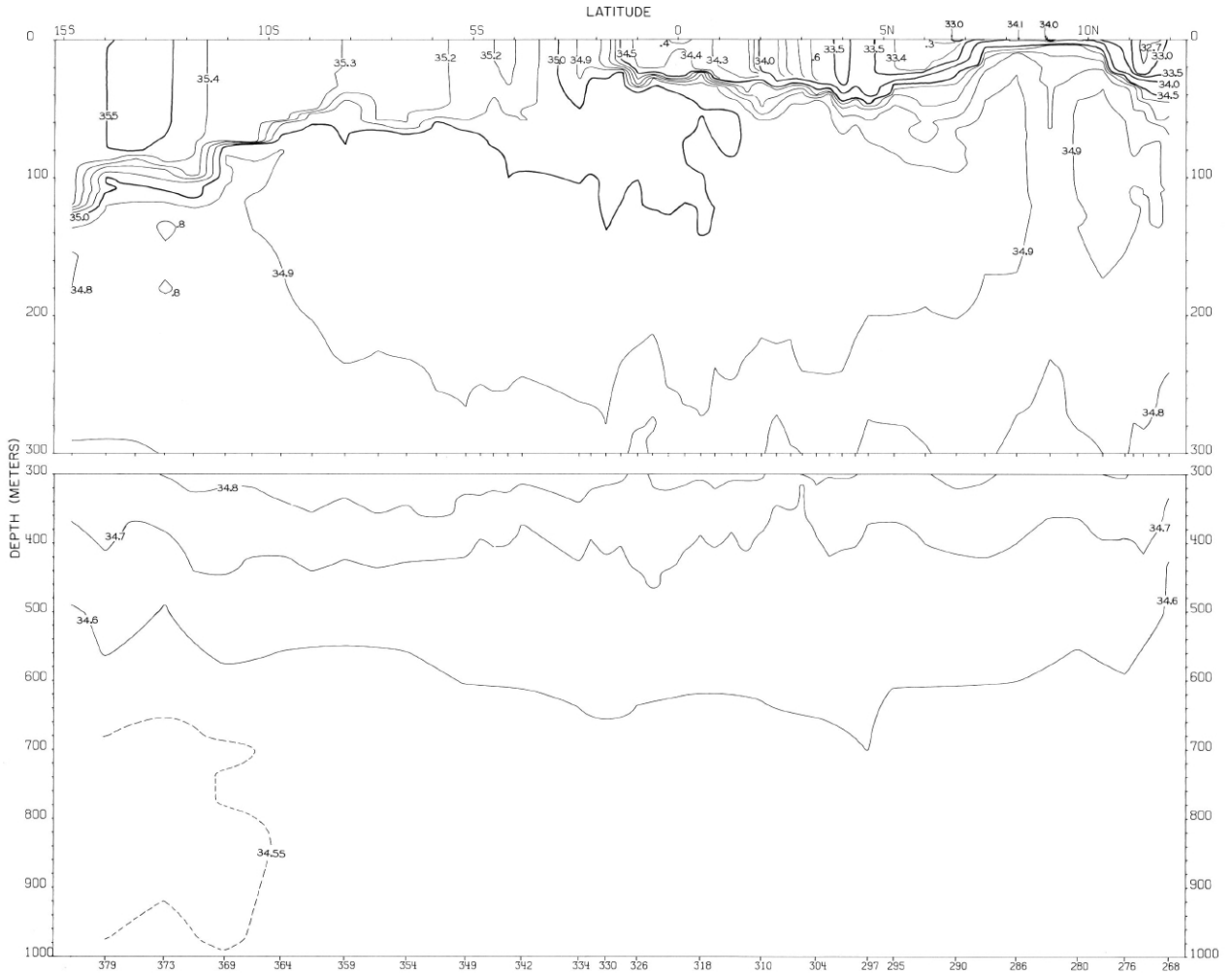

FIGURE 47-S-v10.—Vertical distribution of salinity (‰) along 88° W., August 31-September 10, 1967. These contours are based on STD data read from analog traces.

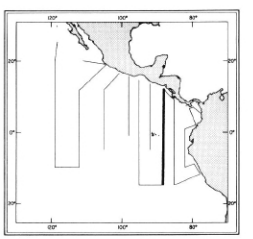

47-S-v10.

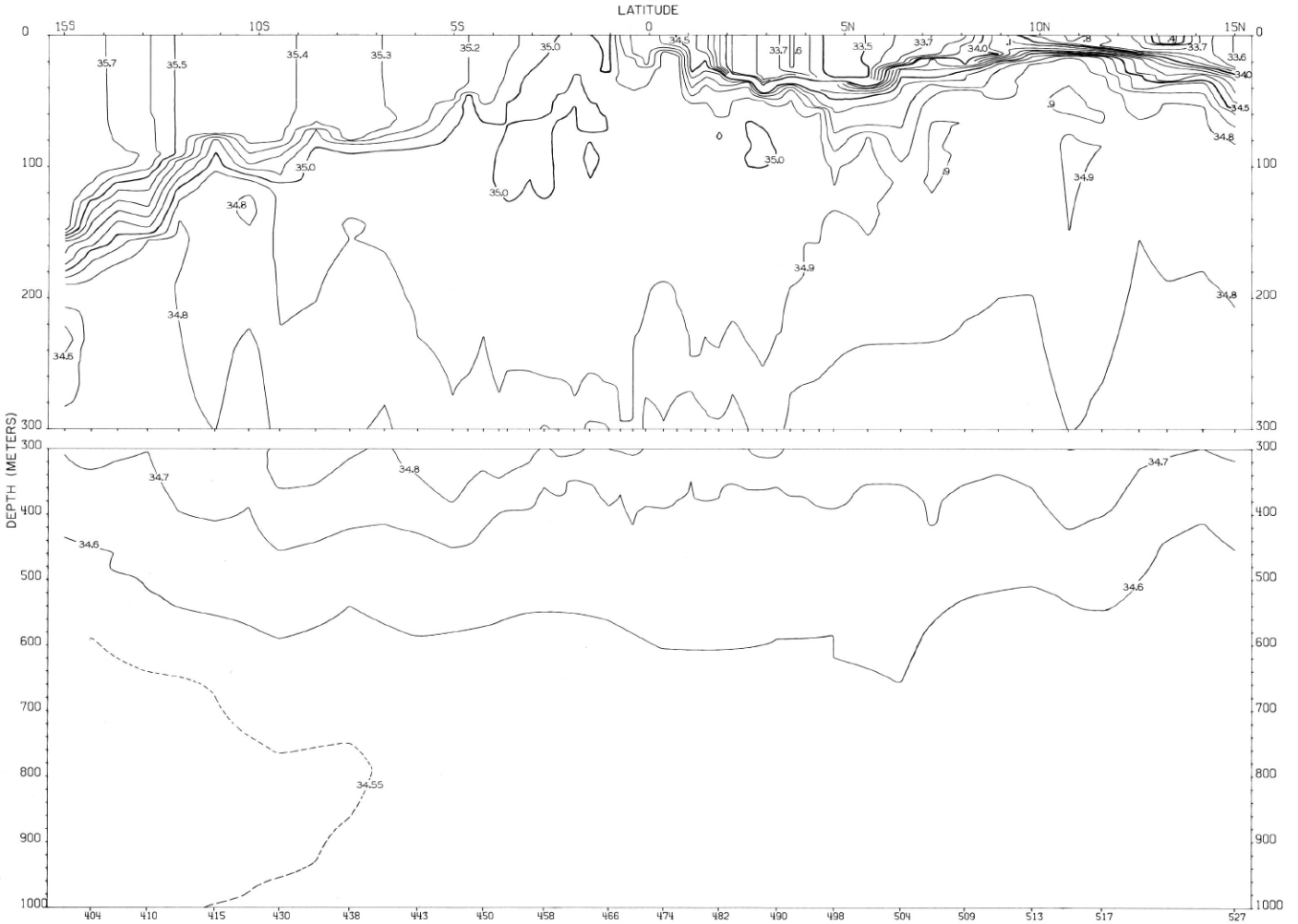

FIGURE 47-S-v12.—Vertical distribution of salinity (‰) along 95° W., September 12-23, 1967. These contours are based on STD data read from analog traces.

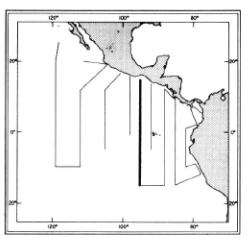

47-S-v12.

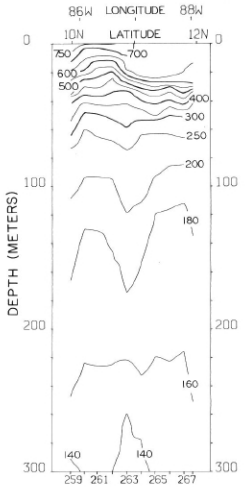

FIGURE 47-δ-v9.—Vertical distribution of thermosteric anomaly, δ_T, (cl./t.) along the coasts of Costa Rica and Nicaragua from 85°52′ W. to 88°02′ W., August 30-31, 1967. These contours are based on STD data read from analog traces.

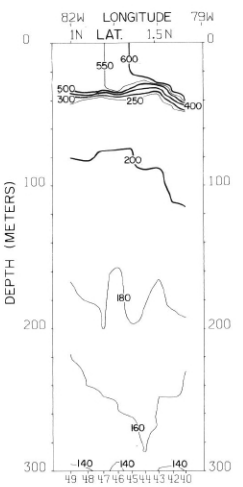

FIGURE 47-δ-v3.—Vertical distribution of thermosteric anomaly, δ_T, (cl./t.) along 1°20′ N. from the coast of Colombia to 82° W., August 5, 1967. These contours are based on STD data read from analog traces.

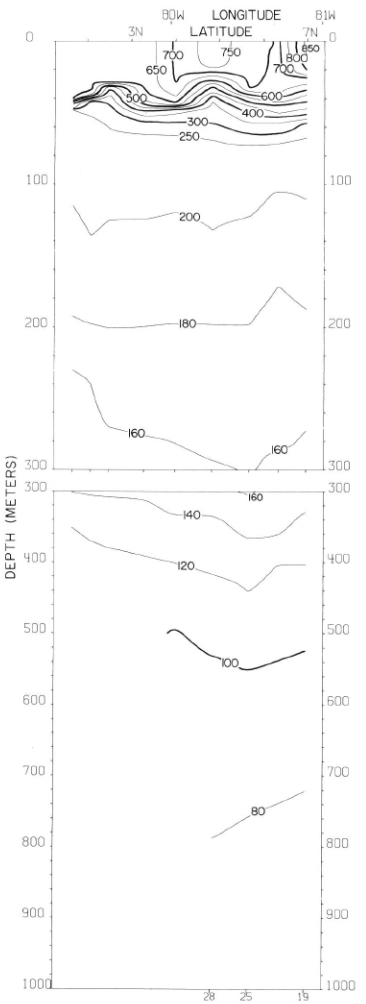

FIGURE 47-δ-v2.—Vertical distribution of thermosteric anomaly, δ_T, (cl./t.) along a northwest-southeast section in the central portion of the Panama Bight from Peninsula de Azuero, Panama, to the coast of Colombia, August 3-5, 1967. These contours are based on STD data read from analog traces.

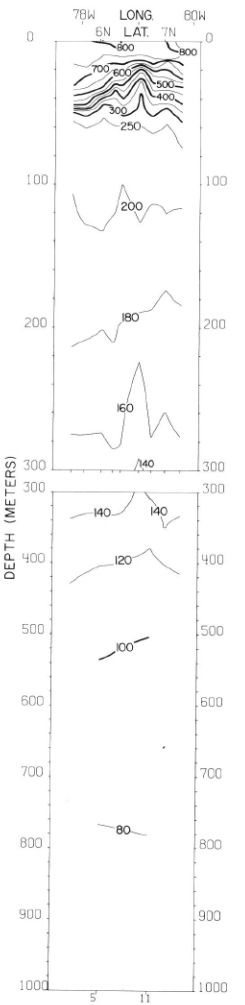

FIGURE 47-δ-v1.—Vertical distribution of thermosteric anomaly, δ_T, (cl./t.) across the northern portion of the Panama Bight from the coast of Colombia to Cabo Mala, Panama, August 1-2, 1967. These contours are based on STD data read from analog traces.

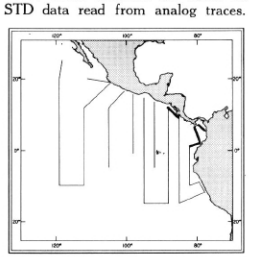

47-δ-v1.

47-δ-v2.

47-δ-v3.

47-δ-v9.

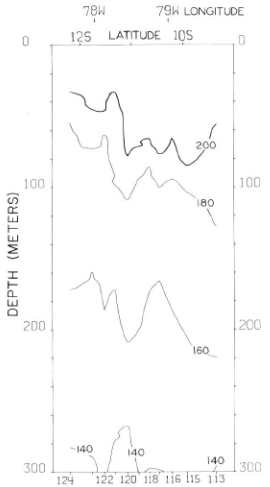

FIGURE 47-δ-v6.—Vertical distribution of thermosteric anomaly, δ_T, (cl./t.) along the coast of Peru from 9°22′ S. to 12°12′ S., August 13-16, 1967. These contours are based on STD data read from analog traces.

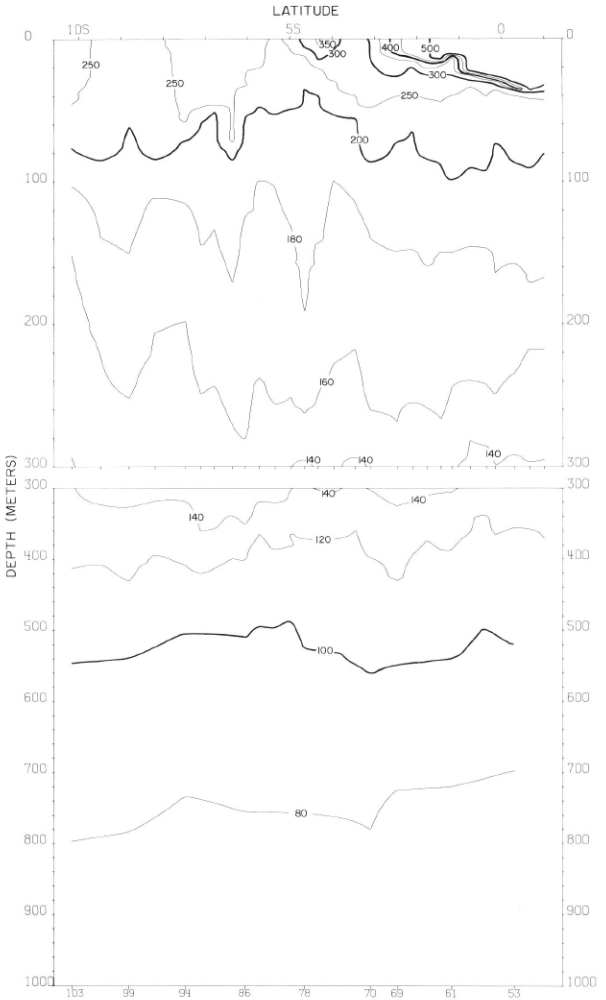

FIGURE 47-δ-v4.—Vertical distribution of thermosteric anomaly, δ_T, (cl./t.) along 82° W., August 5-12, 1967. These contours are based on STD data read from analog traces.

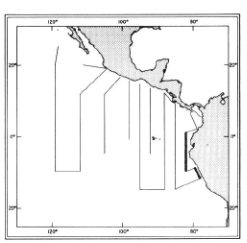

47-δ-v4.

47-δ-v6.

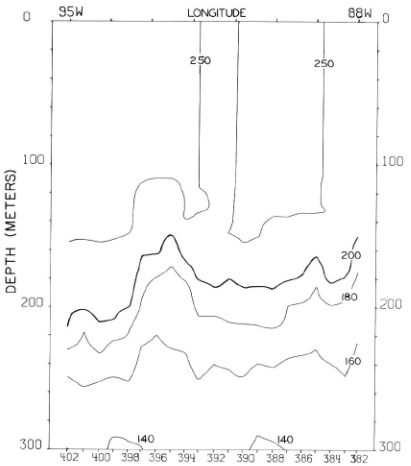

FIGURE 47-δ-v11.—Vertical distribution of thermosteric anomaly, δ_T, (cl./t.) along 15° S., September 10-12, 1967. These contours are based on STD data read from analog traces.

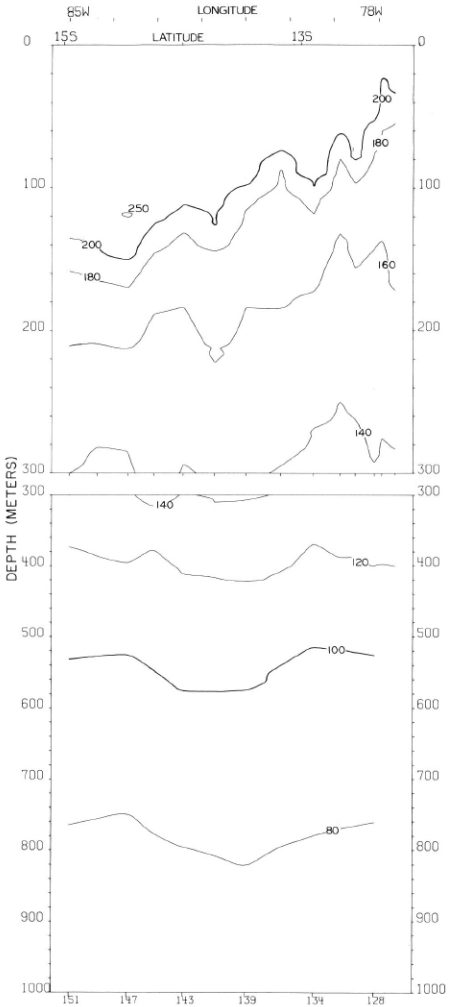

FIGURE 47-δ-v7.—Vertical distribution of thermosteric anomaly, δ_T, (cl./t.) along a northeast-southwest section from the coast of Peru to 15° S., 85° W., August 16-19, 1967. These contours are based on STD data read from analog traces.

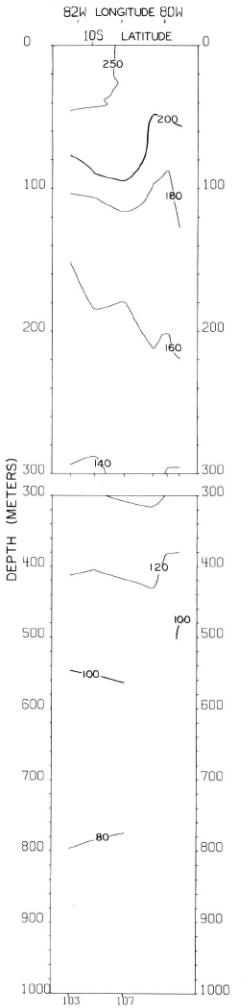

FIGURE 47-δ-v5.—Vertical distribution of thermosteric anomaly, δ_T, (cl./t.) along a southwest-northeast section from 10°09′ S., 82°09′ W. to the coast of Peru, August 12-13, 1967. These contours are based on STD data read from analog traces.

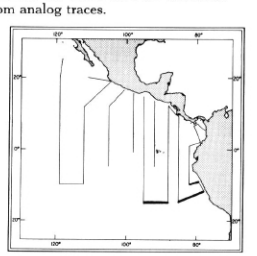

47-δ-v5.

47-δ-v7.

47-δ-v11.

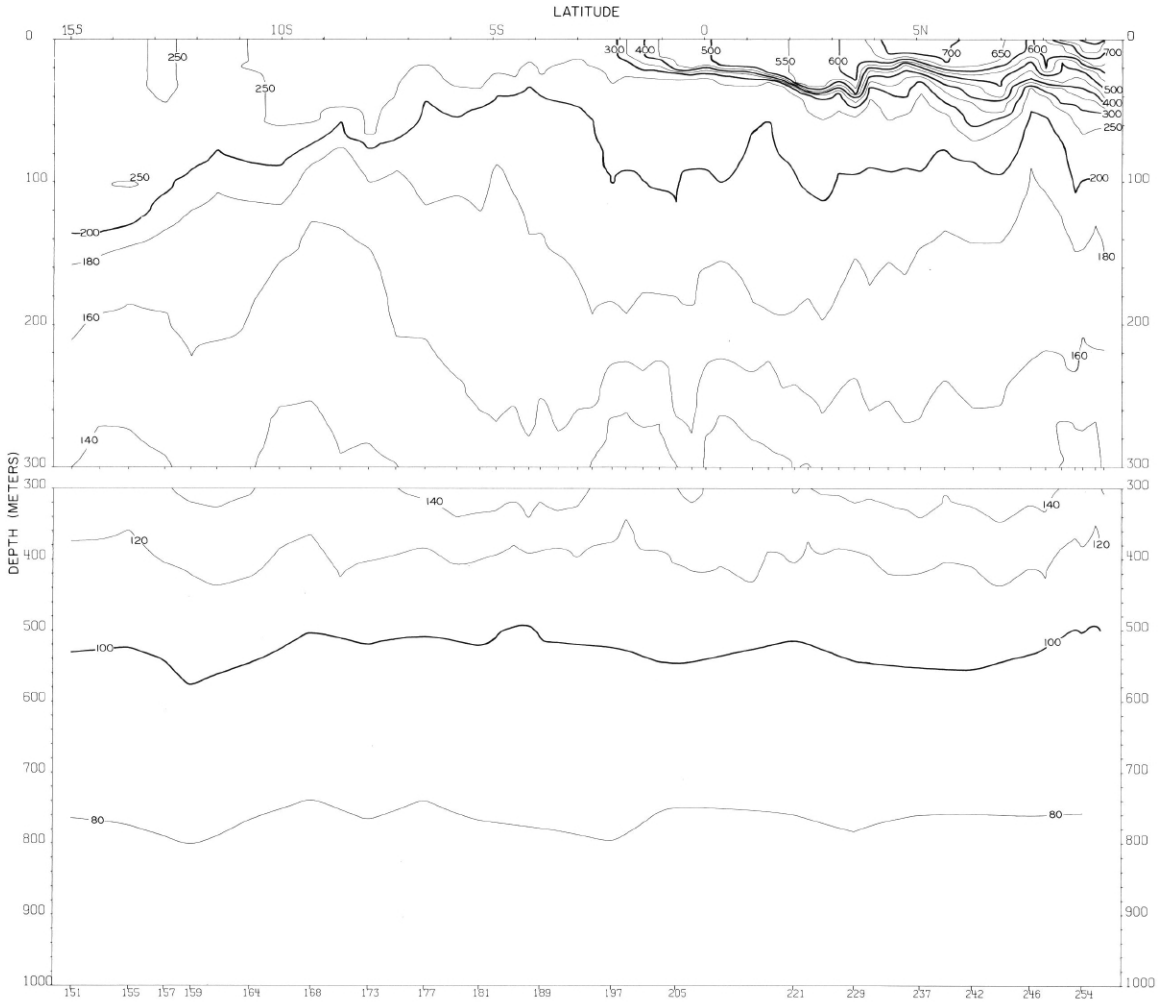

FIGURE 47-δ-v8.—Vertical distribution of thermosteric anomaly, δ_T, (cl./t.) along 85° W., August 19-28, 1967. These contours are based on STD data read from analog traces.

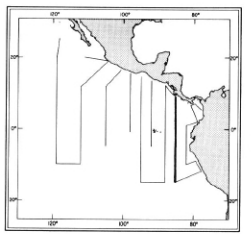

47-δ-v8.

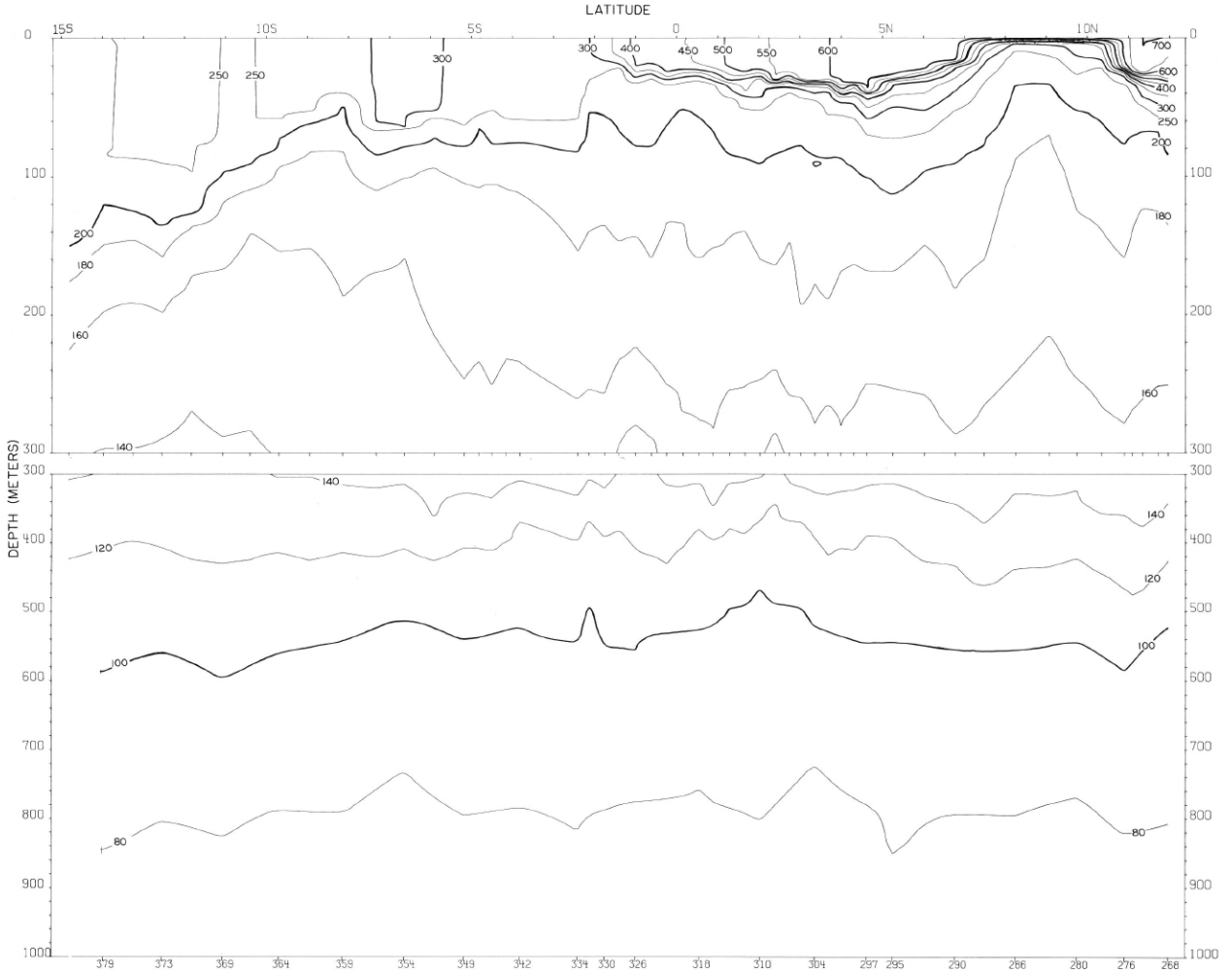

FIGURE 47-δ-v10.—Vertical distribution of thermosteric anomaly, δ_T, (cl./t.) along 88° W., August 31-September 10, 1967. These contours are based on STD data read from analog traces.

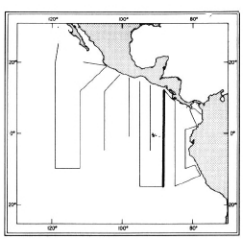

47-δ-v10.

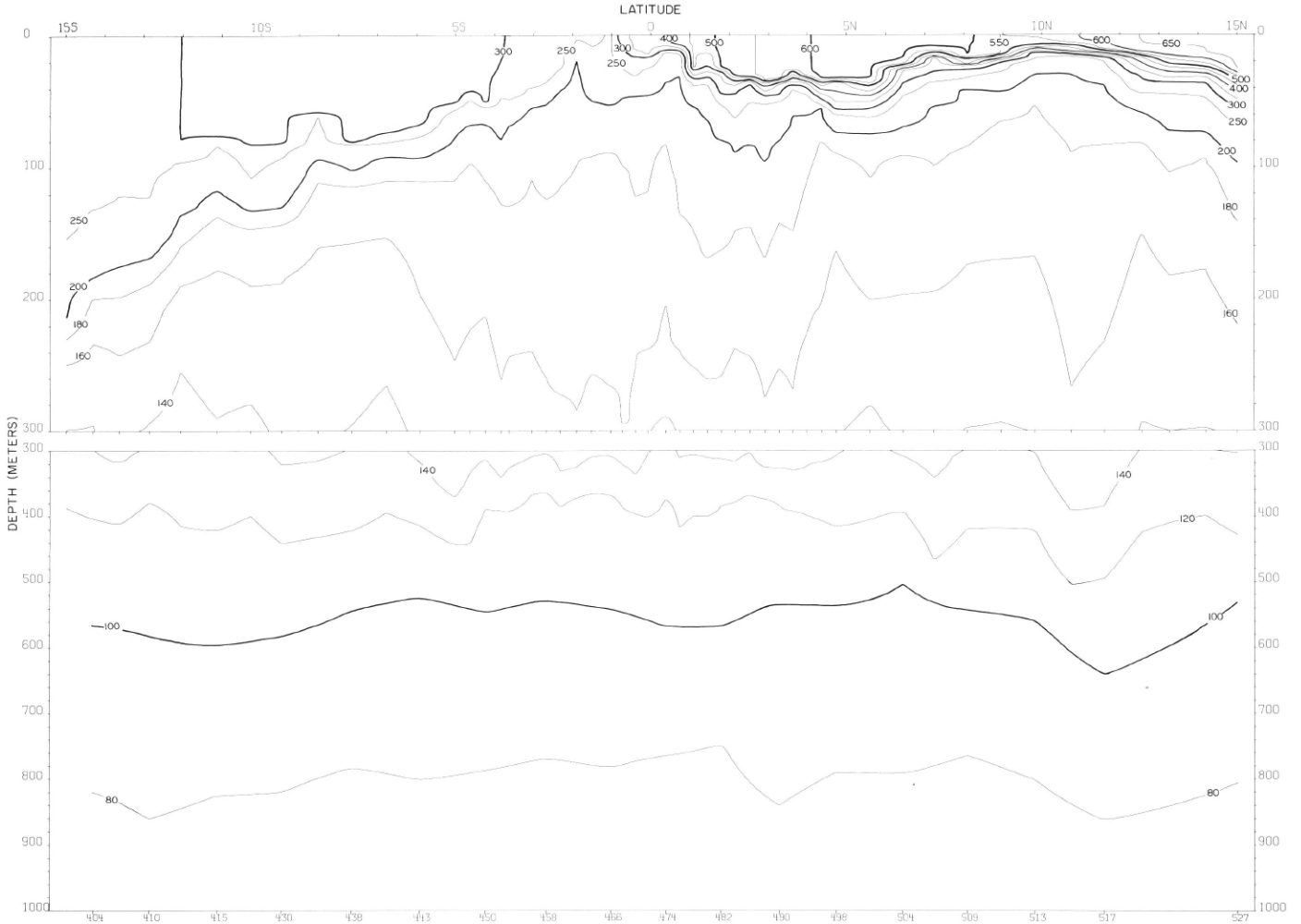

FIGURE 47-δ-v12.—Vertical distribution of thermosteric anomaly, δ_T, (cl./t.) along 95° W., September 12-23, 1967. These contours are based on STD data read from analog traces.

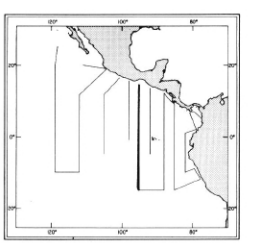

47-δ-v12.

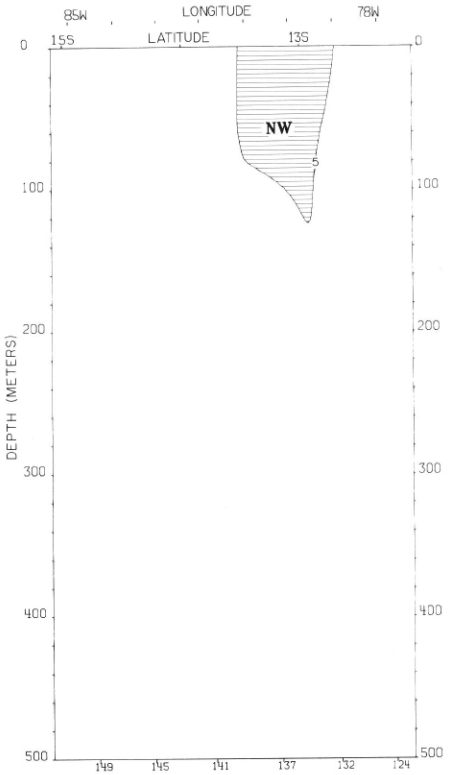

FIGURE 47-G-v7.—Vertical distribution of the component of geostrophic velocity (cm./sec.), relative to 500 db., normal to a northeast-southwest section from the coast of Peru to 15° S., 85° W., August 16-19, 1967. The light shading indicates flow toward the northwest with a velocity greater than 5 cm./sec.

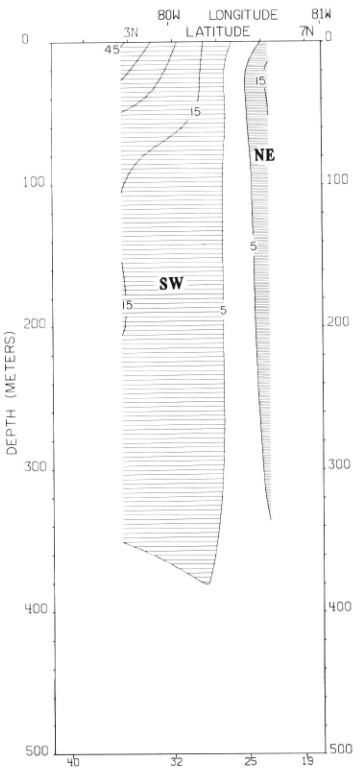

FIGURE 47-G-v2.—Vertical distribution of the component of geostrophic velocity (cm./sec.), relative to 500 db., normal to a northwest-southeast section in the central portion of the Panama Bight from Peninsula de Azuero, Panama, to the coast of Colombia, August 3-5, 1967. Dark shading indicates flow toward the northeast with a velocity greater than 5 cm./sec.; light shading indicates flow toward the southwest with a velocity greater than 5 cm./sec.

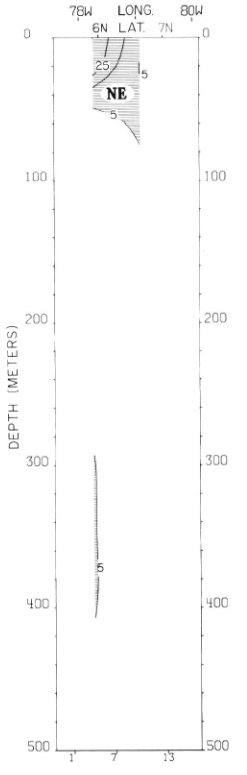

FIGURE 47-G-v1.—Vertical distribution of the component of geostrophic velocity (cm./sec.), relative to 500 db., normal to a section across the northern portion of the Panama Bight from the coast of Colombia to Cabo Mala, Panama, August 1-2, 1967. Dark shading indicates flow toward the northeast with a velocity greater than 5 cm./sec.

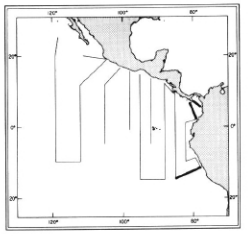

47-G-v1.

47-G-v2.

47-G-v7.

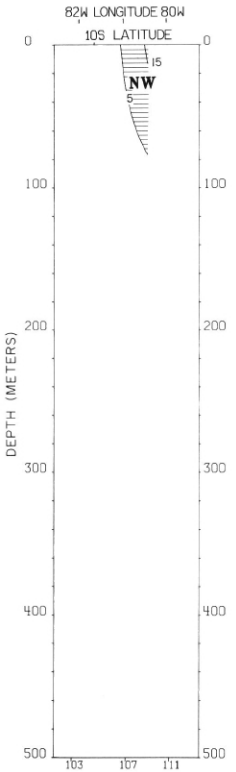

FIGURE 47-G-v5.—Vertical distribution of the component of geostrophic velocity (cm./sec.), relative to 500 db., normal to a southwest-northeast section from 10°09′ S., 82°09′ W. to the coast of Peru, August 12-13, 1967. The light shading indicates flow toward the northwest with a velocity greater than 5 cm./sec.

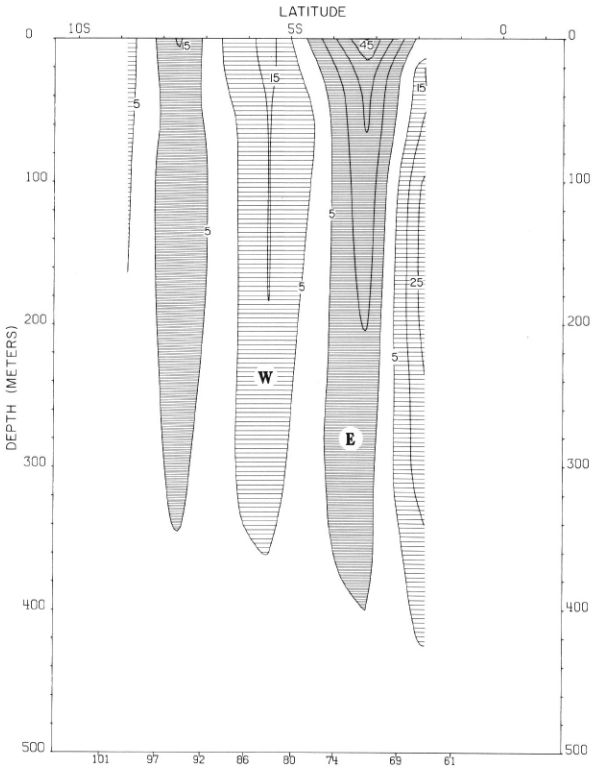

FIGURE 47-G-v4.—Vertical distribution of the zonal component of geostrophic velocity (cm./sec.), relative to 500 db., along 82° W., August 6-12, 1967. Dark shading indicates eastward flow with a velocity greater than 5 cm./sec.; light shading indicates westward flow with a velocity greater than 5 cm./sec.

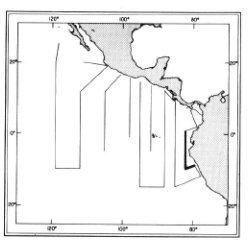

47-G-v4.

47-G-v5.

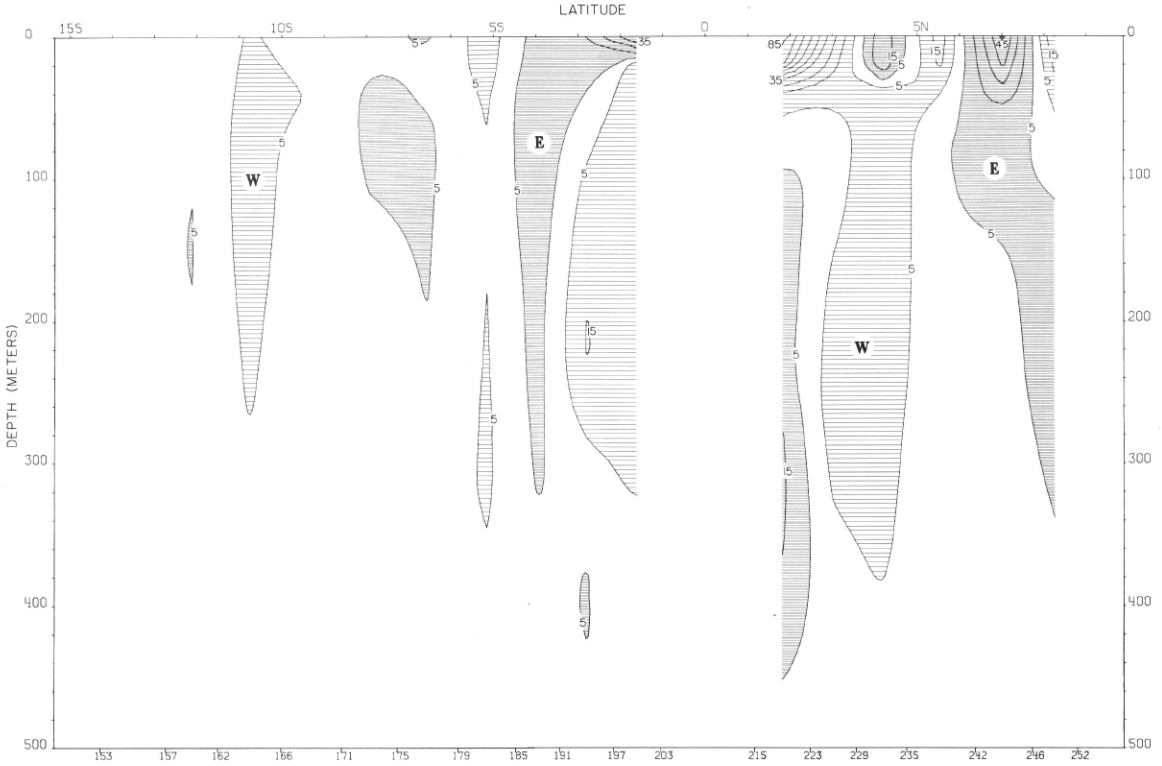

FIGURE 47-G-v8.—Vertical distribution of the zonal component of geostrophic velocity (cm./sec.), relative to 500 db., along 85° W., August 19-28, 1967. Dark shading indicates eastward flow with a velocity greater than 5 cm./sec.; light shading indicates westward flow with a velocity greater than 5 cm./sec.

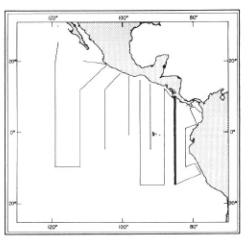

47-G-v8.

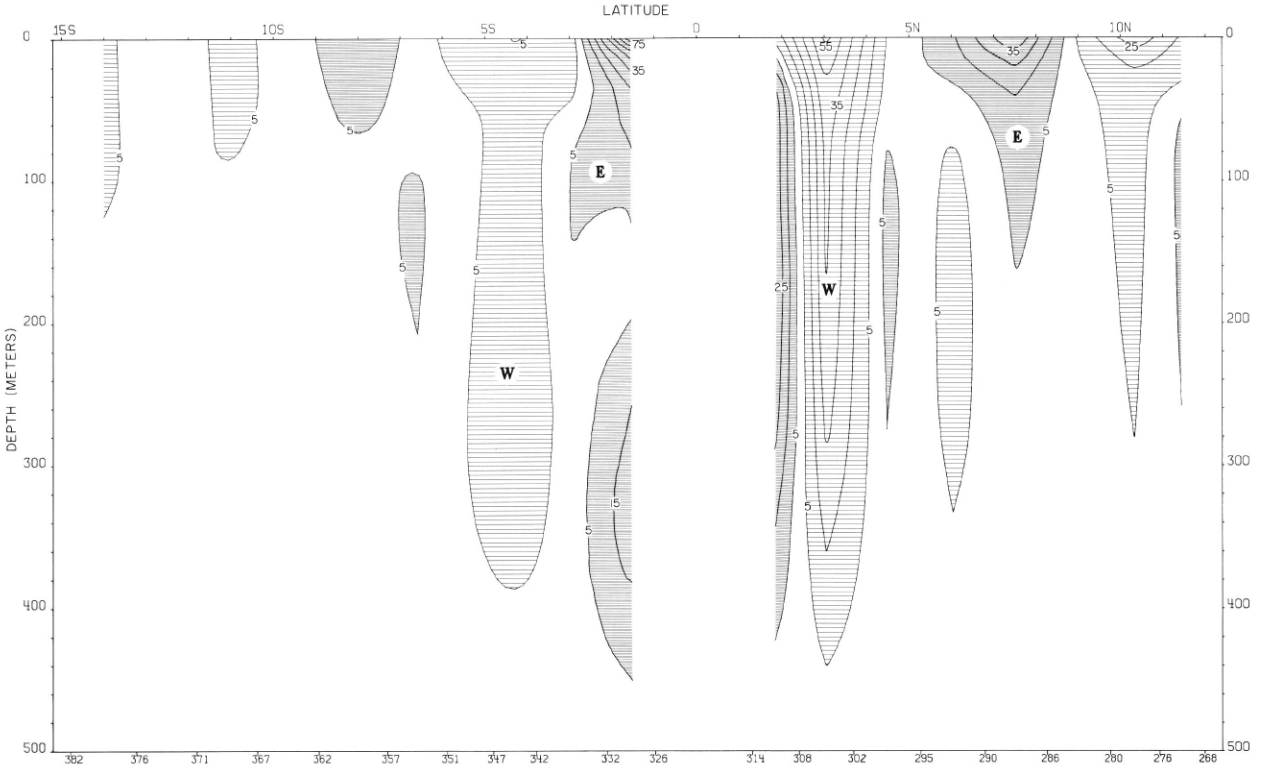

FIGURE 47-G-v10.—Vertical distribution of the zonal component of geostrophic velocity (cm./sec.), relative to 500 db., along 88° W., August 31-September 10, 1967. Dark shading indicates eastward flow with a velocity greater than 5 cm./sec; light shading indicates westward flow with a velocity greater than 5 cm./sec.

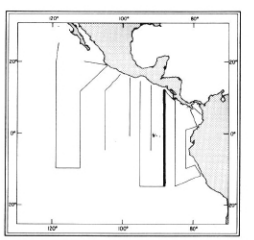

47-G-v10.

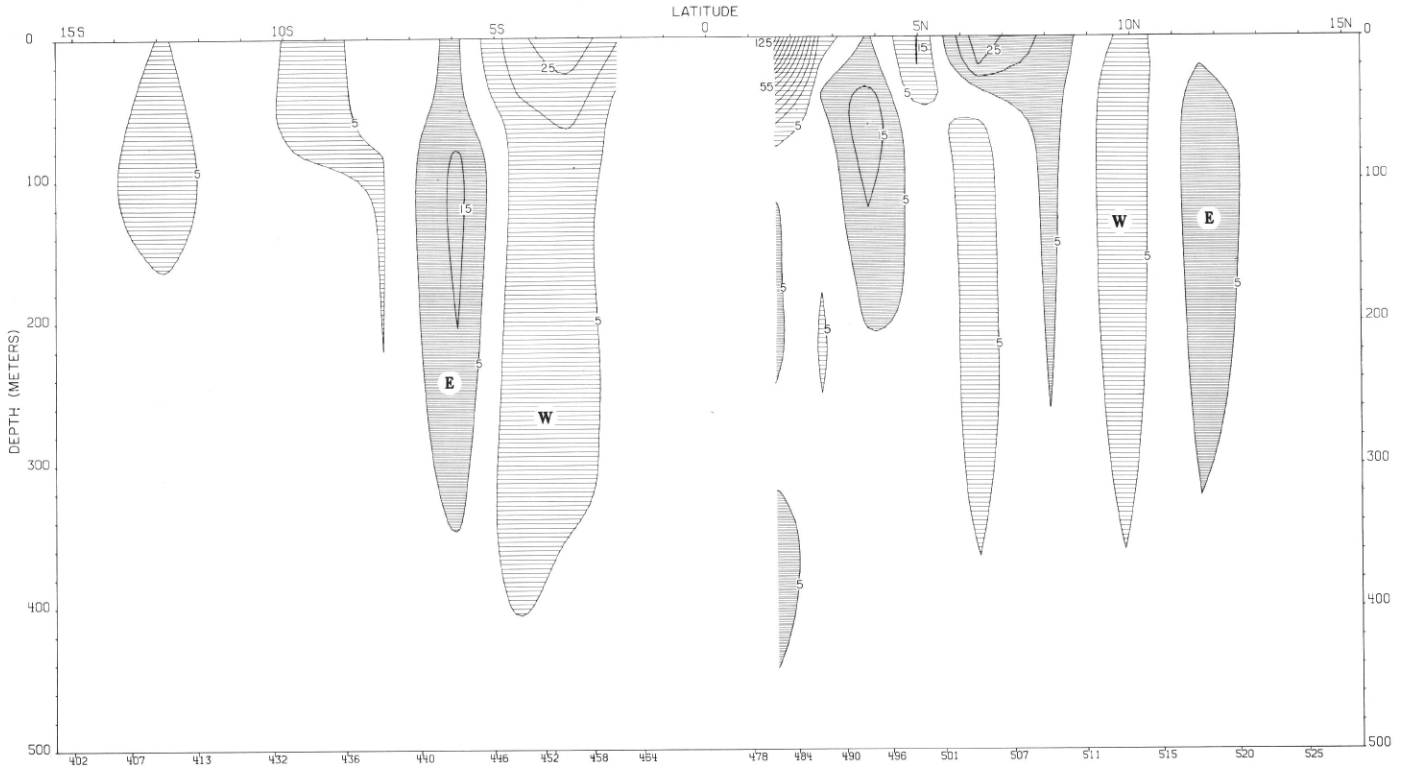

FIGURE 47-G-v12.—Vertical distribution of the zonal component of geostrophic velocity (cm./sec.), relative to 500 db., along 95° W., September 12-22, 1967. Dark shading indicates eastward flow with a velocity greater than 5 cm./sec.; light shading indicates westward flow with a velocity greater than 5 cm./sec.

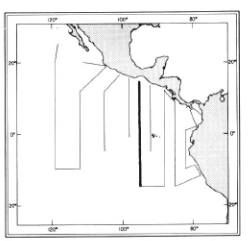

47-G-v12.

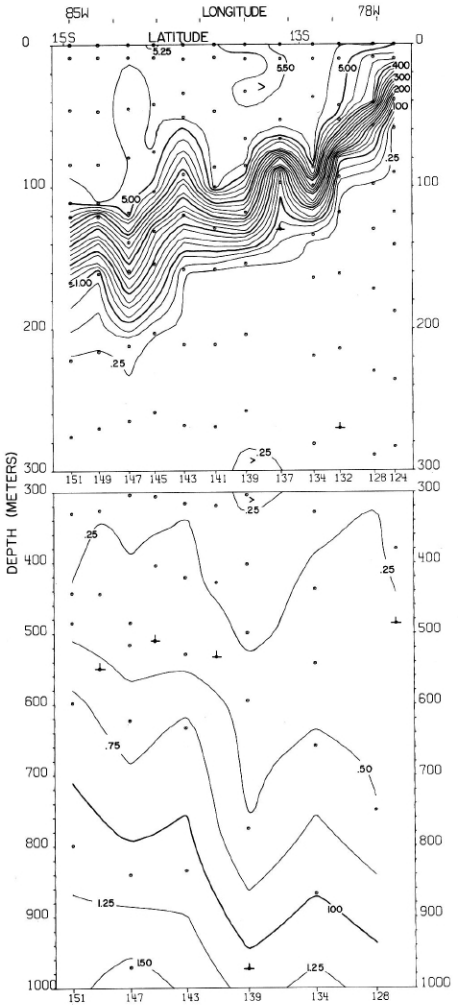

FIGURE 47-O_2-v7.—Vertical distribution of oxygen (ml./l.) along a northeast-southwest section from the coast of Peru to 15° S., 85° W., August 17-19, 1967.

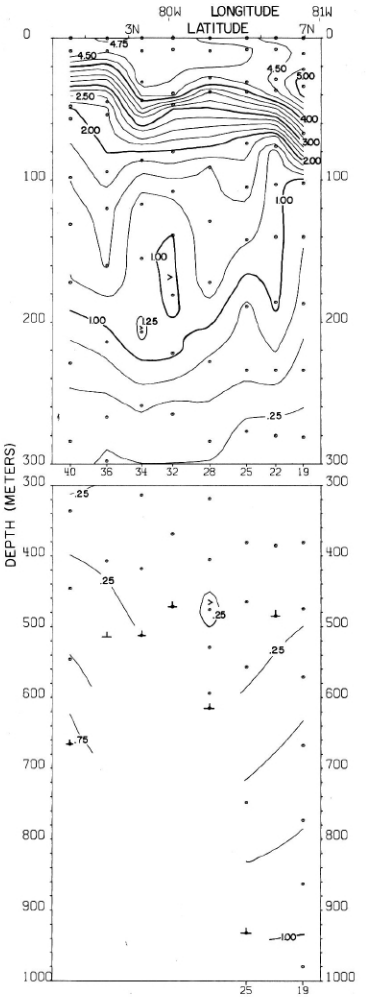

FIGURE 47-O_2-v2.—Vertical distribution of oxygen (ml./l.) along a northwest-southeast section in the central portion of the Panama Bight from Peninsula de Azuero, Panama, to the coast of Colombia, August 3-4, 1967.

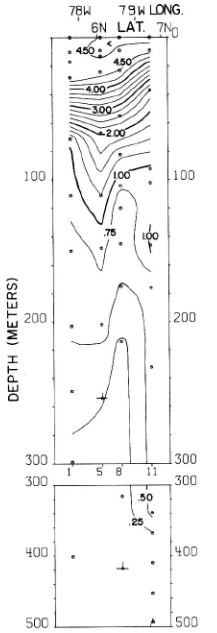

FIGURE 47-O_2-v1.—Vertical distribution of oxygen (ml./l.) across the northern portion of the Panama Bight from the coast of Colombia to Cabo Mala, Panama, August 1-2, 1967.

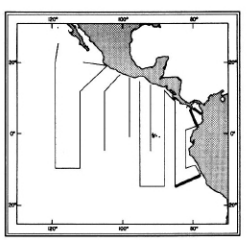

47-O_2-v1.

47-O_2-v2.

47-O_2-v7.

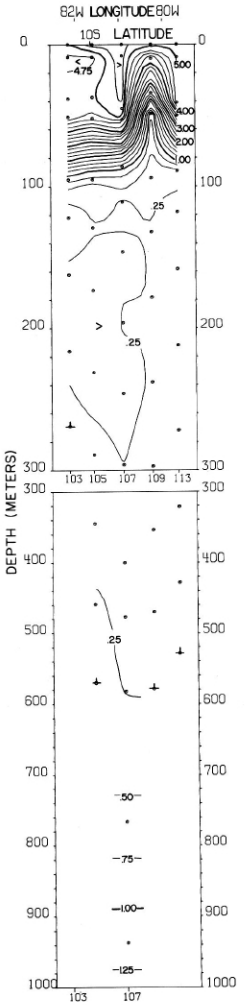

FIGURE 47-O₂-v5.—Vertical distribution of oxygen (ml./l.) along a southwest-northeast section from 10°09′ S., 82°09′ W. to the coast of Peru, August 12, 1967.

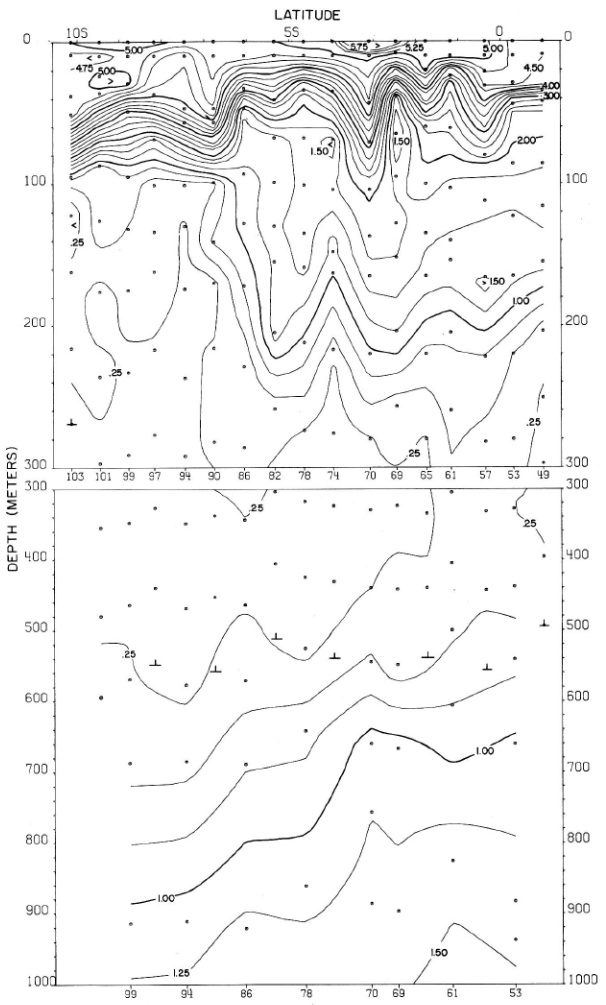

FIGURE 47-O₂-v4.—Vertical distribution of oxygen (ml./l.) along 82° W., August 6-12, 1967.

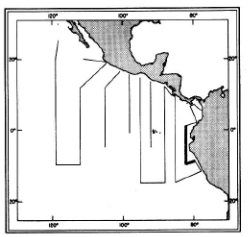

47-O₂-v4.

47-O₂-v5.

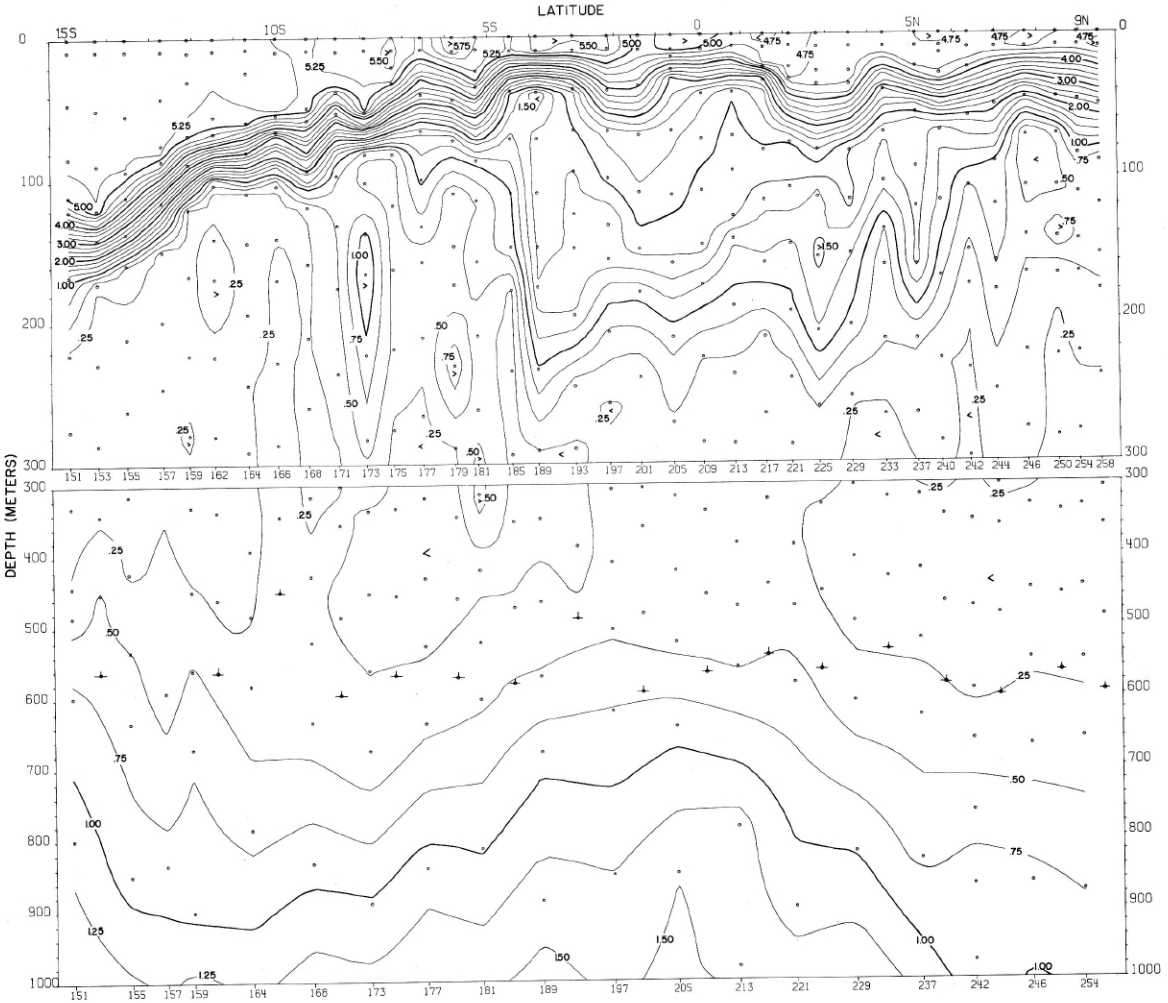

FIGURE 47-O2-v8.—Vertical distribution of oxygen (ml./l.) along 85° W., August 19-28, 1967.

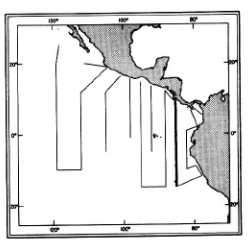

47-O2-v8.

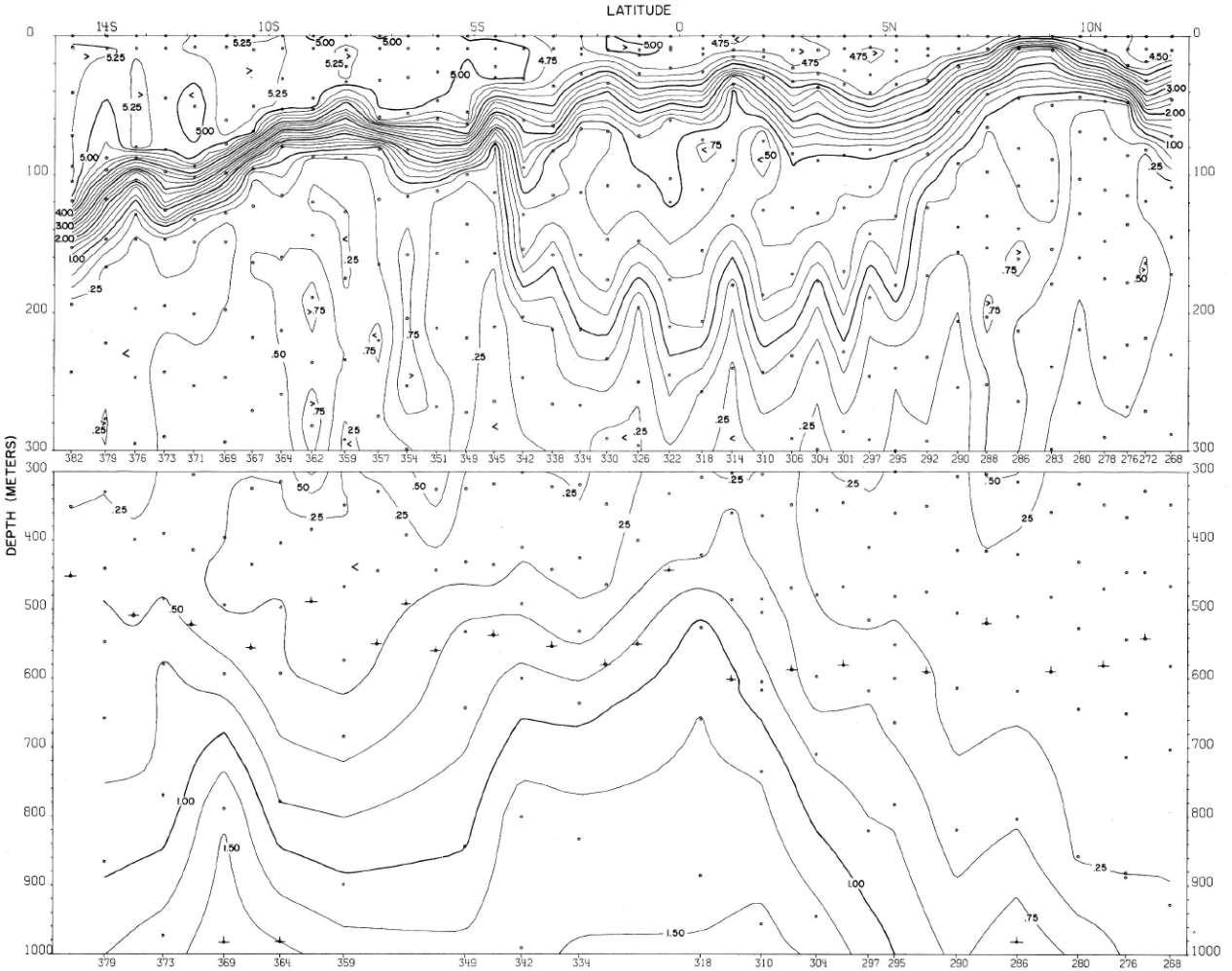

FIGURE 47-O₂-v10.—Vertical distribution of oxygen (ml./l.) along 88° W., August 31-September 10, 1967.

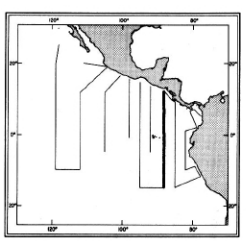

47-O₂-v10.

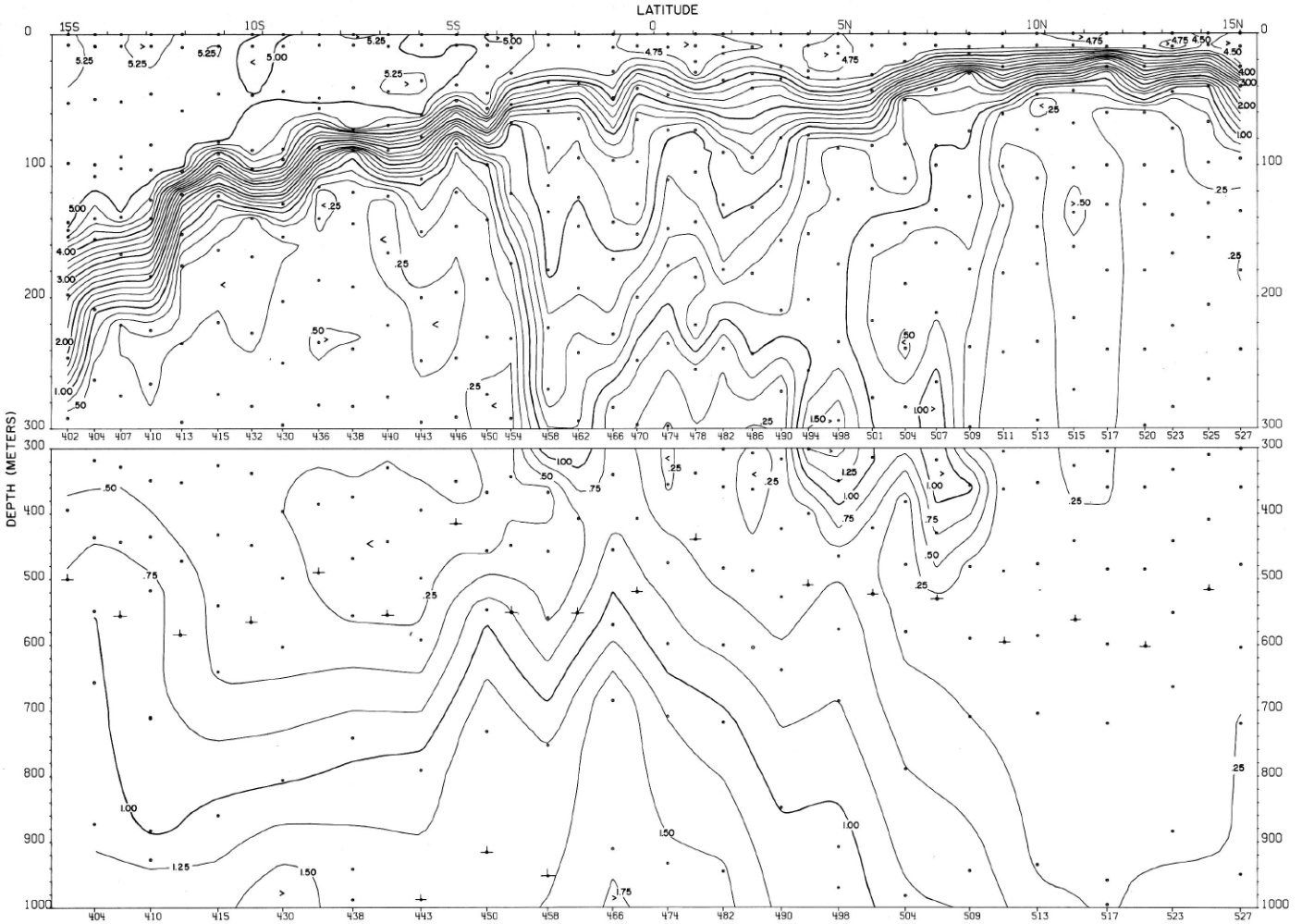

FIGURE 47-O₂-v12.—Vertical distribution of oxygen (ml./l.) along 95° W., September 12-23, 1967.

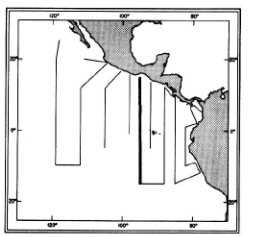

47-O₂-v12.

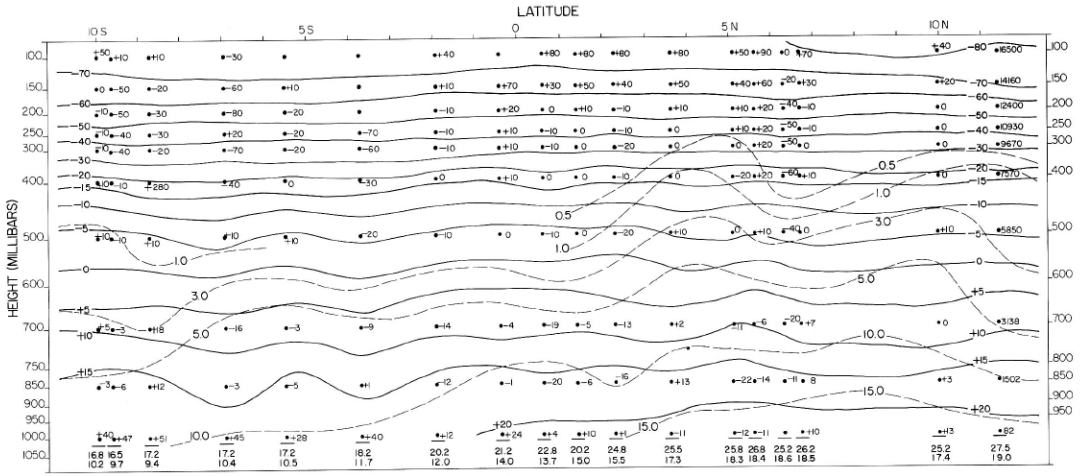

FIGURE 47-UA-v4.—Vertical section of the atmosphere along 82° W., August 2-12, 1967. Solid lines are isotherms of air temperature (°C.). Dashed lines are isopleths of mixing ratio of the air (g./kg.). Surface air temperature is plotted above surface mixing ratio and below a base line representing the surface pressure (mb.). The computed height (m.) of each standard pressure surface is plotted for the northernmost radiosonde station of the section. At other stations the difference of computed height minus the corresponding height at the northern station is shown at each standard level.

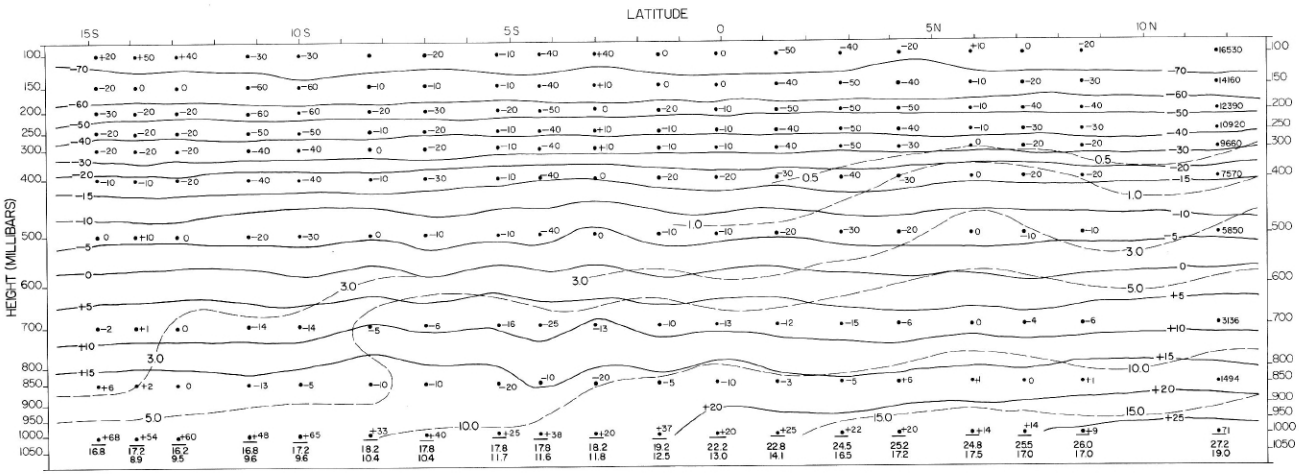

FIGURE 47-UA-v8.—Vertical section of the atmosphere along 85° W., August 19-31, 1967. Solid lines are isotherms of air temperature (°C.). Dashed lines are isopleths of mixing ratio of the air (g./kg.). Surface air temperature is plotted above surface mixing ratio and below a base line representing the surface pressure (mb.). The computed height (m.) of each standard pressure surface is plotted for the northernmost radiosonde station of the section. At other stations the difference of computed height minus the corresponding height at the northern station is shown at each standard level.

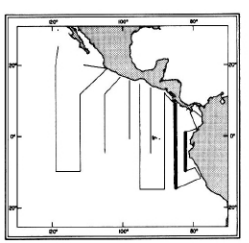

47-UA-v4.

47-UA-v8.

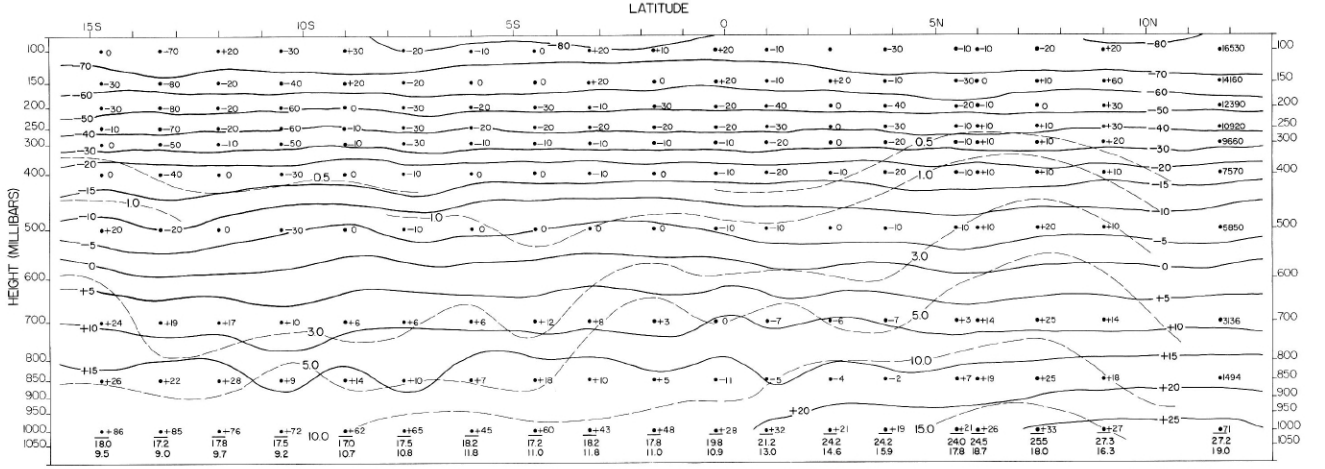

FIGURE 47-UA-v10.—Vertical section of the atmosphere along 88° W., August 31-September 11, 1967. Solid lines are isotherms of air temperature (°C.). Dashed lines are isopleths of mixing ratio of the air (g./kg.). Surface air temperature is plotted above surface mixing ratio and below a base line representing the surface pressure (mb.). The computed height (m.) of each standard pressure surface is plotted for the northernmost radiosonde station of the section. At other stations the difference of computed height minus the corresponding height at the northern station is shown at each standard level.

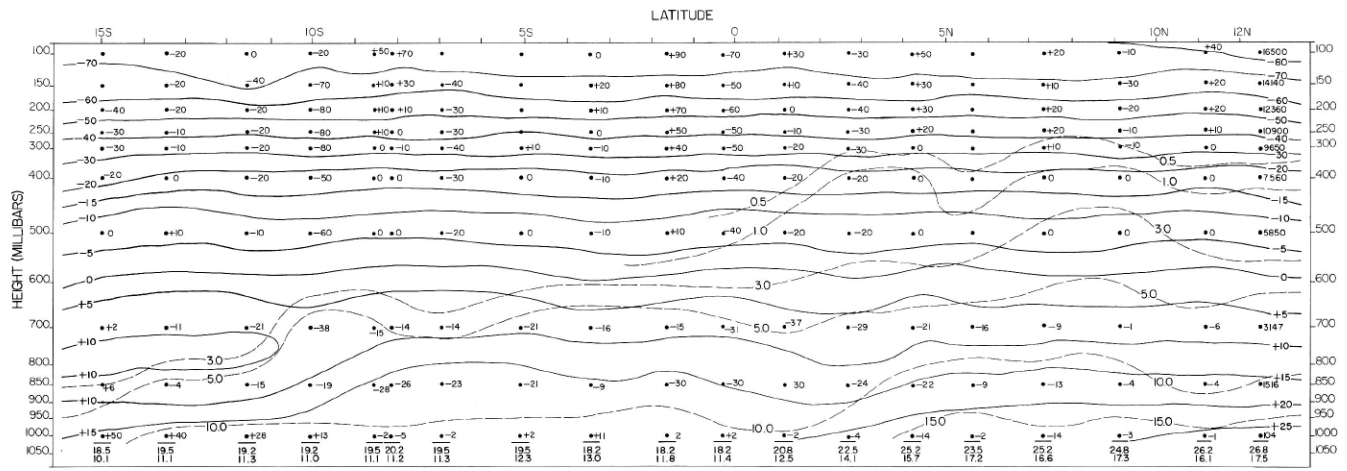

FIGURE 47-UA-v12.—Vertical section of the atmosphere along 95° W., September 12-22, 1967. Solid lines are isotherms of air temperature (°C.). Dashed lines are isopleths of mixing ratio of the air (g./kg.). Surface air temperature is plotted above surface mixing ratio and below a base line representing the surface pressure (mb.). The computed height (m.) of each standard pressure surface is plotted for the northernmost radiosonde station of the section. At other stations the difference of computed height minus the corresponding height at the northern station is shown at each standard level.

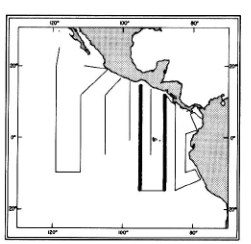

47-UA-v10.

47-UA-v12.